IOWA STATE UNIVERSITY
Digital Repository

Graduate Theses and Dissertations

Iowa State University Capstones, Theses and Dissertations

2019

Investigating the viability of bio-additives with rejuvenating properties in 50% RAP HMA mix designs: A multi-faceted approach of analyzing mix performance

Nicholas Manke
Iowa State University

Follow this and additional works at: https://lib.dr.iastate.edu/etd

 Part of the Civil Engineering Commons, and the Sustainability Commons

Recommended Citation
Manke, Nicholas, "Investigating the viability of bio-additives with rejuvenating properties in 50% RAP HMA mix designs: A multi-faceted approach of analyzing mix performance" (2019). *Graduate Theses and Dissertations*. 17051.
https://lib.dr.iastate.edu/etd/17051

This Dissertation is brought to you for free and open access by the Iowa State University Capstones, Theses and Dissertations at Iowa State University Digital Repository. It has been accepted for inclusion in Graduate Theses and Dissertations by an authorized administrator of Iowa State University Digital Repository. For more information, please contact digirep@iastate.edu.

www.manaraa.com

Investigating the viability of bio-additives with rejuvenating properties in 50% RAP HMA mix designs: A multi-faceted approach of analyzing mix performance

by

Nicholas David Manke

A dissertation submitted to the graduate faculty

in partial fulfillment of the requirements for the degree of

DOCTOR OF PHILOSOPHY

Major: Civil Engineering (Civil Engineering Materials)

Program of Study Committee:
R. Christopher Williams, Major Professor
Vernon Schaefer
Eric Cochran
Stephen Vardeman
Jeramy Ashlock
Ashley Buss

The student author, whose presentation of the scholarship herein was approved by the program of study committee, is solely responsible for the content of this dissertation. The Graduate College will ensure this dissertation is globally accessible and will not permit alterations after a degree is conferred.

Iowa State University

Ames, Iowa

2019

Copyright © Nicholas David Manke, 2019. All rights reserved.

www.manaraa.com

DEDICATION

I dedicate this dissertation to my family who have supported me throughout my education and life. My father who taught me that anything worth doing is worth doing your best and there is nothing hard work and perseverance can't accomplish. My mother who supported me and greeted my trips home with a warm hug and a home-cooked meal. And to my siblings, extended family, and close friends, the countless hours poured into my education and career were made much easier with the time spent in between with all of you.

www.manaraa.com

TABLE OF CONTENTS

www.manaraa.com

www.manaraa.com

LIST OF FIGURES

www.manaraa.com

www.manaraa.com

LIST OF TABLES

www.manaraa.com

www.manaraa.com

ACKNOWLEDGEMENTS

I would first like to thank Dr. Christopher Williams for giving me the opportunity to take my academic career far further than I ever thought was possible. Dr. Williams has helped me open doors to opportunities I never knew existed and I was able to advance my career and knowledge to a level where I'm more excited than ever for the future. His guidance, support, and feedback throughout this process has been extremely appreciated and I'm forever grateful to have had the opportunity to work with him.

I would also like to thank the professors on my POS committee, Dr. Vern Schaefer, Dr. Ashley Buss, Dr. Stephen Vardeman, Dr. Jeramy Ashlock, and Dr. Eric Cochran. Their assistance and guidance were much appreciated. An additional thank you to all other faculty, staff, and mentors who have taught me, shared their wisdom, and offered me guidance throughout my duration at Iowa State University. They provided me with a solid foundational footing on which to expand and develop my knowledge which was essential in the preparation of this dissertation.

I would like to thank all of my friends and colleagues in the asphalt labs who helped me greatly with both procedural guidance, material preparation and testing, and analysis. Zahra Sotoodeh-Nia, Paul Ledtje, and Dr. Joseph Podolsky all offered their experience, thoughts, ideas, and time to assist me throughout my graduate studies.

Finally, I would like to thank all of the partners on the BioRePavation team for their support, feedback, and contributions to this research. I would like to thank those in the Infravation program for funding this research and allowing for the data collection and analysis which has lead to these findings.

www.manaraa.com

ABSTRACT

Reclaimed asphalt pavement (RAP), though the most recycled material by weight in the U.S. and Europe, is not currently most effectively utilized. The material RAP is readily available due to the vast amount of infrastructure surfaced with flexible pavements. Recycled materials are often desired for reduced material costs in construction, reduced environmental costs, and reduced impacts on non-renewable resources. While RAP has been a commonly used material for decades in the U.S. and other nations, it has been used primarily as base aggregate material, construction site fill, and as a partial aggregate and binder replacement in HMA mixes. Many U.S. state agencies are reluctant to use RAP in significant amounts in HMA mixes with many limiting RAP contents to 15% to 30% depending on the agency and the roadway.

Reluctancy to increase the allowable RAP content in new mixes is largely due to the incorporation of a significant amount of aged, stiff binder which, if not properly designed for, can decrease a pavement's resistance to brittle failure mechanisms and moisture damage. During aging, the ratio of asphaltene to maltene molecules increase which in turn reduces the viscous damping and strain dissipation ability of the pavement. Rejuvenators and specifically engineered non-bituminous bio-binders with rejuvenating properties can both be used to chemically restore the molecular ratios within the aged RAP binder to allow for a greater amount of RAP to be used.

This research uses a multi-faceted approach to analyze the performances of two organically-derived rejuvenators and one novel bio-binder in HMA mixes incorporating 50% RAP by mix weight. One rejuvenator used is derived from soybean chemistry and is applied as a binder additive while the other rejuvenator is derived from pine chemistry and is applied directly to the RAP material. The novel bio-binder is a polymer-modified non-bituminous binder made from

www.manaraa.com

refined pine chemistry with rejuvenation properties. The first phase of this research was to validate the performance of the novel bio-binder in the laboratory using disc-shaped compact tension (DCT) testing, beam fatigue testing, dynamic modulus and flow number testing, and moisture damage testing. As a control, a mix using the same aggregate gradations, sources, and binder content with a PG 58-28 bituminous neat binder was used. Testing showed that the novel bio-binder with 50% RAP passed all U.S. performance and volumetric criteria for a pavement with a 20-year design load of greater than 10 million but less than 30 million ESALs. Additionally, intermediate and low-temperature test results showed the rejuvenating ability of the bio-binder in restoring the viscous damping and stiffness dissipation properties of the mix at critical temperatures.

The second phase of this research was the analysis of mix sensitivity to process control variations such as mixing temperature, curing times, and other variables associated with increasing the mixing scale from a laboratory-mixed scale to a continuous mixing plant operation in the field. Both rejuvenators and the novel bio-binder were assessed for process control and mix scale variation impacts on pavement performance. Performance test results indicated that the bio-binder had little to no sensitivity regarding mix performance to process control variations associated with the change in mix scales. Both rejuvenators showed an increased stiffness with an increase in mix scale and associated increase in mixing temperature, storage time, and increase in aggregate fines content. However, the rejuvenator applied directly to the RAP material showed less stiffness sensitivity to mix scale increase process control variables at both low and intermediate temperatures relative to the rejuvenator used as a binder additive. All three bio-additives reduced the mix stiffness at low and intermediate temperatures below that of a high-performance control mix with just 20% RAP while providing adequate rutting resistance at high temperatures. The

www.manaraa.com

three bio-additives met or surpassed laboratory performance test criteria at both the small-scale and large-scale mixing operations for pavements with 20-year design loads of greater than 10 million but less than 30 million ESALs.

Mechanistic-empirical software modeling along with in-situ accelerated pavement testing results were used in the third phase of research to analyze how mixes with bio-additives and 50% RAP content perform beyond laboratory-scale testing. The same mix designs were used as the second phase field-produced mixes. Accelerated pavement testing measured both rutting accumulation and cracking as a percentage of surface area. Rutting measurement analysis showed that although the mixes with bio-additives softened the mixes to a degree at high temperatures, the total predicted asphaltic layer rutting was still very similar to the high-performance control. Crack measurements showed that the pavement mixes with bio-additives significantly reduced the amount of early cracking as compared to the control mix. Software predictions were used to project the accelerated pavement test rutting measurements and develop fitted models predicting rutting progression with high-temperature ESALs. Software predictions do not account for aging effects on pavement performance which would have an impact on long-term performance. These models predict that all three mixes with bio-additives will experience less than 10-mm of asphaltic layer rutting with 640,000 cumulative ESALs applied when surface temperatures are in excess of 30°C. In the climate considered, this equates to a total 20-year design traffic load of 9.75 million ESALs. Fatigue cracking predictions showed that lower air void contents significantly increase the mixes' resistance to both top-down and bottom-up cracking. While all mixes showed exceptional performance against bottom-up fatigue cracking, the three mixes with bio-additives in addition to the control mix were predicted to experience top-down fatigue cracking as the critical design distress.

www.manaraa.com

CHAPTER 1: GENERAL INTRODUCTION

An increase in demand for new and replaced flexible pavements in the U.S. and other nations along with limited available funding, volatile crude oil prices, and rising construction costs has led many to seek new methods of lowering infrastructure costs while maintaining performance. The use of reclaimed asphalt pavement (RAP, or RA in EU terminology) in hot mix asphalt (HMA) pavements is a popular method of reducing material costs while simultaneously reducing environmental costs and usage of non-renewable aggregate resources. Asphalt pavement is the most recycled material by weight in the U.S. at over 80 million tons annually [1,2] and in the EU at over 40 million tons annually [3]. Even though RAP as a material is recycled at an astonishing rate, much of it is not used in new pavement mixes due to several concerns. Use in new pavements is the most efficient way to recycle RAP as it utilizes not only the valuable aggregate resources, but also recycles the binder content.

1.1. Reclaimed Asphalt Pavement (RAP)

RAP material is produced by the milling or removal and subsequent crushing of aged pavements that are to be repaired or replaced. One concern with using RAP in new pavements is the quality control of the RAP material processing and storage. Because RAP can be produced from many pavements that used different materials and were at different levels of aging, the mixing of RAP from multiple small projects can make it difficult to assess the quality of the material. Additionally, storage of RAP stockpiles with exposure to precipitation, soil intrusion, and deleterious and organic material inclusion and overgrowth further inhibits the chances of the RAP being a quality addition to a new HMA mix. However, if the RAP materials are known and have

www.manaraa.com

been appropriately processed and stockpiled, the material is a good potential resource for use in new pavements.

Besides process and storage concerns with RAP materials, there are inherent concerns with the aged binder content included in RAP. During aging, asphalt binder undergoes volatilization and polycondensation of smaller maltene molecules [4]. The result of these phenomena is a larger ratio of larger asphaltene molecules to smaller lubricating maltene molecules and a shifting of the viscoelastic response. Aged binders become stiffer, less viscous, and more prone to brittle failure mechanisms such as thermal and fatigue cracking. Without properly addressing and re-balancing these properties, a mix's longevity can be drastically reduced. Adsorbed hardened binder films around the RAP aggregate can also cause blending limitations between the RAP binder and the neat binder. Localized incomplete blending is known as "black rock" which can create stripping, localized rutting, and early crack propagation distresses from weak, pervious aggregate-binder interfaces [5,6].

1.2. Bio-Additives with Rejuvenating Properties

The Federal Highway Administration (FHWA) suggests that special design considerations should be used when exceeding 30% RAP by mix weight [1]. At high RAP contents, the potential for adverse effects from the added stiff binder content increase substantially. To offset the imposed "stiffness" of the RAP, soft bituminous binders, petroleum-derived rejuvenators, organic material-derived rejuvenators, and partial binder replacements have been used. Research has shown that organically-derived rejuvenators can chemically break weak intermolecular associations of polycondensed asphaltene molecules to restore the viscoelastic properties of the aged binder [5,7]. Studies on rejuvenated mixes with 40% RAP by mix weight have shown that rejuvenators can

www.manaraa.com

improve a mix's resistance to thermal and fatigue cracking but can also improve the diffusibility of the neat binder with the RAP binder interface [8]. While rejuvenating additives can effectively soften the mix at low and intermediate temperatures, it is desirable to retain a degree of stiffness at high temperatures to resist rutting. A bio-binder derived from pine chemistry was used as a complete replacement of bituminous neat binder in a mix with 50% RAP content and shown to have primary rejuvenation effects on the RAP binder in addition to desirable viscoelastic properties [9,10]. The use of a bio-binder with rejuvenating properties means that not only can it chemically restore the molecular ratios of the aged binder and improve diffusibility, it can also supplement the RAP content by specific design for the viscoelastic properties desired.

1.3. Organization of Dissertation

This research uses a multi-faceted approach to analyze the mix performance of two rejuvenators and a novel bio-binder made from refined pine chemistry. All three additives are made from refined organic co-products or by-products and are used in HMA mixes incorporating 50% RAP by mix weight. Chapter 2 focuses on the performance and viability of the novel bio-binder against a control with 50% RAP and a conventional PG 58-28 neat bitumen. Test specimens were laboratory-mixed and compacted. Performance tests include disc-shaped compact tension (DCT) testing, beam fatigue, dynamic modulus and flow number testing, and moisture testing. Performance test results are statistically compared and cross-validated against applicable Superpave and U.S. industry recommendations for conventional mixes for a pavement with a 20-year design life of greater than 10 million but less than 30 million ESALs. Chapter 3 presents analyses that explore the sensitivity of the three mixes with bio-additives to process control and mix scale variable associated with changing from a small-scale laboratory operation to full-scale asphalt plant operation. DCT, beam fatigue, dynamic modulus and flow number testing, as well as

www.manaraa.com

Hamburg wheel-track testing (HWTT) were used to assess the mixtures' sensitivities to changes in mix scale and associated process control variables.

Chapter 4 analyzes data collected from large-scale in-situ accelerated pavement testing as well as mechanistic-empirical software modeling results. In-situ test rutting results are used to fit computer modeling predictions and develop extrapolated rutting progression predictions for each mix based on critical ESALs. Computer modeling fatigue cracking predictions are used to examine and explain differences in observations seen in in-situ testing cracking trends. Analysis results are then used to determine conservative prediction methods and critical distresses for each mix. Construction and traffic variables are also analyzed for their effect on predicted rutting and fatigue cracking to determine optimum air void contents, traffic speeds, and traffic volumes for each mix. Finally, Chapter 5 provides a general summary with conclusions and recommendations for future research.

References

1. FHWA, U.S. Department of Transportation Federal Highway Administration. "Reclaimed Asphalt Pavement in Asphalt Mixtures: State of the Practice." *FHWA Publication No. FHWA-HRT-11-021*. April 2011.

2. National Center for Asphalt Technology (NCAT): *Hot Mix Asphalt Materials, Mixture Design and Construction, 3rd ed.*, NCAT. 1991.

3. EAPA (European industry association), Asphalt in Figures, 2016. [www.eapa.org]

4. Ali, Hesham. "Long-Term Aging of Recycled Binders." Florida International University: Civil and Environmental Engineering Department; submitted to the Florida Department of Transportation. July 2015.

5. Haghshenas et al. "Research on High-RAP Asphalt Mixtures with Rejuvenators and WMA Additives." University of Nebraska-Lincoln: Nebraska Department of Roads Research Reports. September 2016.

www.manaraa.com

6. Kowalski et al. “Thermal and Fatigue Evaluation of Asphalt Mixtures Containing RAP Treated with a Bio-Agent.” *Applied Sciences, Vol. 7, Issue 3*. February 2017.

7. Zaumanis et al. “Influence of Six Rejuvenators on the Performance Properties of Reclaimed Asphalt Pavement (RAP) Binder and 100% Recycled Asphalt Mixtures.” *Construction and Building Materials.* November 2014.

8. Mogawer, Walaa & Booshehrian, Abbas & Vahidi, Siavash & Austerman, Alexander. (2013). “Evaluating the effect of rejuvenators on the degree of blending and performance of high RAP, RAS, RAP/RAS mixtures.” *Road Materials and Pavement Design*. 14. 10.1080/14680629.2013.812836.

9. Jiménez del Barco Carrión, A., Pérez-Martínez, M., Themeli, A., Lo Presti, D., Marsac, P., Pouget, S., Chailleux, E., Airey, G. D. (2017). Evaluation of bio-materials’ rejuvenating effect on binders for high-reclaimed asphalt content mixtures. *Materiales de Construcción*, *67*(327), 1–11.

10. Jiménez del Barco Carrión, A., Lo Presti, D., Pouget, S., Airey, G., & Chailleux, E. (2017). Linear viscoelastic properties of high reclaimed asphalt content mixes with biobinders. *Road Materials and Pavement Design*, 1–11.

www.manaraa.com

CHAPTER 2: PERFORMANCE OF A SUSTAINABLE ASPHALT MIX INCORPORATING HIGH RAP CONTENT AND NOVEL BIO-DERIVED BINDER

Modified from a paper submitted to Road Materials and Pavement Design

Nicholas D. Manke[a]*, R. Christopher Williams[a], Zahra Sotoodeh-Nia[a], Eric W. Cochran[b], Laurent Porot[c], Emmanuel Chailleux[d], Simon Pouget[e], Francois Olard[e], Ana Jimenez Del Barco Carrion[f], Jean-Pascal Planche[g], Davide Lopresti[f]

[a] *Department of Civil, Construction, and Environmental Engineering, Iowa State University, Ames, Iowa, 50011*
[b] *Department of Chemical, and Biological Engineering, Iowa State University, Ames, Iowa, 50011*
[c] *Kraton Corporation, Arizona Chemical*
[d]*Department of Materials and Structures, IFSTTAR*
[e]*EIFFAGE Infrastructures,France*
[f]*Department of Civil Engineering, Nottingham Transportation Engineering Centre, University of Nottingham*
[g]*Western Research Institute, Laramie, Wyoming, 82072*
**Corresponding author: nmanke@iastate.edu*

Abstract

The recent drive to find ways to increase sustainability and decrease costs in asphalt paving has led researchers to find innovative ways to incorporate more recycled materials and bio-derived binders into mixes with varying success. With greater recycled material contents, especially reclaimed asphalt pavement (RAP), the more potential issues arise that demand unique solutions. Reclaimed binder contents are typically oxidized, brittle, and pose both unknown degree of binder blending and increased cracking potential in the new asphalt mix. A new novel bio-derived binder made from refined pine derivate chemistry stabilized with an SBS polymer can both increase the sustainability of asphalt mixes by alleviating the need for virgin crude oil-derived binders as well as allowing for the increase in RAP content. Laboratory performance testing was conducted on

www.manaraa.com

asphalt mixes containing 50% RAP by mix weight and the novel bio-derived binder in an effort to show that unconventional binders can perform as adequately as conventional crude oil-derived binders in high RAP content mixes. The natural softness of the bio-derived binder balances the stiffness of the aged binder content while maintaining sufficient resistance to high temperature rutting. Additionally, the nature of the bio-derived binder may have a rejuvenating effect by chemically interacting with the aged RAP binder. Several performance tests were conducted on laboratory-prepared mix specimens containing the bio-derived binder. The same tests were also conducted on specimens of the same mix design containing a control 50/70 pen virgin crude oil-derived bitumen. Low temperature thermal cracking, intermediate temperature fatigue cracking, rutting, stiffness, and moisture susceptibility were all evaluated using disc-shaped compact tension (DCT) testing, beam fatigue testing, flow number testing, dynamic modulus testing, and indirect tension (IDT) testing, respectively. Results showed that the bio-derived binder outperformed the conventional binder with respect to resistance to thermal cracking and adequately passed all requirements for additional testing to qualify for pavements with 20-year design loadings of less than 30 million ESALs. The overarching conclusion of this research is that asphalt mixes containing 50% RAP and a bio-derived binder can be designed to pass performance criteria at low, intermediate, and high temperatures without the need of additional virgin crude-oil derived bitumen.

2.1. Introduction

The current conditions of infrastructure around the world coupled with limited government funding and rising material and labor costs have increased the drive for finding ways to effectively cut paving costs by incorporating more recycled materials. Depleting sources of quality virgin aggregates and high and fluctuant crude oil prices lead to ever-increasing material costs in paving

www.manaraa.com

that can best be offset by partial or total replacement of conventional virgin materials in asphalt mixes. Additionally, maximizing the use of recycled materials is critical in terms of environmental cost savings related to aggregate quarrying. Reclaimed asphalt pavement (RAP), here being synonymous with RA in EU standards, has been used in asphalt mixes for decades and started becoming popular in the 1970s. Today, RAP is the most recycled material in the U.S. at over 80 million tons being re-used annually in paving, fill, and base material [1, 2]. Likewise, in Europe, more than 40 million tons of RAP is re-used each year [3]. However, RAP as a material is largely underutilized throughout the world by limiting specifications, lacking guidance, and hesitation to put laboratory findings into practice.

Much of the hesitation to allow high RAP contents in asphalt mixes is attributed to the stiffness of the aged binder introduced into the mix. Highly aged binders lose much of their flexibility and ability to dissipate stresses through viscoelastic relaxation making them susceptible to brittle failures such as fatigue cracking and low temperature thermal cracking. The increased stiffness does; however, have the positive influence of increasing the mix's resistance to high temperature shearing deformations like rutting and shoving. A critical balance must be made to increase or restore the ability to relax stress of the asphalt mix incorporating a high RAP content while retaining sufficient stiffness to resist rutting. Such a balance can be achieved through the use of RAP rejuvenation or utilizing a specifically designed binder as was done in this research.

Partial binder replacement by bio-derived materials has been a recent focus of numerous research studies to further increase the sustainability of asphalt pavements and lower paving costs. This research goes a step further by using an asphalt mix incorporating 100% conventional virgin binder replacement by reclaimed binder and a novel sustainable binder derived from refined pine

www.manaraa.com

chemistry stabilized with polymers. In addition to the use of no virgin crude oil-derived binder, the mix tested in this research incorporates 50% RAP by mix weight.

This research, as part of the BioRePavation project, is intended to show that in a post-fossil fuel scenario where crude oil is unavailable, economically unfeasible, or its extraction deemed unsustainable, bio-asphalt mixes manufactured with bio-derived binder and high RAP content can be successfully developed. This study provides evidence that even with no addition of neat bituminous binder, bio-asphalt mixes under investigation pass all applicable specifications for pavements designed with 20-year design loads of less than 30 million ESALs.

2.2. Background

The push for greater degrees of sustainability in asphalt paving have been focused largely on two major categories of research: rejuvenation of recycled materials to successfully incorporate higher percentages of RAP in mixes, and partial crude oil-derived binder replacement by sustainably-produced binders from waste and/or recycled materials. There has been much research and implementation of the prior category, whereas the latter category has been less thoroughly explored. The novel sustainable binder presented in this research presents; however, the possibility for a complete conventional binder replacement along with incorporation of high RAP contents.

Recycled asphalt pavement (RAP) contains aged binder which has undergone chemical changes resulting in altered physical responses to loading. Oxidation, moderate polycondensation, and volatilization of asphalt fractions increases the ratio of larger, or associating, asphaltene molecules to smaller lubricating maltene molecules like saturates, aromatics, and resins [4]. The result of such changes is a much stiffer material with substantially reduced flexibility and elastic responses to stresses. The primary function of a rejuvenator is to rebalance the strong intermolecular associations of the large, often polycondensed, asphaltene molecular binder

www.manaraa.com

fraction [5]. Common rejuvenator types include paraffinic oils, aromatic extracts, naphthenic oils, tall oils, and bio-rejuvenators refined from natural resources such as rapeseed, linseed, and pine oils. Research has shown that properly designed rejuvenation can result in adequate HMA mix designs incorporating up to 100% RAP by aggregate weight [6]. Additionally, rejuvenators have been shown to increase pavement life by up to nine years in mixes containing RAP [4]. Rejuvenation; however, has a key uncertainty pertaining to mix completion of the virgin binder with the aged RAP binder and rejuvenator [6]. Incomplete blending known as "black rock" can lead to moisture damage, rutting, and premature cracking. Additionally, many agencies currently do not include rejuvenators in specifications or are hesitant to allow them due to the wariness that they may increase rutting and moisture damage potential [5,7].

The rejuvenating effect and linear viscoelastic properties of bio-binders manufactured from pine resin and by-products of the paper industry in asphalt mixes with 50% RAP and bio-binders as the only virgin binder has also been investigated [8,9]. The bio-binders showed great potential to rejuvenate RAP and the bio-recycled asphalt mixes had acceptable viscoelastic properties compared to conventional mixes while being composed only of RAP and non-petroleum-based binders.

These studies and more show that industrial and consumer waste products can be valuable resources in flexible pavement materials. Not only can the developed materials increase the sustainability of pavements by increasing the allowable quantity of recycled materials, but they can also allow for the partial or total replacement of crude oil-derived binders. The usage of otherwise waste materials not only offers promise of substantial material savings, but also the real possibility of offering economic incentives to the industries producing the waste materials.

www.manaraa.com

2.3. Materials

Binders, aggregates, and RAP materials were provided by EIFFAGE for this research. Binders used included a virgin 50/70 pen grade (PG 64-22) conventional binder as well as a novel bio-binder referred to as Biophalt® (BF). BF is derived from polymer-modified refined pine sap and does not contain any source of petroleum products other than the polymer [10,11]. The RAP was delivered fractionated in coarse (8/12 mm) and fine (0/8 mm) fractions. Both the RAP and virgin aggregates were oven-dried and split to ensure uniformity of the materials in each mixed batch for preparing test specimens. RAP binder content was determined according to ASTM D 2172 [12] and ASTM D 7906 [13] standards. Each RAP fraction's binder content was determined individually by using toluene to dissolve the aged binder off of the aggregates and then using a series of centrifuges to separate the toluene-binder solution from the aggregates. A rotary evaporator was then used to distill the binder from the toluene. Because this paper focuses on mix performance comparisons, only a brief summary of material properties is included for reference.

Table 2.1 provides a summary of binder grades as determined using all applicable ASTM and AASHTO testing standards and following the Superpave methodology of binder grading using the performance grading (PG) system.

Table 2.1: Binder PG Grade Summary

Binder	PG Grade	Penetration (x0.1mm)	Softening point (°C)	Fraass breaking point (°C)
Control	PG 64-22	55.0	49.0	-7
BF	N/A*	146.5	73.5	-15
RAP	PG 94-4	6.5	81.0	+14
Control + RAP	PG 76-16	25.0	61.8	+1
BF + RAP	PG 58-22	80.0	68.8	-7

www.manaraa.com

The BF binder was unable to be tested using the DSR due to the sticky nature of the virgin binder. However, the conventional characterization shows that it is a soft binder and the blended grade with RAP is significantly lower than the control, so it is reasonable to assume that the virgin BF binder has a grade softer than PG 58-xx. By comparing the unblended and blender binder grades and conventional properties shown in Table 2.1, one can conclude that the BF binder lends itself well to use in mix designs containing high RAP contents.

2.4. Mix Design

To directly compare the effectiveness of the novel bio-binder, BF, with the control binder, mix designs for all performance testing were controlled to consist of the same binder contents and aggregates. Mixes for both binders contained 50% RAP by aggregate weight, 2.7% virgin binder by mix weight, and 1.7% recycled binder by mix weight.

Table 2.2 summarizes the aggregate gradations for virgin aggregate, blended RAP fractionations, and the final design aggregate blend used in all performance test mixes. The blend gradation is designed based on aggregate packing volumetric concepts to optimize interlock and densities. Minimum and maximum requirements are as suggested by the Superpave mix design methodology. It should be noted that these gradations were used for laboratory-prepared mixes and a slightly different gradation curve was used for large-scale field testing. However, the focus of this study is on the comparison of the binders, so only the consistency of the gradations among mix sub-groupings is of importance for validation of subsequent comparative results.

www.manaraa.com

Table 2.2: Aggregate Gradations

Sieve Size		Percent Passing			Requirements	
U.S. Customary	mm	Virgin	RAP	Blend	Min	Max
1”	25	100	100	100.0	100	
3/4”	19	98.9	99.9	99.4	90	100
1/2”	12.5	66.9	92.4	80.0		90
3/8”	9.5	29.6	60.6	45.5		
#4	4.75	23.5	29.9	26.8		
#8	2.36	22.6	24.7	23.7	23	49
#16	1.18	17.1	7.6	12.2		
#30	0.60	12.9	3.6	8.1		
#50	0.30	10.0	1.3	5.5		
#100	0.15	8.1	0.4	4.1		
#200	0.075	6.6	0.1	3.2	2	8

The nominal maximum aggregate size (NMAS) of the design blend is 19.0 mm which increases surface friction and mandates a minimum pavement lift thickness of 76 mm (3 inches) [14].

All specimens prepared for performance testing were mixed in small batches in the laboratory, short-term oven aged, and subsequently compacted using a gyratory compactor. The volumetric properties of mixes using each binder were tested against Superpave requirements for 20-year design ESAL ratings in excess of 10 million but less than 30 million [14]. Table 2.3 provides a summary of all tested and calculated volumetric properties of primary importance for each mix. AASHTO T 331 testing standards [15] using the CoreLok method were used to determine mix bulk specific gravities (G_{mb}), while maximum theoretical specific gravities (G_{mm}) of mixes were determined according to the AASHTO T 209 specification [16].

www.manaraa.com

Table 2.3: Mixture Volumetrics

Property	Control	BF	Requirement
P_b	4.49	4.49	-
P_b (virgin)	2.8	2.8	-
P_b (RAP)	1.69	1.69	-
VMA	13.2	14.2	>13.0
VFA	69.5	71.6	65-78
DP	0.7	0.6	0.6-1.2
P_{ba}	0.8	0.4	-
P_{be}	3.7	4.1	-
G_{mm}	2.63	2.60	-
G_{mb}	2.52	2.50	-
$\%V_a$	4.0	4.0	4
G_b	1.047	1.035	-
G_{se}	2.831	2.799	-
G_{sb}	2.778	2.778	-

As is shown in Table 2.3, both mix designs meet all applicable Superpave mixture volumetric requirements for pavements with 20-year design loads in excess of 10 million but less than 30 million ESALs. Slight variations in mix volumetrics consisting of the same relative gradations and binder contents is most likely attributable to the variation of the binder absorption into aggregate surface voids and binder specific gravity. Using the standard ESAL equations and associated factors attributable to an urban arterial or highway, a 20-year design load of 30 million ESALs equates to approximately 27,500-32,500 vehicles/day whereas a 10 million ESAL design load equates to approximately 7,500-12,500 vehicles/day as an idea for associative traffic levels being discussed.

2.5. Performance Testing

Several types of testing were carried out on laboratory-mixed and compacted specimens to assess the performance of the novel bio-binder in comparison to a standard crude oil-derived binder. Because asphalt mixes contain viscoelastic materials, it is important to test mixture

www.manaraa.com

performance at a variety of temperatures and loading conditions to ensure the pavement can withstand a wide variation of environmental and traffic loading conditions in the field. Disc-shaped compact tension (DCT) testing was chosen to assess the asphalt mixes' resistance to low temperature thermal cracking while beam fatigue testing was selected to assess their resistance to intermediate temperature fatigue cracking. To predict high temperature rutting resistance, flow number testing was used. Additionally, dynamic modulus testing was used to construct master curves and indirect tension testing was used to assess moisture susceptibility.

2.5.1. Testing procedures

This section outlines the procedures used to carry out laboratory testing on the materials under consideration. All applicable ASTM and AASHTO standards followed are referenced in addition to laboratory and research-specific testing conditions and material preparations.

2.5.1.1. Disc-shaped compact tension (DCT)

Low-temperature thermal cracking is a distress initiated by environmental loading effects. In geographic areas where daily and annual thermal fluctuations can be extreme, thermal cracking in pavements can significantly increase the required maintenance of the pavement and/or shorten the lifespan of the pavement. As temperatures decrease, pavements shrink dimensionally generating significant tensile stresses within the system. At very low temperatures, tensile stresses can exceed the tensile strength of the pavement resulting in cracking [17]. Thermal cracking is typically transverse to travel direction and is top-down in nature due to the more rapid surface cooling, geothermal heating and thus thermal gradation that exists within a pavement cross-section in cold weather [2]. Cyclic thermal fluctuations exacerbate micro-fractures and cold weather loading further deteriorate the distress due to the brittleness of binders at low temperatures. While

www.manaraa.com

thermal cracking is typically not associated with traffic loading, the presence of transverse thermal cracks in short intervals allows for moisture penetration into the subgrade and general discontinuity of the pavement system to effectively distribute loading.

Disc-shaped compact tension (DCT) testing was performed in accordance with ASTM D 7313 procedural standards to assess the low temperature tensile strength of the mixes [18]. Three specimens were prepared for each test subset as outlined in Table 2.4.

Table 2.4: DCT Testing Subset Parameters

Binder	% Air Voids	Test Temperature (°C)
Control	4	-6
	7	-6
	7	-12
BF	4	-12
	7	-12

Specimens at both four and seven percent air voids were tested to replicate air voids at the end of the design life (4%) and immediately post-construction (7%). Control mixes were tested at both -6 and -12°C because the binder low performance grade of the control mix (-16°C) varied from that of the BF mix (-22°C). ASTM standards suggest DCT testing to be performed at 10°C greater than the low grade of the binder; however, the control mix was also tested at -12°C as a direct comparison to the BF mix under the same conditions.

Each specimen was laboratory-mixed and compacted using a Superpave gyratory compactor. Compacted specimens were then cored using a water-cooled drill press and cut using water-cooled saws. Prepared specimens were of the dimensions and configuration shown in Figure 2.1 as provided in ASTM D 7313 [18].

www.manaraa.com

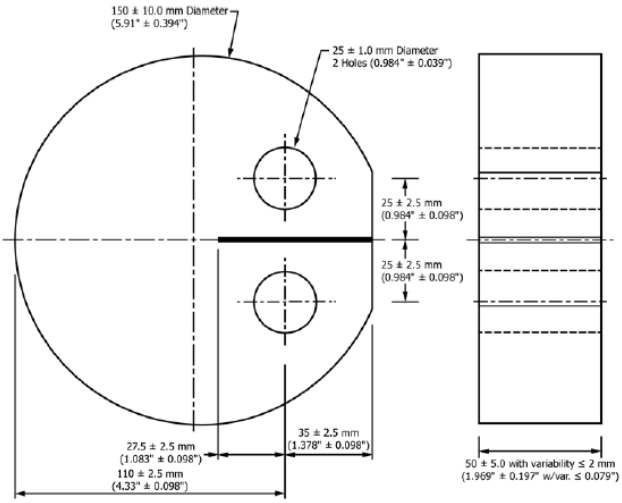

Figure 2.1: ASTM Standard DCT Specimen Dimensions (ASTM D 7313)

Prepared specimens were allowed to dry at room temperature for a minimum of 24 hours and fitted with metal gauge points. Air-dried specimens were then conditioned at the test temperature in an environmentally-controlled unit for 8 to 16 hours prior to testing in an environmentally-controlled testing apparatus. A crack mouth opening displacement (CMOD) gauge was clipped into the metal gauge points and the specimen was loaded to failure at a controlled CMOD rate of 0.0017 mm/sec. The failure criteria was the point at which tensile load resistance was reduced to less than 0.1 kN.

Data collected included CMOD versus loading. The data plotted to specimen failure was then used to calculate the fracture energy (G_f) of each specimen using Equation 2.1 and normalized to individual specimen dimensions.

$$G_f = \frac{A_f}{l*t} \qquad \text{[Eq.2.1]}$$

where:

A_f = Area under the load vs. CMOD plot (J),

l = Length of the fractured face (m), and

t = Specimen thickness (m).

www.manaraa.com

2.5.1.2. Beam fatigue

Beam fatigue results are useful in predicting the fatigue behavior of HMA mixes. Fatigue cracking is attributed to high loading repetitions at temperatures intermediate relative to the environment the pavements are placed and is thus linked to the effective binder grade of the mix. Effective binder grade in this instance refers to the blended binder grades of both virgin binder and RAP binder in the respective mixes. The significance of predicting fatigue behavior at intermediate temperatures is that these conditions dictate the working conditions the pavement will be subjected to through much of its life. Fatigue cracking begins as top-down or bottom-up micro fractures that develop through repeated strain cycling as flexible pavements deflect and recover through loading-unloading cycles. As cracking evolves, it isolates sections of the pavement from the system which accelerates pavement deterioration and results in the familiar alligator skin-like pattern of interconnected fractures.

Beam fatigue testing was completed in accordance with AASHTO T 321 procedural standards [19]. For each binder, six beams were made with the following nominal dimensions: 380 mm in length x 63 mm in width x 50 mm in thickness. Sets of six beams were cut from two slabs (three beams per slab) made at seven percent air voids and compacted using a linear kneading slab compactor. Slabs were oversized in width to ensure each beam consisted of two saw-cut edges. Prepared beams were then normalized in an environmentally-controlled chamber with the testing device at a temperature of 20°C. Specimens were then loaded individually into a four-point flexural bending apparatus and axially haversine loaded at a frequency of 10 Hz. Figure 2.2 shows a sample beam in the testing device used as a reference.

www.manaraa.com

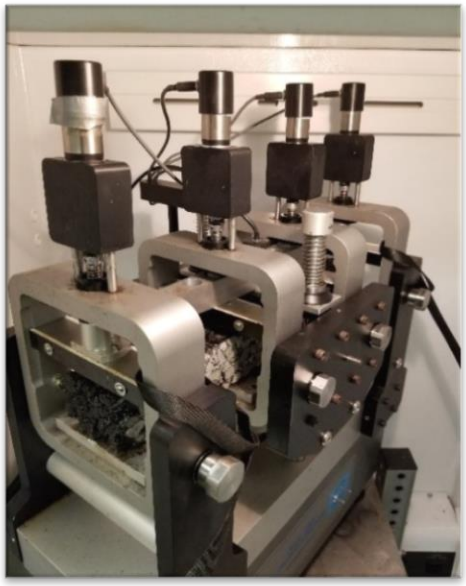

Figure 2.2: Beam Fatigue Testing Apparatus

Tests were run in strain control mode on each individual beam, with the group of six beams for each binder/mix combination generating one data set for analysis covering varying strain amplitude levels. Strain control mode loading is more relevant to performance of thin pavement layers less than 130 mm (5-inches) in thickness since the mechanical response is driven by the soil stiffness in this case [2]. The six strain amplitude levels chosen ranged from 1200 to 300 micro-strain. Data collected for analysis were the strain level and cycles to failure which is described by AASHTO T 321 as the maximum value of the product of measured flexural stiffness and number of load cycles during testing [19]. The failure criteria was 50% of the initial flexural stiffness determined at the 50th load cycle. Fifty load cycles ensured the beams were appropriately seated and thus the initial flexural stiffness is representative. Strain and load cycles to failure can be plotted on a log-log plot to determine best-fit flexural coefficients K1 and K2 described using the power law relationship shown in Equation 2.2.

$$N_f = K1\left(1/\epsilon_0\right)^{K2} \qquad \text{[Eq. 2.2]}$$

www.manaraa.com

where:

N_f = number of load cycles to failure,

ε_0 = flexural strain amplitude in micro-strain, and

K1, K2 = regression constants.

2.5.1.3. Flow number

The most common type of high temperature distress in flexible pavements is rutting. Rutting can occur as a result of a weak subgrade or shear deformation of the asphalt mix itself under loading. The latter mode is in part the focus of this research. Although the incorporation of RAP with its stiff, aged binder typically increases a pavement's resistance to rutting, the influence of a non-conventional binder on rutting resistance is of interest. A mix's susceptibility to rutting is dependent on both aggregate characteristics (i.e. angularity, gradation, etc.) and the binder's properties including shear modulus. Because the same aggregate sources were used for both mixes in this study, any variation in rutting resistance can be attributed to binder effects.

Flow number testing was performed on four specimens per mix in accordance with AASHTO T 378 [20]. Test specimens were previously used to conduct non-destructive dynamic modulus testing. Testing was completed using a UTM 25 asphalt mixture performance tester (AMPT) at a controlled temperature of 54°C under unconfined conditions. Each specimen was compacted to 7% air voids using a Superpave Gyratory Compactor to the specified nominal dimensions of 100-mm in diameter by 150-mm in height. An air void content of 7% is representative of the upper threshold of many conventional mixes post-construction. Samples were subjected to a 600 kN haversine axial compression load at a frequency of 1 Hz. Each load cycle consisted of a 0.1 s load pulse followed by a 0.9 s rest period. Tests were ended once the specimen reached 5% permanent axial strain or 10,000 load cycles, whichever occurred first. Reported

www.manaraa.com

results included the flow number of each specimen which is defined as the load cycle corresponding to the minimum permanent strain rate per cycle. The flow number (FN) is usually considered to be the onset of tertiary flow, or creep within the specimen and is a measurement of matrix shearing under repetitive loading cycles.

During flow number testing, an asphalt specimen can undergo three phases of deformation: primary, secondary, and tertiary. Primary deformation is the initial consolidation of voids and other preliminary densification phenomena. Secondary deformation is the viscoelastic response consisting of deformation-relaxation cycles. Tertiary deformation is a plastic, or creep response of the specimen indicating shear failure. Figure 2.3 shows a plot of accumulated permanent strain and strain rate per cycle vs. load cycles and the three phases of deformation. The results shown in Figure 2.3 are an illustrative example.

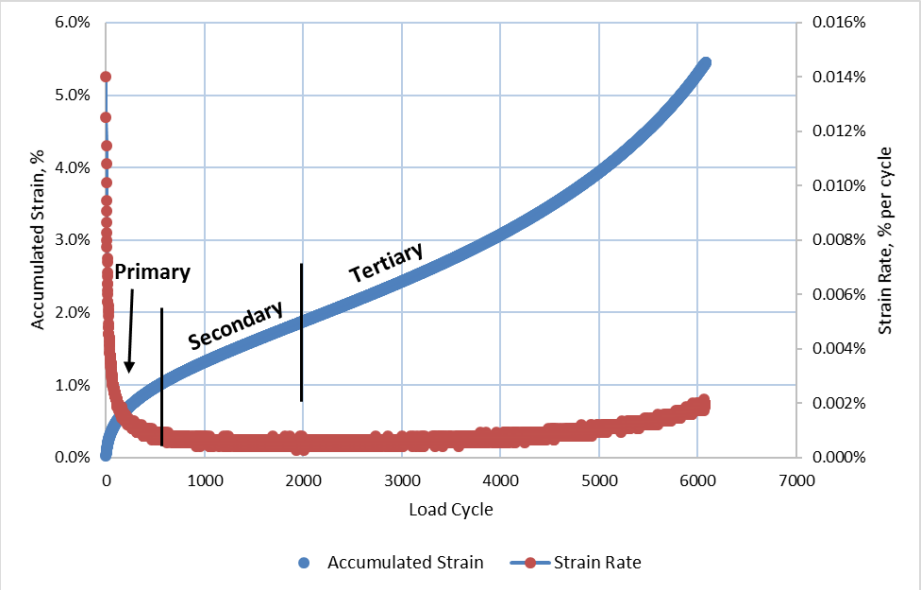

Figure 2.3: Example of Deformation Under Loading

www.manaraa.com

2.5.1.4. Dynamic modulus

Dynamic modulus testing was used in accordance with AASHTO TP 79 specifications to determine the stress-strain behavior of the mixes over a wide range of temperatures and frequencies in the linear viscoelastic domain [21]. Recorded dynamic modulus values (E*) over the range of temperatures and frequencies were used to construct sigmoidal master curves. Master curves show how the mix's stiffness varies with loading rates. At low temperatures and high frequencies, pavements are more susceptible to brittle cracking failures. At high temperatures and low frequencies, pavements are more susceptible to viscous shear failures like rutting. At intermediate temperatures and frequencies, pavements are most susceptible to fatigue cracking where a moderate stiffness balancing deformation-resistance and elasticity to prevent brittle failure is desired. Master curves can therefore help predict pavement distressing problems over a wide range of scenarios.

Each test subset consisted of four specimens except for five control mix specimens tested at 7% air voids. There were four subsets: each mix compacted to 4% and 7% air voids. Each specimen was compacted to nominal dimensions of 100 mm in diameter and 150 mm in height using a Superpave gyratory compactor. Specimens were then subjected to sinusoidal axial loading to a reference stress using a universal testing machine (UTM) in a temperature-regulated chamber. Specimen axial strains were measured using linear variable differential transformers (LVDTs). Three temperatures (4, 21, and 37°C) and eight frequencies (25, 10, 5, 2, 1, 0.5, 0.2, and 0.1 Hz) were used to construct subsequent master curves for each data subset.

Master curves were plotted using frequencies shifted to an intermediate reference temperature of 21°C and plotted on a log-log scale to form sigmoidal curves. Curves were fitted using both the shifted data from the dynamic modulus testing as well as predicted curves for

www.manaraa.com

extrapolation of trends at frequencies beyond those tested. Predicted curves are best-fit sigmoidal functions that minimize standard error between actual and predicted stiffness values through the reduced frequency sections for which data is available. The sigmoidal function used can be seen in Equation 2.3.

$$Log|E^*| = a + \frac{b}{1+e^{\beta+\gamma(logf_R)}} \quad \text{[Eq. 2.3]}$$

where:

f_R = reduced frequency at reference temperature in Hz,

a = minimum value of E* in MPa,

a + b = maximum value of E* in MPa, and

β, γ = fitting coefficients.

2.5.1.5. Moisture susceptibility

Moisture damage is a common problem for pavements, especially those in areas where seasonal freeze-thaw cycles are prevalent. Due to aggregates' higher affinity for water than binder, water is able to diffuse through thin aggregate coatings and break the bonds between aggregates and binder. This type of damage is adhesive damage; however, cohesive damage is also possible as water molecules diffuse into the binder and soften it. Compounding moisture damage is the opening of surface shrinkage microcracks due to differential surface binder aging, pore pressures generated within air voids upon loading cycles, and hydrostatic pressures within saturated air voids from volumetric expansion as water freezes. While there is no consensus agreement among agencies and researchers about how RAP use in asphalt mixtures influences moisture resistance, some claim that high RAP contents generally improve a mix's moisture resistance [5]. Moisture resistance improvement is attributable to the pre-coating of hardened binder on aggregates that do not fully diffuse with the added virgin binder. A resulting thicker coating of binder of high

www.manaraa.com

viscosity should reduce the amount of adhesive (stripping) damage that occurs within the mix as moisture cannot diffuse across the thicker aggregate-binder interface [2].

Moisture damage susceptibility of both mixes were assessed in accordance with AASHTO T 283 standards [22]. This method subjects one set of specimens to a freeze-thaw cycle (wet) while one set remains unsaturated (dry). Specimens were lab-mixed and compacted to dimensions of 100 mm in diameter by 60 mm in height using a gyratory compactor. Each specimen was compacted around a target air void (AV) content of 7% to assess early-life moisture resistance. Once conditioned, specimens were loaded to failure in indirect tension at a displacement rate of 50 mm/min. Failure was deemed to be the point at which the specimen fractured, and load resistance fell below the recorded peak load. Peak loads were converted to peak strengths (kPa) by using specimen nominal dimensions. Using wet and dry peak strengths of specimens of comparable air void contents, the tensile stress ratio (TSR) can be evaluated using Equation 2.4 and is an indicator of moisture damage susceptibility.

$$TSR = \frac{S_1}{S_2} \qquad \text{[Eq. 2.4]}$$

where:

S_1 = peak strength of the wet conditioned specimen in kPa, and

S_2 = peak strength of the dry unconditioned specimen in kPa.

2.5.2. Testing results

This section provides the results gained from used the testing procedures outlined in subsection 2.5.1. Performance results are summarized graphically and in tables and are accompanied by appropriate statistical analyses.

www.manaraa.com

2.5.2.1. Disc-shaped compact tension (DCT)

The DCT test results for each mixture parameters tested are summarized in Table 2.5.

Table 2.5: DCT Results Summary

Binder	Air Voids (%)	Test Temp. (°C)	Average G_f (J/m^2)	CV, G_f (%)	Average Peak Load (kN)
Control	4	-6	624	22.7%	3.77
BF	4	-12	599	23.6%	3.55
Control	7	-6	717	8.2%	3.73
Control	7	-12	383	9.8%	3.25
BF	7	-12	581	18.0%	4.11

Table 2.5 shows the variation in average fracture energies, peak loads, and fracture energy coefficient of variation (CV). The CV is a statistical measure of data point dispersion where lower CVs indicate less scatter. To put the fracture energies presented in Table 2.5 into context, a comprehensive study has shown that G_f values greater than 400 J/m^2 indicate low potential of widespread thermal cracking within pavements [23]. Only the control mix tested at -12°C and 7% air voids resulted in an average fracture energy below the 400 J/m^2 value. Peak load values are presented but not statistically compared due to the large standard deviations observed and relative closeness of values among mixes. Statistical comparisons among the mean fracture energies between mixes at comparable conditions are summarized in Table 2.6.

Table 2.6: Statistical Comparison Summary Between Mixes

Binder	Air Voids (%)	Test Temp. (°C)	Average G_f (J/m^2)	P-value (ANOVA)	95% C.I. for $\mu_{Control}-\mu_{BF}$
Control	4	-6	624	0.8349	(-295, 346)
BF	4	-12	599		
Control	7	-6	717	0.1192	(-55, 329)
BF	7	-12	581		
Control	7	-12	383	0.0365	(-376, -20)
BF	7	-12	581		

www.manaraa.com

Table 2.6 shows comparative statistics among binder subsets' average fracture energies. One-way analysis of variance (ANOVA) p-values were calculated for differences among compared means with lower values indicating higher probability of difference. The only statistically significant differences in means occurs at 7% air voids. The control mix tested at -6°C shows a somewhat significantly greater mean measured fracture energy than the BF mix tested at -12°C. When both mixes were tested at -12°C, the BF mix shows a strongly statistically significant difference between mean measured fracture energies, with the BF mix being the greater of the two. In addition to ANOVA p-values, 95% confidence intervals (C.I.) for mean differences are shown.

The second and third set of comparisons are important because it shows variation between binder performance when the mixes are tested at the same temperature and at temperatures 10°C greater than their respective low binder grade. When tested 10°C above their respective low binder grade, results show that the control mix will provide mean fracture energy values greater than those of the BF mix at roughly 88% confidence. When tested at the same temperature (-12°C), the BF mix will provide mean fracture energy values greater than those of the control mix at over 95% confidence.

In addition to comparisons between the mixes, comparisons were also analyzed within each mix. These investigations show mean fracture energy variations within mixes at varying air voids and test temperatures. Table 2.7 provides a summary of within mix statistical analyses.

Table 2.7: Statistical Comparison Summary Within Mixes

Binder	Air Voids (%)	Test Temp. (°C)	Average G_f (J/m^2)	P-value (ANOVA)	95% C.I.
Control	4	-6	624	0.3525	$\mu_{CI4\%}-\mu_{CI7\%}$ (-339, 153)
Control	7	-6	717		
Control	7	-6	717	0.0011	$\mu_{CI-6}-\mu_{CI-12}$ (223, 446)
Control	7	-12	383		
BF	4	-12	599	0.8676	$\mu_{BF4\%}-\mu_{BF7\%}$ (-263, 299)
BF	7	-12	581		

www.manaraa.com

Table 2.7 shows that the only statistically significant difference in mean fracture energies within mixes occurs between the control mix when tested at -6°C and -12°C. However, by looking at the differences between mixes tested at 4% and 7% air voids, one can see that there is a greater likelihood of the control mix mean fracture energy decreasing as voids decrease during compaction through field loading. The BF mix; however, slightly increases in mean fracture energy with densification indicating sustenance of its resistance to thermal cracking throughout the pavement's life.

2.5.2.2. Beam fatigue

A power law relationship was used to determine K1 and K2 values for each binder. Figure 2.4 shows the log-log plot used to determine the best-fit regression constants for each binder.

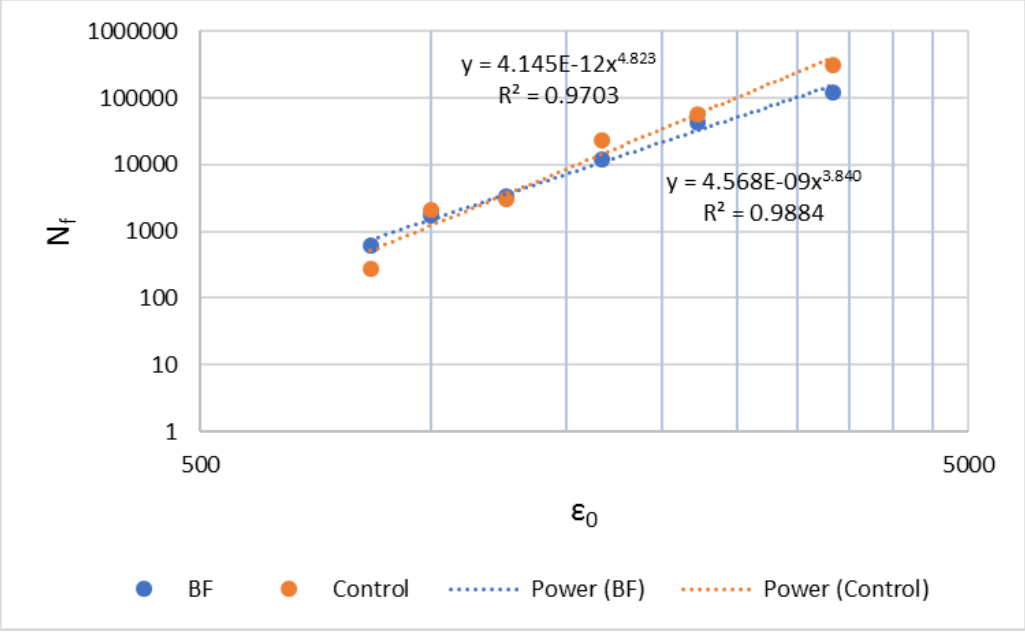

Figure 2.4: Fatigue Coefficient Determination

Results of Figure 2.4 are summarized in Table 2.8 for the important values under consideration.

www.manaraa.com

Table 2.8. Fatigue Coefficients

Binder	K1	K2	R^2
Control	4.145E-12	4.823	0.9703
BF	4.568E-09	3.840	0.9884

As seen in Table 2.8, testing of both binders result in very small K1 values and high coefficient of determination values (R^2) close to unity signifying that the best-fit models account for 97.0% and 98.8% of the variance in predicted load cycles to failure for control and BF binders, respectively. The K2 fatigue exponent is indicative of damage rate accumulation within a beam specimen [24]. Due to the exponential nature, lower K2 values show a quicker rate of damage accumulation. Recommended values of K2 are based on laboratory prepared specimens and include 4.32 by the Transport and Road Research Laboratory to 4.76 by the Belgian Road Research Center [15]. A K2 range of 3.5 to 4.5 was recommended to the Illinois Department of Transportation by Carpenter [25]. It therefore stands that acceptable K2 values lie in a range of about 3.5 to 4.76 with more agencies recommending a K2 value of 4.0 or greater. Both binders tested provide reasonable K2 values ranging from 3.8 to 4.8 with the BF mix showing potential for a slightly faster rate of fatigue damage accumulation than the control.

Beam fatigue test results were also used to generate fatigue curves for the two binders considered. Figure 2.5 shows both curves on the same log-log plot for ease of comparison.

www.manaraa.com

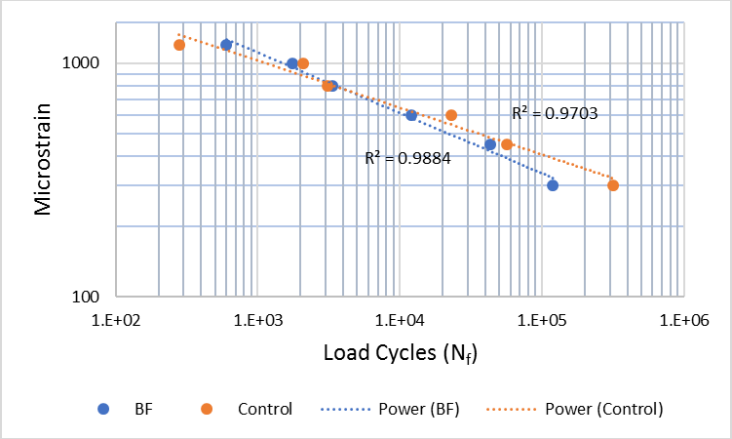

Figure 2.5: Fatigue Curves

Figure 2.5 shows that both binders have very similar fatigue curves with the BF mix having the slightly steeper slope due to the lower K2 value. The fatigue curve similarity indicates that both binders offer similar fatigue cracking resistance in the mixes tested. While each dataset of six beams was not repeated for statistical analysis in this study, the R^2 value of near unity for each dataset shows a desired log-log linearity and sufficient fatigue coefficient precision using a best-fit power trendline.

Figure 2.6 shows typical mix stiffness dissipation with progressive loading cycles at flexural strain amplitudes of 600 and 1000 micro-strain. These curves allow one to further assess the slightly lower K2 value determined for the BF mix and therefore more rapid rate of damage accumulation.

www.manaraa.com

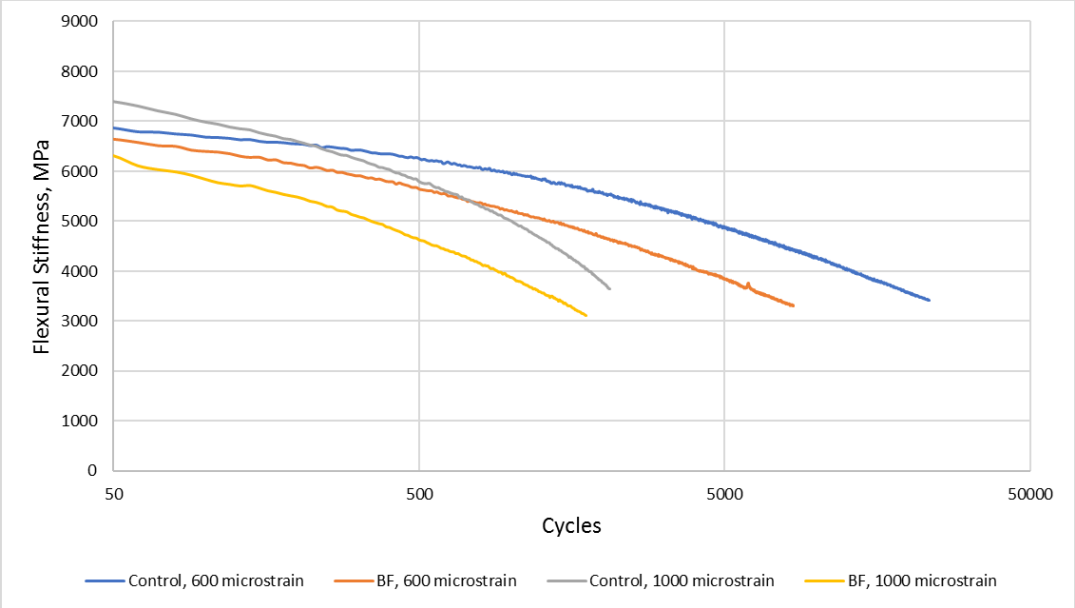

Figure 2.6: Flexural Stiffness Dissipation with Load Cycle Accumulation

Figure 2.6 clearly shows that the BF mix exhibits a more rapid rate of flexural stiffness dissipation with load cycles as compared to comparable control mixes. This observation is in agreement with the K2 evaluation predicting a more rapid rate of damage accumulation for the BF mixes. These phenomena are likely explained by the more viscous response under load at intermediate temperatures by the BF mix. More viscous behavior within a mix under repeated load cycles will generate internal heating that will further lower the flexural stiffness and account for a more rapid rate of damage accumulation and flexural stiffness dissipation.

2.5.2.3. Flow number

Flow number test results and accompanying statistical summaries for each mix are provided in Table 2.9. In addition to the average FN for each mix, FN coefficient of variances (CV) are shown as a measure of data dispersion.

www.manaraa.com

Table 2.9: Statistical Comparison Summary

Binder	Average FN	CV, FN (%)	P-value (ANOVA)	95% C.I. for $\mu_{Control}-\mu_{BF}$
Control	863	6.2%	0.0050	(123, 447)
BF	578	20.9%		

As seen in Table 2.9, the control mix specimens had a greater average FN than the BF mix as well as a much lower CV meaning that control mix specimen measured FNs exhibited about one-third less data dispersion than the BF mix specimens. A one-way analysis of variance (ANOVA) was used to test the difference in mean FNs between the mixes. As shown, the comparison results in a p-value of 0.0050 indicating that the control mix mean FN is statistically significantly greater than that of the BF mix. A 95% confidence interval (C.I.) for the mean difference is shown to be between 123 and 447 load cycles.

The difference in mean flow numbers as well as the large variances observed for the BF mix specimens is most likely attributable to the difference in respective binder high temperature grades (see Table 2.1). A significantly softer BF binder + RAP binder at high temperatures relative to the control binder + RAP binder is expected to result in the observations found here. Additionally, the softness of the BF binder and the relatively high air void content of 7% may have also led to some additional lowering of the flow number. However, from a purely comparative standpoint of these two binders, the trends observed here are only meant to show that under the same conditions, the BF mix has slightly less resistance to rutting than the control mix as it pertains to flow number testing.

While the control mix had greater mean FN values, and subsequently greater resistance to rutting by shear deformation than the BF mix, it is important to analyze the mean FNs in terms of acceptable design ESALs each mix is suitable for. Table 2.10 shows recommended minimum FN

www.manaraa.com

values for varying degrees of design ESAL ratings [26]. These recommendations are compared with 95% C.I.s for each mix's mean FN.

Table 2.10: NCHRP Recommended FN Values (NCHRP Report 673, Table 8-20)

ESALs (Millions)	Minimum FN	Control 95% C.I. μ_{FN}	BF 95% C.I. μ_{FN}
<3	-	(779, 948)	(386, 771)
3 to <10	53		
10 to <30	190		
≥30	740		

As seen in Table 2.10, the control mix provides acceptable rutting resistance based on flow number testing to qualify for design traffic loadings in excess of 30 million ESALs with 95% confidence based on these results. The BF mix is shown to qualify for design traffic loadings up to but not exceeding 30 million ESALs with 95% confidence based on these results.

2.5.2.4. Dynamic modulus

Dynamic modulus (E*) values and master curves are compared both between and within mixes at 4% and 7% air voids. The dynamic modulus of a mix is the absolute value of the complex modulus and includes both the elastic stiffness and internal damping component generated by the viscoelastic binder [17]. Master curves for both mixes compacted at 4% air voids shifted at a standard intermediate reference temperature of 21°C are shown in Figure 2.7 which reflects expected mix response after post-construction consolidation without considering binder aging effects. Also shown in Figure 2.7 are mix phase angles over the reduced frequencies tested. Phase angles are an indication of viscous or elastic behavioral response to loading with lower phase angles indicating more elastic (stress relaxation) responses and greater phase angles indicating more viscous (plastic deformation) behavior.

www.manaraa.com

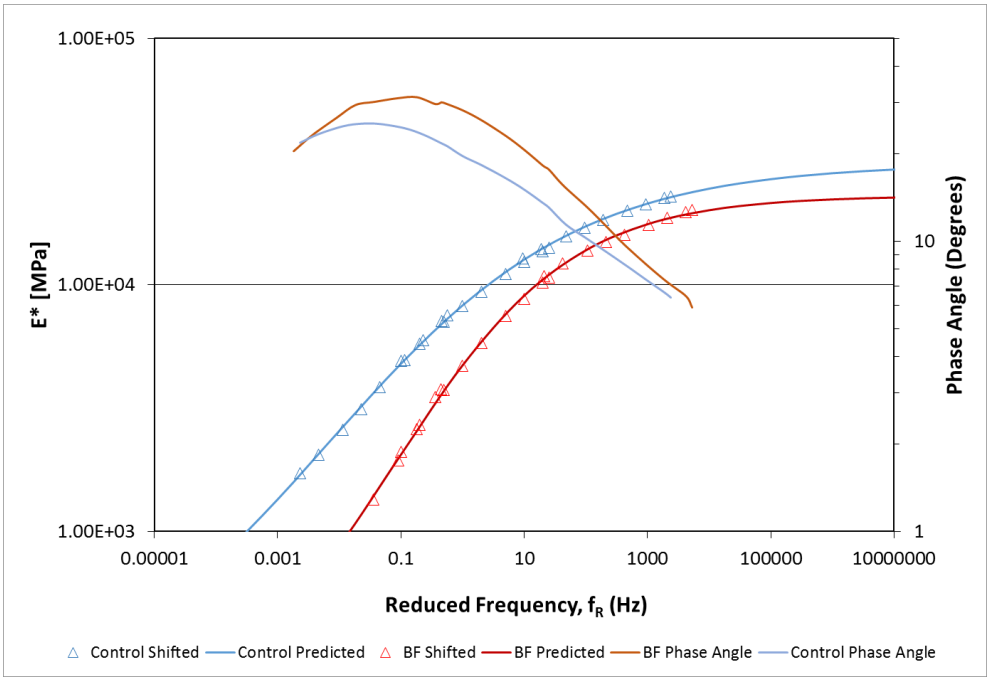

Figure 2.7: DM Master Curves at 4% Air Voids

Figure 2.7 shows that the control mix displays greater stiffnesses than the BF mix over all frequencies at 4% air voids. The greater gap at low frequencies indicates that the control mix may provide greater rutting resistance at high temperatures where low loading frequencies are critical. The control mix's greater stiffness at high frequencies indicates that the control mix may be more prone to thermal cracking distress due to the more brittle behavior associated with high stiffnesses at low temperatures [2]. Select frequencies and temperatures were selected for statistical comparisons between the two mixes. Results are shown in Table 2.11.

Table 2.1: Summary Statistics Between Binders at 4% Air Voids

Binder	Temp. (°C)	Freq. (Hz)	Avg. E* (MPa)	CV, E*	P-value (ANOVA)	95% C.I. for $\mu_{Control}$-μ_{BF} (MPa)
Control	4	10	21291	8.9%	0.0470	(48, 5165)
BF			18684	4.7%		
Control	21	1	8208	15.1%	0.0025	(1776, 5219)
BF			4710	14.1%		
Control	37	0.1	1753	9.1%	<0.0001	(1013, 1410)
BF			541	5.1%		

www.manaraa.com

As shown in Table 2.11, the control mix exhibits statistically significantly greater stiffnesses at low temperature and high frequency, intermediate temperatures and frequency, and high temperature and low frequency. These results substantiate the findings of the master curves to be statistically significant at 95% confidence. Differences of means were evaluated using one-way analysis of variance (ANOVA) and includes coefficient of variations for tested means as a measure of data spread as well as 95% confidence intervals (C.I.) for the difference between mean dynamic modulus values of the control and BF mixes.

Master curves for both mixes compacted at 7% air voids and shifted to a standard reference temperature of 21°C are shown in Figure 2.8. These master curves reflect how the mixes are expected to perform in the early stages of the pavement's life as no long-term aging of the mix was done. Figure 2.8 also includes phase angle master curves of both mixes at 7% air void to assess the degree of viscous response under load through a range of reduced frequencies.

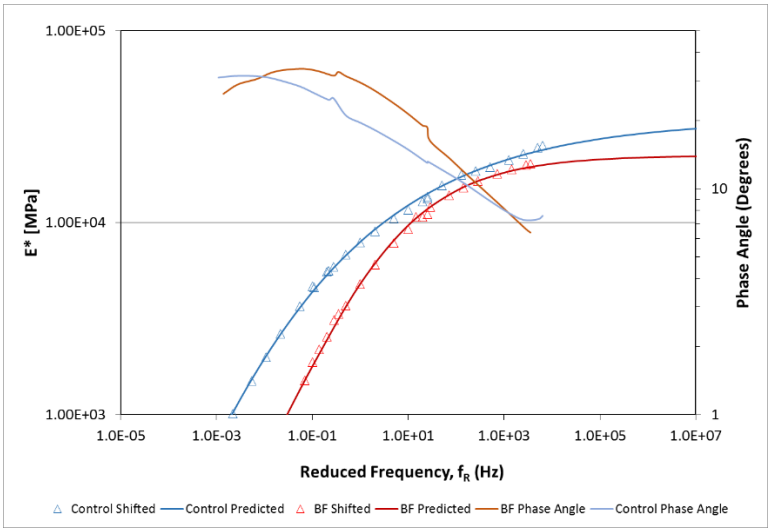

Figure 2.8: DM Master Curves at 7% Air Voids

As seen in Figure 2.8, the control mix has greater estimated dynamic modulus values at frequencies of about 5E-05 and greater. At 7% air voids, the master curves show expectations of

www.manaraa.com

the control mix showing superior resistance to rutting at high temperatures (low frequencies) until the BF mix shows the superior rutting resistance at very high temperatures likely a result of the polymer modification (very low frequencies) although this observation contradicts the general trends at 7% air voids through flow number testing and analysis as was previously discussed. At low temperatures, the BF mix again graphically shows a greater resistance to brittle low temperature cracking (high frequencies). Table 2.12 shows statistical comparisons between mixes at critical temperature and frequency selections.

Table 2.2: Summary Statistics Between Binders at 7% Air Voids

Binder	Temp. (°C)	Freq. (Hz)	Avg. E* (MPa)	CV, E*	P-value (ANOVA)	95% C.I. for $\mu_{Control}$-μ_{BF} (MPa)
Control	4	10	22792	6.8%	0.0096	(1257, 6346)
BF			18991	8.9%		
Control	21	1	7910	4.7%	<0.0001	(2258, 3962)
BF			4799	14.6%		
Control	37	0.1	724	11.3%	<0.0001	(319, 544)
BF			292	17.8%		

As seen in Table 2.12, the control mix again portrays statistically significantly greater dynamic modulus values at all compared temperatures and frequencies. These results validate the trends shown in the master curves of Figure 2.8 as statistically significant differences among the binders at 7% air voids.

A comparison of mix stiffnesses within mixes at varying air void contents was also desired to assess if mixes undergo significant dynamic modulus variations during loading. These changes are not completely associated with changes over the life of the pavements as binder aging conditions were not varied with air void contents. Results of the within mix comparisons are summarized in Table 2.13.

www.manaraa.com

Table 2.3: Statistical Summary Within Binders

Binder	AV, %	Temp. (°C)	Freq. (Hz)	Avg. E* (MPa)	CV, E*	P-value (ANOVA)	95% C.I. for $\mu_{4\%}$-$\mu_{7\%}$ (MPa)
Control	4%	4	10	21291	8.9%	0.2302	(-4203, 1201)
	7%			22792	6.8%		
	4%	21	1	8208	15.1%	0.6214	(-1066, 1662)
	7%			7910	4.7%		
	4%	37	0.1	1753	9.1%	<0.0001	(836, 1222)
	7%			724	11.3%		
BF	4%	4	10	18684	4.7%	0.7581	(-2631, 2017)
	7%			18991	8.9%		
	4%	21	1	4710	14.1%	0.8596	(-1268, 1090)
	7%			4799	14.6%		
	4%	37	0.1	541	5.1%	0.0002	(175, 323)
	7%			292	17.8%		

Table 2.13 shows that both mixes showed statistically significant increases in mean E* values at only high temperature (37°C) and low frequency (0.1 Hz) when the mix was compacted at 7% air voids and 4% air voids to understand the effect of post-construction consolidation. These results show that brittle cracking susceptibility should not vary significantly for either mix during densification; however, resistance to rutting increases during pavement densification as would be expected. The similarity in trends shows that the BF mix behaves similar to the control mix with regard to dynamic modulus changes due to the anticipated densification over the life of the pavement.

Because HMA mixes are composed of elastic and viscoelastic materials, it is important to also consider the mix phase angle in addition to the dynamic modulus. The phase angle (δ) varies from 0 to 90° and is a measure of the degree of elastic and viscous behavior within the mix under load. A lower phase angle indicates a greater degree of elastic behavior while a higher phase angle indicates more viscous behavior at the same complex modulus. The viscous component of the load response is attributable to energy loss through non-recoverable deformation while the elastic

www.manaraa.com

component of the load response is attributable to stored energy that is recoverable upon matrix relaxation [17]. Figure 2.9 shows both mix's phase angle variations with dynamic moduli variations at 7% air voids. Phase angles at 4% air voids were not compared due to the inability to replicate the binder aging that will exist when the pavement is at 4% air voids and the great degree of impact binder aging has on the phase angle of the mix.

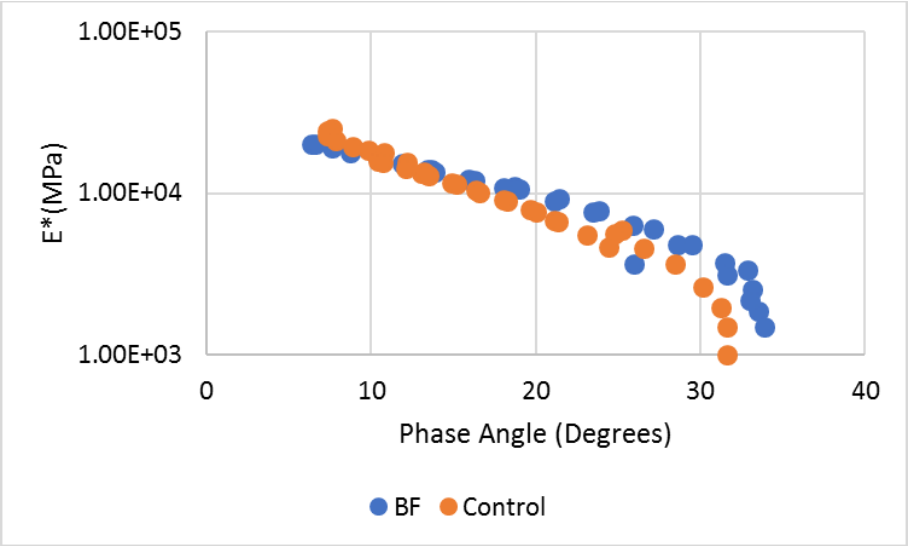

Figure 2.9: E vs δ at 7% Air Voids*

Figure 2.9 shows that the BF mix reaches a peak phase angle of 31° at a dynamic modulus of 1500 MPa while the control mix reaches a peak phase angle of 25° at a dynamic modulus of 1500 MPa. Both mixes trend the same with lower phase angles at the greatest moduli corresponding to low temperatures. As test temperatures increase and load frequencies decrease, the mix phase angles increase to a maximum and then began to decrease again at high temperatures and low frequencies. This decrease beyond maximum is likely attributable to an increased influence of aggregate interlock within the mixes as the binders began to display more viscous behavior beyond the linear viscoelastic region. A statistical analysis of phase angles at critical temperatures and frequencies is summarized in Table 2.14.

www.manaraa.com

Table 2.4: Statistical Comparison Summary of δ at 7% Air Voids

Binder	Temp. (°C)	Freq. (Hz)	Avg. δ (°)	CV, δ	P-value (ANOVA)	95% C.I. for $\mu_{Control}$-μ_{BF} (°)
Control	4	10	7.3	1.0%	0.7068	(-2.4, 1.8)
BF			7.6	13.2%		
Control	21	1	19.6	0.5%	<0.0001	(-12.0, -7.7)
BF			29.5	4.8%		
Control	37	0.1	31.1	1.9%	0.1564	(-2.9, 12.5)
BF			26.3	18.1%		

Table 2.14 shows that the BF mix has a statistically significantly greater phase angle at intermediate temperatures and 1 Hz frequency. The mixes showed comparable phase angles at low temperature and high frequency. At high temperature and low frequency, the BF mix shows a slightly significantly lower phase angle. These analyses show that the BF mix exhibits a comparable ability to relax stress to the control mix at low temperatures, less ability to relax stress at intermediate temperatures, and potentially greater ability to relax stress at high temperatures. The more viscous response by the BF mix at intermediate temperatures (greater average phase angle) as compared to the control mix helps explain why the BF mix exhibited a more rapid rate of damage accumulation in the beam fatigue testing presented earlier in this report.

2.5.2.5. Moisture susceptibility

Compacted specimens for both mixes resulted in varying air void contents. In order to investigate and normalize TSR values, trends between air voids and measured peak strengths were determined for each specimen subset. These results and trends can be seen in Figure 2.10.

www.manaraa.com

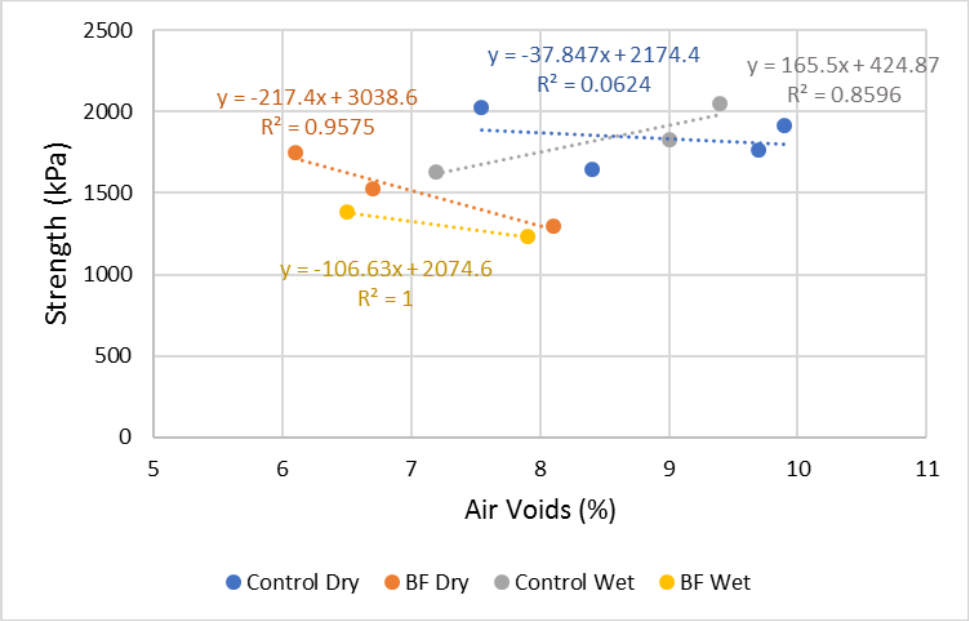

Figure 2.10: Air Voids vs. Peak Strength

Trends shown in Figure 2.10 were used to compare measured TSR values with TSR values calculated based on predicted peak strengths at the same air void content ($TSR_{adjusted}$). Both TSR values are shown in Table 2.15 along with specimen pair average air void content and difference in respective air void contents between the wet and dry specimens. A TSR value of 1.0 indicates no moisture damage was incurred during one freeze-thaw cycle.

Table 2.5: TSR Value Comparison

Binder	Avg. AV (%)	ΔAV (%)	$TSR_{measured}$	$TSR_{adjusted}$
Control	7.4	0.4	0.80	0.87
Control	8.7	0.6	1.11	1.01
Control	9.6	0.7	1.16	1.11
BF	6.3	0.4	0.79	0.84
BF	6.6	0.2	0.90	0.85
BF	8.0	0.2	0.95	0.94

As shown in Table 2.15, both mixes show trends of increasing TSR with increasing air voids. To assess statistically significant trends, a one-way ANOVA and F-test modeling analysis was used. Results of the statistical testing show that a statistically significant difference occurs for

www.manaraa.com

air void content's role in TSR value (p=0.0414) and a non-statistically significant difference occurs for binder's role in TSR value (p=0.5120). These findings suggest no significant difference in mix moisture susceptibility at the same relative air void content.

Both the peak strength trends and the statistical models were used to estimate TSR values for each mix at 7.0% air voids. For the control mix, the peak strength trends estimate a TSR of 0.83 and the statistical model estimates a TSR of 0.76 at 7.0% air voids. For the BF mix, the peak strength trends estimate a TSR of 0.87 and the statistical model estimates a TSR of 0.88 at 7.0% air voids. These results imply that the BF mix provides a slightly greater resistance to moisture damage than the control mix. A standard recommended TSR value of 0.80 or greater is widely accepted as indication that a mix is sufficiently resistant to moisture damage [14]. By comparison, the control mix provides moderate-sufficient resistance to moisture damage while the BF mix provides sufficient resistance to moisture damage. Sufficient resistance to moisture damage may also be a good indicator of the degree of blending compatibility between the bio-derived binder and the RAP binder content as there was no significant strength loss through fracturing of binder to aggregate interfaces. Presence of black rock, or insufficient binder blending with the RAP binder content, often leads to increased stripping due to weak bond interfaces allowing for the easy diffusion of water [6].

2.6. Summary and Conclusions

A potential complete replacement of conventional crude-oil derived binder by a novel non-petroleum-based binder in use with 50% RAP by aggregate and bitumen weight was evaluated in this research. Mix evaluation focused on mixture performance with the independent variable being the binder. Low temperature DCT testing showed that both the control and BF mixes yield mean fracture energies greater than the recommended 400 J/m2 at test temperatures 10°C above their

www.manaraa.com

respective low temperature binder grade. However, when tested at the same low temperature of -12°C, only the BF mix averaged fracture energies greater than 400 J/m2. These findings show that the BF mix provides greater resistance to thermal cracking at lower temperature ranges due to the relative softness of the virgin bio-binder as compared to the control at low operative temperatures. Furthermore, the BF mix showed rather consistent mean fracture energies at both 4% and 7% air voids indicating that post-construction compaction alone will not improve thermal cracking potential for this mix.

Testing showed that at intermediate working temperatures, the BF mix performed similarly to the control mix with the BF mix showing only slight potential for higher rates of fatigue damage accumulation. These findings did not; however, imply that the BF mix will undergo greater percentages of fatigue cracking in the field than the control mix. The BF mix fatigue coefficients fall within industry-suggested bounds to prevent excessive fatigue cracking at working temperatures.

At high temperatures, flow number testing showed that while the BF mix portrayed statistically significantly lower mean FN values than the control mix, the BF mix still showed acceptable rutting resistance for 20-year design ESALs of greater than 10 million but less than 30 million. While the BF mix is of a softer grade than the control mix, the mix is still able to resist high temperature shear deformations.

During evaluation of mix moisture susceptibility, it was determined that the BF mix has statistically-similar resistance to moisture damage as the control mix at 7% air voids with a tensile strength ratio greater than 0.80. By direct comparison, the BF mix has a slightly greater predicted resistance to moisture damage than the control possibly due to the higher adhesion characteristics of the binder in a mix consisting of 50% RAP.

www.manaraa.com

The overarching conclusion of this research is that engineering an asphalt mixture with a complete crude-derived binder replacement and incorporation of 50% RAP is possible. The novel pine-derived sustainable bio-binder passed industry standards for performance at a 20-year design ESAL level of greater than 10 million but less than 30 million at low, intermediate, and high temperature criterion. It is noteworthy to add that these performance tests and test criteria were developed for mixes using conventional petroleum-based bitumen. Therefore, the full advantages of this bio-binder may not be fully appreciated within the confines of these performance tests alone but rather the results prove that such mixes yield performance results sufficient to pass conventional specifications. Further work undertaken within the BioRePavation project has shown that when compared to traditional petroleum-based mixes for binder and surface courses such bio-asphalt mixes generally provides better environmental performance and exhibit promise for longer lifespans with less maintenance in a full-scale test scenario.

References

1. FHWA, U.S. Department of Transportation Federal Highway Administration. "Reclaimed Asphalt Pavement in Asphalt Mixtures: State of the Practice." *FHWA Publication No. FHWA-HRT-11-021*. April 2011.

2. National Center for Asphalt Technology (NCAT): *Hot Mix Asphalt Materials, Mixture Design and Construction, 3rd ed.*, NCAT. 1991.

3. EAPA (European industry association), Asphalt in Figures, 2016. [www.eapa.org]

4. Ali, Hesham. "Long-Term Aging of Recycled Binders." Florida International University: Civil and Environmental Engineering Department; submitted to the Florida Department of Transportation. July 2015.

5. Haghshenas et al. "Research on High-RAP Asphalt Mixtures with Rejuvenators and WMA Additives." University of Nebraska-Lincoln: Nebraska Department of Roads Research Reports. September 2016.

www.manaraa.com

6. Zaumanis et al. “Influence of Six Rejuvenators on the Performance Properties of Reclaimed Asphalt Pavement (RAP) Binder and 100% Recycled Asphalt Mixtures.” *Construction and Building Materials.* November 2014.

7. Kowalski et al. “Thermal and Fatigue Evaluation of Asphalt Mixtures Containing RAP Treated with a Bio-Agent.” *Applied Sciences, Vol. 7, Issue 3*. February 2017.

8. Jiménez del Barco Carrión, A., Pérez-Martínez, M., Themeli, A., Lo Presti, D., Marsac, P., Pouget, S., Chailleux, E., Airey, G. D. (2017). Evaluation of bio-materials’ rejuvenating effect on binders for high-reclaimed asphalt content mixtures. *Materiales de Construcción, 67*(327), 1–11.

9. Jiménez del Barco Carrión, A., Lo Presti, D., Pouget, S., Airey, G., & Chailleux, E. (2017). Linear viscoelastic properties of high reclaimed asphalt content mixes with biobinders. *Road Materials and Pavement Design*, 1–11.

10. Biophalt patent US 8,652,246 B2

11. Pouget S. & Loup L. "Thermo-mechanical behaviour of mixtures containing bio-binders", Road Material and Pavement Design, vol.14, Special Issue EATA, pp. 212-226, 2013.

12. ASTM D2172. “Standard Test Methods for Quantitative Extraction of Asphalt Binder from Asphalt Mixes.” Standard Specifications for Transportation Materials and Methods of Sampling and Testing, Washington D.C., 2007.

13. ASTM D7906. “Standard Practice for Recovery of Asphalt from Solution Using Toluene and the Rotary Evaporator.” Standard Specifications for Transportation Materials and Methods of Sampling and Testing, Washington D.C., 2007.

14. Asphalt Institute. Asphalt Mix Design Methods, 7th Edition. MS-2. 2014.

15. AASHTO T 331-13. “Standard Method of Test for Bulk Specific Gravity (Gmb) and Density of Compacted Hot Mix Asphalt (HMA) Using Automatic Vacuum Sealing Method.” Standard Specifications for Transportation Materials and Methods of Sampling and Testing, Washington D.C., 2015.

16. AASHTO T 209. “Theoretical Maximum Specific Gravity and Density of Hot Mix Asphalt (HMA).” Standard Specifications for Transportation Materials and Methods of Sampling and Testing, Washington D.C., 2015.

www.manaraa.com

17. Y.H. Huang. Pavement Analysis and Design. Second Edition, Prentice Hall, New Jersey, 2004.

18. ASTM D7313. "Standard Test Method for Determining Fracture Energy of Asphalt-Aggregate Mixtures Using the Disk-Shaped Compact Tension Geometry." Standard Specifications for Transportation Materials and Methods of Sampling and Testing, Washington D.C., 2007.

19. AASHTO T 321. "Determining the Fatigue Life of Compacted Asphalt Mixtures Subjected to Repeated Flexural Bending." Standard Specifications for Transportation Materials and Methods of Sampling and Testing, Washington D.C., 2017.

20. AASHTO T 378. "Determining the Dynamic Modulus and Flow Number for Asphalt Mixtures Using the Asphalt Mixture Performance Tester (AMPT)." Standard Specifications for Transportation Materials and Methods of Sampling and Testing, Washington D.C., 2017.

21. AASHTO TP 79-13. "Determining the Dynamic Modulus and Flow Number for Asphalt Mixtures Using the Asphalt Mixture Performance Tester (AMPT)." Standard Specifications for Transportation Materials and Methods of Sampling and Testing, Washington D.C., 2013.

22. AASHTO T 283-14. "Standard Method of Test for Resistance of Compacted Asphalt Mixtures to Moisture-Induced Damage." Standard Specifications for Transportation Materials and Methods of Sampling and Testing, Washington D.C., 2015.

23. W.G. Buttlar, S. Ahmed, E.V. Dave, and A.F. Braham. "Comprehensive Database of Asphalt Concrete Fracture Energy and Links to Field Performance." Paper presented at the 89th Annual Meeting of the Transportation Research Board, Washington, D.C., January 2010.

24. Cascione et al. "Laboratory Evaluation of Field Produced Hot Mix Asphalt Containing Post-Consumer Recycled Asphalt Shingles and Fractionated Recycled Asphalt Pavement." Asphalt Paving Technology 2011, Association of Asphalt Paving Technologies, Vol. 80.

25. S.H. Carpenter. "Fatigue Performance of IDOT Mixtures." Research Report FHWA-ICT-07-007, Illinois Center for Transportation, July 2006.

www.manaraa.com

26. National Cooperative Highway Research Program. “NCHRP Report 673: A Manual for Design of Hot Mix Asphalt with Commentary.” Transportation Research Board, Washington D.C., 2011.

www.manaraa.com

CHAPTER 3: PERFORMANCE OF HMA MIXES INCORPORATING 50% RAP AND NOVEL BIO-ADDITIVES: INVESTIGATION OF MIX SCALE INFLUENCE ON PERFORMANCE RESULTS

Modified from a paper to be submitted to the Journal of Construction and Building Materials

Nicholas D. Manke[a]*, R. Christopher Williams[a], Zahra Sotoodeh-Nia[a], Eric W. Cochran[b], Laurent Porot[c], Emmanuel Chailleux[d], Simon Pouget[e], Francois Olard[e]

[a] *Department of Civil, Construction, and Environmental Engineering, Iowa State University, Ames, Iowa, 50011*
[b] *Department of Chemical, and Biological Engineering, Iowa State University, Ames, Iowa, 50011*
[c] *Kraton Corporation, Arizona Chemical*
[d]*Department of Materials and Structures, IFSTTAR*
[e]*EIFFAGE Infrastructures,France*
**Corresponding author: nmanke@iastate.edu*

Abstract

Around the world, researchers and agencies are developing new ways to reduce costs while simultaneously increasing sustainability in the asphalt paving industry with varying success. Limited funding, the depletion of quality aggregate resources, and a growing awareness of eco-consciousness has led many to find new ways to incorporate more recycled materials into pavement mixes. Reclaimed asphalt pavement (RAP) is a readily available, economical resource in most industrialized nations. The aged binder content of RAP while a valuable resource, if not addressed appropriately, can cause premature thermal and fatigue cracking as well as stripping, difficult compaction, and moisture damage. In order to balance the stiffness of the RAP binder content, rejuvenators or engineered "soft" binders and additives can be used as partial or complete replacements to conventional neat bituminous binder. This research serves to address the

www.manaraa.com

performance of two bio-additive rejuvenators with different means of application and one novel bio-binder with rejuvenating properties as a complete replacement of conventional neat bitumen in mixes with 50% RAP by mix weight. Performance test results were conducted at two mix scales (lab-mixed and plant-produced) and compared to two control mixes with 50% RAP and 20% RAP, respectively, and bituminous binder. Performance results of lab-scale mixes and plant-produced mixes were analyzed for differences to assess any performance variability with mix scale and associated process control variability. Selected performance tests include: disc-shaped compact tension (DCT), beam fatigue, flow number and dynamic modulus, and Hamburg wheel-track testing (HWTT). These tests allow for the analysis of mix performance at a range of temperatures and loading conditions for the prediction of thermal cracking, fatigue cracking, rutting resistance, and moisture susceptibility. Results show that the novel bio-binder and both rejuvenators with 50% RAP by mix weight pass all performance criteria for pavements with 20-year design loads of greater than 10 million but less than 30 million ESALs based on U.S. standard criteria. The novel bio-binder and both rejuvenators increased the thermal cracking resistance while maintaining sufficient stiffness at high temperatures. The novel bio-binder performance was not significantly affected by process control variations attributable to varying mix scales showing it is likely less sensitive to quality control tolerances. Both rejuvenated mixes; however, did show performance result differences and sensitivity between lab-scale and plant-produced mixes at intermediate and high temperature performance.

3.1. Introduction

In the U.S. and other countries around the world, aging infrastructure has put significant strains on limited government funds and quality material resources. Rising labor costs, depleting quarry resources, and volatile crude oil prices have led many agencies, owners, and researchers to

www.manaraa.com

search for viable ways to produce flexible pavements more economically without reducing performance quality. One popular method of lowering material costs and sourcing aggregate is by incorporating recycled materials into hot mix asphalt (HMA) pavements. In the U.S., asphalt pavement is the most recycled material by weight with over 80 million tons recycled annually [1,2]. Europe similarly recycles over 40 million tons of asphalt pavement annually [3]. Reclaimed asphalt pavement (RAP, or RA in EU standards) has been used to various degrees in the U.S. since the 1970s. The bitumen content of RAP; however, has been widely underutilized as a large percentage of recycled pavement is used as a cheap aggregate material alternative in site work. By incorporating both the aggregate and bitumen contents of RAP in greater percentages in new pavements, the full benefit of this readily available material can be reached. Not only can using high RAP contents in asphalt pavements reduce material costs and save nonrenewable resources for other uses, it can positively impact environmental costs associated with aggregate quarrying and landfilling of RAP.

Many current governmental agency specifications in the U.S. show great hesitation to allow more than 30% RAP in asphalt mixes which is a point where the stiffer RAP bitumen content is enough to mandate special considerations for mix designs [1]. Recycled pavements include aged binders which through a range of phenomena greatly increase the stiffness of the bitumen and therefore increase the potential for brittle failure mechanisms. While the increased stiffness is welcomed to enhance high temperature rutting resistance, it must be balanced to not significantly inhibit the ability of the new mix to relax and recover incurred strains in conditions where brittle fatigue and thermal cracking are prevalent. One method of balancing these properties is by using a rejuvenator to physically or chemically alter key molecular interactions within the blended

www.manaraa.com

bituminous binder. Another novel method to balance these properties is by using partial or total neat bituminous binder replacement by specifically-designed viscoelastic materials.

As part of the BioRePavation project, this research explores the performance of high RAP content mix designs incorporating two rejuvenators and a novel bio-binder as a complete replacement for neat bitumen. Design life criteria for these performance investigations consist of 20-year design lives of greater than 10 million ESALs but less than 30 million ESALs, categorizing these mixes as moderate-high design loading pavements. The primary focus of this research study is to address the impact of mix scale on performance indicators for two variations of rejuvenator applications and a novel bio-binder with 50% RAP content mix designs while at the same time showing the performance viability of such mixes. Such an investigation can shed light on how to move forward in translating lab-mixed performance test results to field performance predictability in high RAP content mix designs.

3.2. Background

The incorporation of high RAP contents (>30% by mix weight) into asphalt pavements presents several potential challenges that must be carefully considered and overcome. Reclaimed asphalt pavement (RAP) contains binder that has undergone volatilization of the smaller asphalt fractions and polycondensation which increases the ratio of larger associating asphaltene molecules to smaller lubricating maltene molecules [4]. These changes result in a stiffer binder that is more prone to brittle failure mechanisms and reduced pavement longevity. Another potential challenge when using RAP is the presence of “black rock” which occurs from the incomplete blending of the aged RAP binder coating the RAP aggregate with the virgin binder. Presence of “black rock” creates weak aggregate-binder interfaces that can lead to premature moisture damage, localized rutting, and early crack propagation [5,6].

www.manaraa.com

Two major areas of research to balance the blended binder stiffness and improve binder blending have focused on rejuvenators and partial neat bitumen replacement with softer viscoelastic materials. Rejuvenators can be used to treat the RAP material itself or as a binder additive and primarily serve to rebalance the intermolecular associations of the polycondensed large molecular fraction of the RAP binder [5]. The use of partial neat bitumen replacement with specifically designed softer viscoelastic materials can serve a dual purpose: to effectively balance the stiffness of the mix at low and intermediate temperatures and serve as a rejuvenating component. In the past, petroleum-based oils have been used inadequately as rejuvenators by diluting the aged binder. Recently with the increase in performance demands and interest for introducing more RAP in asphalt mixes, a new generation of engineered rejuvenators has emerged. Research on rejuvenated mixes have shown that at 40% RAP content, a rejuvenator can significantly improve the low-temperature thermal and fatigue cracking of a mix while additionally improving the diffusibility of the virgin binder with the hardened RAP binder interface [7.8]. Other research has shown that rejuvenated mixes can provide adequate performance for low-volume roadways with incorporation of up to 100% RAP as an aggregate source [9]. However, some rejuvenators can potentially adversely affect a mix's rutting and stripping resistance at high doses but could be combated with the addition of a polymer [7,9]. A bio-binder manufactured from polymer-stabilized pine chemistry as the only neat binder in a mix consisting of 50% RAP has been shown to have positive rejuvenating effects and linear viscoelastic properties suitable for use in paving [10,11].

Because of the complex nature of developing a balanced asphalt mix design incorporating both a high RAP content and bio-derived rejuvenating additives, a multitude of mix volumetrics and performance tests should be carried out for analysis. Disc-shaped compact tension (DCT)

www.manaraa.com

testing is used to assess a mix's resistance to low-temperature thermal cracking. Tensile stresses develop within the pavement system due to plastic shrinkage and are further expounded by thermal gradients within the pavement due to air temperature and geothermal temperature heat variants at the surface and bottom of the pavement section, respectively [2]. Eventually, these tensile stresses can exceed the available tensile strength of the pavement and transverse, top-down brittle cracking is initiated [2,12]. The existence of thermal cracking at short intervals promotes further pavement degradation through moisture-intrusion and increasing mechanical load stresses at crack edges.

Beam fatigue test results can be used to predict a mix's resistance to fatigue cracking at intermediate temperatures. The intermediate reference temperature used for testing is linked to both climatic influence as well as the effective binder grades of the mixes. Some research has suggested that in colder climates, selecting an intermediate reference temperature based more heavily on climatic influences more appropriately predicts field performance of high RAP content mixes [13]. Over time, successive strain cycles from repetitive traffic loading can result in top-down or bottom-up micro-fracturing which can be premature in stiff mixes.

Flow number and Hamburg wheel-track testing results can be used to help predict a mix's resistance to viscous shear deformations which result in rutting of the pavement. Rutting is one of the most common high-temperature distresses associated with flexible pavements and excessive rutting can lead to serviceability and safety concerns. While the incorporation of RAP typically increases the rutting resistance of a mix, the impact of a rejuvenator or rejuvenating bio-binder is of interest as both reduce the effective blended binder grade stiffness.

www.manaraa.com

3.3. Materials

All materials used to create the laboratory-mixed specimens were provided by EIFFAGE to represent the materials used in the large-scale field testing. These materials included fractionated RAP in two fractionations (8/12 mm and 0/8 mm), virgin coarse aggregate (10/14 mm), virgin 50/70 pen grade bitumen, and a novel bio-binder called Biophalt® (BF). Biophalt® is made from refined pine chemistry, a co-product of the paper industry, and stabilized with SBS polymers to aid in viscoelastic properties as well as storage stability [14,15]. Bulk shipments of the fractionated RAP were oven-dried and split in a way that ensured statistical uniformity of the materials among individual batches. The binder content of the RAP was determined using toluene-aided distillation in accordance with ASTM D 2172 [16] and ASTM D 7906 [17].

Additionally, two rejuvenators derived from sustainable materials were used. The first, SYLVAROAD™ RP1000 (SY), is made from refined tall oil which is a co-product of the paper industry [18]. This rejuvenator is applied to the RAP directly as a treatment prior to mixing. The second rejuvenator used, epoxidized methyl soyate (EMS), is made from refined soybean chemistry and is used as an additive to neat bituminous binder rather than as a direct applicant to the RAP material [19].

Plant mixes were produced in bulk using a continuous hot asphalt mix plant in France using the same aggregates and RAP as the lab mixes except for the plant-mixed control mix designated here as EME which is a French-based standard high-performance asphalt mix. During production the plant mixing conditions varied from the lab mix production including a higher mixing temperature to compensate the long-haul transportation of materials from the plant to the job site.

www.manaraa.com

Table 3.1 shows a summary of virgin and blended binder grades for the various mixes under study using all applicable ASTM and AASHTO testing standards under the Superpave performance grading (PG) methodology to assess asphalt binders and binder blends.

Table 3.1: Binder PG Grade Summary

Binder I.D.	PG Grade
Control: 50/70 pen grade bitumen	PG 64-22
RAP binder content	PG 94-4
BF virgin binder	N/A*
Control + RAP binder*	PG 76-16
BF + RAP binder*	PG 58-22
Control + RAP binder* + SY	PG 76-22
Control + RAP binder* + EMS	PG 70-22
Control + RAP binder* (EME)	PG 82-xx

*Equivalent to 50% RAP in mix
**Equivalent to 20% RAP in mix

Due to its sticky nature, the BF virgin binder was unable to be tested and therefore a confident performance grade could not be assigned to it. Because of the low high temperature grade of the BF + RAP binder blend, it is reasonable to assume that the BF virgin binder is a significantly softer binder than the control bitumen. It can be seen in Table 3.1 that the control binder is unable to restore the low-temperature properties when blended with RAP. However, the BF bio-binder and both rejuvenated blends positively reduce the low temperature blended binder grade to -22°C. This finding is critical because the incorporation of high RAP contents (>30%) are known to otherwise negatively impact the low temperature performance of mixes as is evidenced by the control + RAP binder grade in Table 3.1.

3.4. Mix Design and Volumetrics

Laboratory-mixed specimens consisted of identical blend gradations, overall binder contents, and RAP contents amongst each test subgroup. Large scale plant-mixed specimens

www.manaraa.com

consisted of very similar blend gradations, overall binder contents, and RAP contents as their lab-mixed counterparts except for the plant-mixed control group. The lab-mixed control mix design consisted of the same RAP content, binder content, and blend gradation as the sustainable mixes with bio-additives. The plant-mixed control; however, utilized a conventional high-performance French-based mix design consisting of 20% RAP as opposed to 50%, a higher binder content, a hard binder, rich mortar, and dense-graded blend gradation. Table 3.2 provides a summary of both the lab-mixed and plant-produced mix designs for each test subgroup. This table is intended to highlight significant consistencies and/or variations among binder subgroups and between small-scale (lab-mixed) and large-scale (plant-mixed) mixes.

Table 3.2: Mix Design Summary

Binder I.D.	Mix Scale	RAP Content (by mix wt.)	Binder Content (total by mix wt.)	Bio-additive Dosage	NMAS (mm)
Control (bitumen)	Lab	50%	4.49%	0%	19.0 mm
	Plant (EME)	20%	5.26%		12.5 mm
BF	Lab	50%	4.49%	100% by wt. of virgin binder	19.0 mm
	Plant		4.44%		
SY (bitumen + SY)	Lab	50%	4.49%	6% by wt. of RAP binder	19.0 mm
	Plant		4.49%		
EMS (bitumen + EMS)	Lab	50%	4.49%	3% by wt. of total binder	19.0 mm
	Plant		4.36%		

As seen in Table 3.2, the biggest difference among mix designs is that of the control group. The lab-mixed control mix design replicates the volumetrics of the mixes incorporating bio-additives as a benchmark. In contrast, the plant-mixed control mix design represents a standard high-performance mix as another benchmark for which to compare the sustainable mix performances. A variation in control mix design allows for a multi-point analysis incorporating

www.manaraa.com

comparisons against a control of the same volumetrics as well as a control with different volumetrics and a lower RAP content.

3.4.1. Aggregate blend gradations

Aggregate blend gradations are a key factor in aggregate packing characteristics which in turn impact mixture performance characteristics, workability, and density. Table 3.3 shows a summary of aggregate blend gradations for each mix subgroup along with industry standard recommendations. Individual aggregate and RAP source gradations are not included here because the overall aggregate blend gradation is the key factor in mixture performance and volumetric characteristics. Plant mix gradations from France were standardized to customary U.S. sieve sizes using linear interpolation for ease of comparison.

Table 3.3: Aggregate Blend Gradation Summary

		Blend I.D.				19.0 mm NMAS Requirments		Blend I.D.	12.5 mm NMAS Requirements	
U.S. Customary	Metric, mm	Lab Mixed	BF, Plant	SY, Plant	EMS, Plant	Min	Max	EME, Plant	Min	Max
1"	25	100	100	100	100	100		100		
3/4"	19	99.4	99.7	99.8	99.7	90	100	99.9	100	
1/2"	12.5	80	86.8	84.1	86.4		90	94.5	90	100
3/8"	9.5	45.5	56	55	55.2			80.5		90
#4	4.75	26.8	33.4	33.5	30.3			46.6		
#8	2.36	23.7	27.2	27.1	23.5	23	49	30.5	28	58
#16	1.18	12.2	21.2	21.5	18.7			21.1		
#30	0.6	8.1	16.3	16.8	14.9			15.4		
#50	0.3	5.5	13	13.4	12.2			11.9		
#100	0.15	4.1	10.7	11	10.2			9.6		
#200	0.075	3.2	8.9	9.1	8.2	2	8	7.7	2	10

As shown in Table 3.3, the lab-mixed specimen gradations are very similar to their plant-mixed counterparts for the BF, SY, and EMS mixes with the exception that the plant-mixed blends include significantly more fines (passing #200 sieve) than the lab mixes.

www.manaraa.com

Figure 3.1 shows Table 3.3 graphically as aggregate gradation curves for each mix subgroup. Included in Figure 3.1 are maximum and minimum control points as well as the maximum density line for a 19.0 mm NMAS aggregate blend.

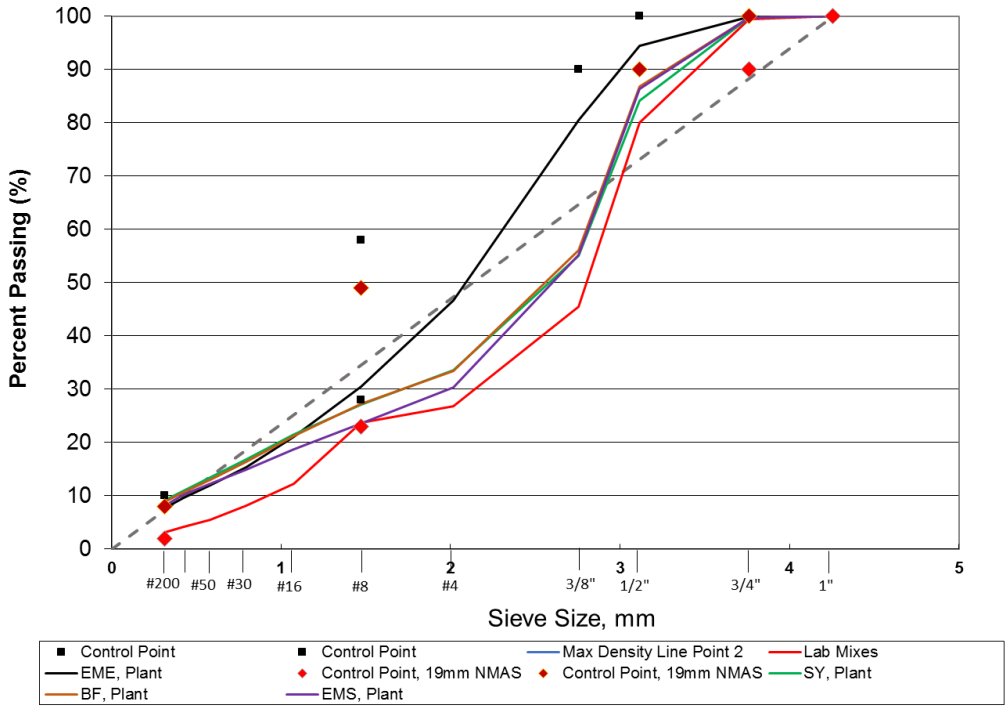

Figure 3.11: Aggregate Blend Gradation Curves

As shown in Figure 3.1, all aggregate blends lie within applicable control points except for the slightly high fines content passing the #200 sieve of the plant-mixed blends (SY, BF, and EMS).

3.4.2. Aggregate blend volumetrics

Aggregate blend volumetrics can be used to assess the aggregate packing characteristics of an asphalt mix. Because dense-graded and gap-graded mixes rely heavily upon aggregate-interlock, such considerations are important in fully understanding the effectiveness of the aggregate blend under loading. The Bailey method utilizes ratios of percent of aggregate retained

www.manaraa.com

on specific sieve sizes based on the NMAS of the blend as a way of predicting aggregate packing characteristics in the asphalt matrix [20]. Pertinent ratios include the coarse aggregate (CA), coarse fraction of the fine aggregate (FA_c) and fine fraction of the fine aggregate (FA_f) ratios. Table 3.4 provides a summary of these ratios for each mix at each scale along with accompanying suggested ratio ranges [20].

Table 3.4: Bailey Method Aggregate Ratio Summary

Ratio	Lab-Mixed	SY (Plant)	BF (Plant)	EMS (Plant)	19.0 mm NMAS Range	Control – EME (Plant)	12.5 NMAS Range
CA	0.34	0.48	0.51	0.56	0.35-0.50	0.57	0.50-0.65
FA_c	0.46	0.64	0.63	0.62	0.60-0.85	0.50	0.35-0.50
FA_f	0.45	0.62	0.61	0.65	0.60-0.85	0.62	0.35-0.50

Suggested ratio ranges shown in Table 3.4 are for a gap-graded coarse blend (19.0 mm NMAS) and dense-graded coarse blend (12.5 mm NMAS) as is most closely shown by the blend gradation curves of Figure 3.1. As the CA ratio decreases below the suggested range and FA ratios increase above the suggested ranges, the mix may exhibit tenderness in the field [20]. Table 3.4 shows that the 19.0 mm NMAS blends show ratio increases from lab-mixed blends to plant-mixed blends indicating that aggregate blend packing characteristics are altered from small-scale lab testing to large-scale field implementation. Such changes must be closely monitored as they could help explain changes in performance test results on the same respective scales.

3.4.3. Mixture volumetrics

A volumetric analysis of an asphalt mixture is important to provide indicators of mixture performance and workability. Mixture volumetrics were assessed for both lab-mixed and plant-mixed samples to determine specific gravities, verify volumetric requirements for mixes with more than 10 million but less than 30 million ESAL 20-year design lives in accordance with Superpave

www.manaraa.com

standards [21], and assess other various volumetric quantities. All specimens used for volumetric quantification were either lab-mixed and short-term oven aged or plant pre-mixed, re-heated, and compacted to the desired air voids using a gyratory compactor.

Table 3.5 provides a summary of volumetric properties associated with the lab-mixed mixes. Table 3.6 similarly provides volumetric properties associated with the plant-mixed mixes. Mixture bulk specific gravities (G_{mb}) were determined according to AASHTO T 331 testing standards using the CoreLok method [22] and maximum theoretical specific gravities (G_{mm}) of the mixes were determined according to AASHTO T 209 testing standards [23]. Other pertinent measurements and ratios such as voids in mineral aggregate (VMA), voids filled with asphalt (VFA), and dust proportion (DP) were calculated according to Superpave standards of practice [20].

Table 3.5: Lab-Mixed Mixture Volumetrics

Property	Control	BF	SY	EMS	Requirement
P_b	4.49	4.49	4.49	4.49	-
P_b (virgin)	2.8	2.8	2.8	2.8	-
P_b (RAP)	1.69	1.69	1.69	1.69	-
VMA	13.2	14.2	13.9	14.2	>13.0
VFA	69.5	71.6	71.0	71.8	65-78
DP	0.7	0.6	0.6	0.6	0.6-1.2
G_{mm}	2.63	2.60	2.61	2.60	-
G_{mb}	2.52	2.50	2.51	2.50	-
$\%V_a$	4.0	4.0	4.0	4.0	4.0

www.manaraa.com

Table 3.6: Plant-Mixed Mixture Volumetrics

Property	Control (EME)	BF	SY	EMS	Requirement
P_b	5.26	4.44	4.49	4.36	-
VMA	18.9	15.8	15.8	15.0	>13.0
VFA	71.6	71.9	71.7	70.9	65-78
DP	1.5	2.4	2.5	2.4	0.6-1.2
G_{mm}	2.55	2.59	2.60	2.61	-
G_{mb}	2.37	2.40	2.42	2.43	-
$\%V_a$	4.0	4.0	4.0	4.0	4.0

As is shown in Table 3.5, all lab-produced mixes meet all Superpave requirements for volumetrics of a mix design with a 20-year design loading of greater than 10 million but less than 30 million ESALs. Table 3.6 shows that while each large-scale plant mix passes VMA and VFA requirements, they do not meet DP requirements. This is attributable to the increase in fines passing the #200 sieve observed in the plant mixes. A high dust proportion (DP) in a dense-graded mix can lead to mix tenderness requiring increased compaction energy, increased optimum binder content from an increased aggregate surface area, and micro-cracking due to stress concentrations upon compaction [20]. The high DP are more in line with what would be expected in a gap-graded SMA mix as opposed to a dense-graded conventional mix.

3.5. Performance Testing

Several kinds of performance tests were carried out on each mix design for both laboratory-mixed and compacted and plant-mixed and laboratory-compacted mixes. The temperature and shear-rate dependence of asphalt binder behavior necessitates low-temperature, intermediate temperature, and high temperature assessment of mixture response under loading. All performance testing in this research was conducted on lab-compacted specimens using a gyratory compactor with a target of 7% air voids to simulate immediate post-construction air void conditions. It should be noted that large-scale field test pavement sections contained significantly lower air void

www.manaraa.com

contents; however, for comparative purposes each subgroup containing the same air void content is enough to draw significant conclusions.

3.5.1. Testing procedures

This section outlines the procedures used to carry out laboratory testing on the materials under consideration. All applicable ASTM and AASHTO standards followed are referenced in addition to laboratory and research-specific testing conditions and material preparations.

3.5.1.1. Disc-shaped compact tension (DCT)

Disc-shaped compact tension (DCT) testing was performed in accordance with ASTM D 7313 standards [24]. The selected test temperature was 10°C above the low temperature blended binder grade of the test mixes containing rejuvenators and BF. It should be noted that due to the warmer low temperature blended binder grade of the control (50/70 bitumen + 50% RAP aggregate content) mix, the -12°C DCT testing temperature does not directly correspond to testing standards for those results. Additionally, field paving trials indicate a lower air void content may be optimal for mixes containing rejuvenators and the BF binder. However, results at a post-construction, pre-traffic loading air void content of 7% provides testing under the same conditions to allow for a direct comparison of binder and rejuvenator influence on low-temperature performance in the same climate location.

Laboratory-mixed specimens were short-term oven aged for two hours after mixing and compacted using a gyratory compactor. Plant-mixed specimens were reheated from bulk to minimize excessive binder aging and gyratory compacted. Compacted specimens were then cut and cored using water-cooled saws and a drill press to the specifications shown in Figure 3.2 as provided by ASTM D 7313 standards [24].

www.manaraa.com

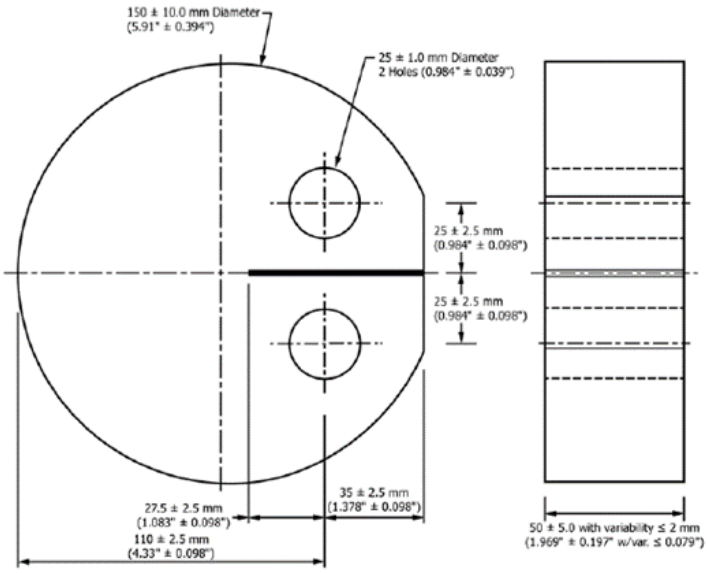

Figure 3.12: DCT Specimen Dimensions as per ASTM D 7313 Standards

Cut specimens were allowed to dry, fitted with metal gage points, and placed in an environmentally-controlled unit for 8 to 16 hours to reach the desired test temperature of -12°C. Once conditioned, individual specimens were loaded into an environmentally-controlled testing apparatus and fitted with a crack mouth opening displacement (CMOD) gage. Each specimen was then loaded to failure at a controlled CMOD rate of 0.0017 mm/sec with failure criteria being the point at which tensile load resistance fell below 0.1 kN.

Data collection consisted of fracture energy (G_f) which is the area under the CMOD versus load curve. Fracture energy was calculated using Equation 3.1 and normalized to individual specimen dimensions including thickness and ligament length.

$$G_f = \frac{A_f}{l*t} \qquad \text{[Eq. 3.1]}$$

where:

A_f = Area under the load vs. CMOD plot (J),

l = Length of the fractured face (m), and

www.manaraa.com

t = Specimen thickness (m).

3.5.1.2. Beam fatigue

Beam fatigue testing was used to assess mix response to repeated loading-unloading cycles at a standard reference temperature of 20°C based on climatic and blended binder grade considerations. Each mix was tested at both small-scale laboratory-mixed and large-scale plant-mixed levels in accordance with AASHTO T 321 standards [25]. For each test subgroup, slabs were prepared using a linear kneading slab compactor to a target of 7% air voids. Each slab was then cut into three individual beams using a water-cooled saw ensuring that every beam consisted of two saw-cut edges and nominal dimensions of 380 mm (L) x 63 mm (W) x 50 mm (T). Compacted beams were allowed to set overnight and then normalized to the test temperature of 20°C. Once beams were thermally-normalized, they were loaded individually into a four-point flexural bending apparatus which subjected beams to haversine axial loads at a rate of 10 Hz. An example of a beam in the testing apparatus is shown in Figure 3.3.

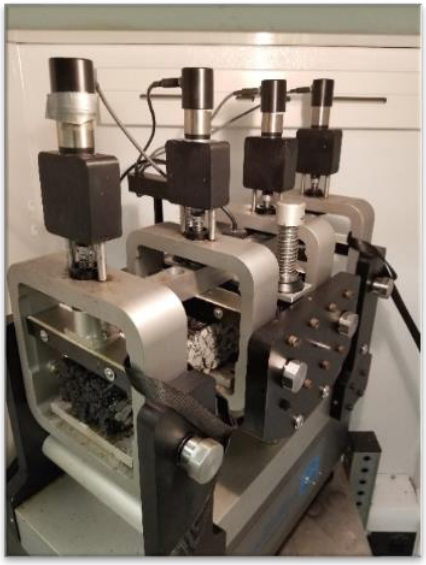

Figure 3.13: Four-Point Flexural Bending Apparatus

www.manaraa.com

Beam fatigue testing was performed in the strain control mode which is more relevant to fatigue performance of pavement layers less than 130 mm (5-inches) in thickness [2]. Strain control mode thus more accurately reflects a pavement whose load-unload mechanical response is largely driven by the subgrade stiffness. Each subgroup of beams constitutes one data set for analysis covering six strain amplitudes ranging from 1200 to 300 micro-strain with one beam tested at each micro-strain level chosen. Micro-strain measured was the amplitude from crest to trough. Failure criteria was the point which each specimen exhibited a flexural stiffness on successive cycles to be 50% of the measured flexural stiffness at the 50th load cycle. The point of reference starting flexural stiffness was measured at the 50th load cycle to ensure proper seating of the beams ensuring the value is representative of the beam's true initial flexural stiffness. Corresponding test strain amplitudes and recorded cycles to failure were plotted on a log-log scale plot to determine flexural coefficients K1 and K2 using the power law relationship shown in Equation 3.2.

$$N_f = K1\left(1/\epsilon_0\right)^{K2} \qquad \text{[Eq. 3.2]}$$

where:

N_f = number of load cycles to failure,

ε_0 = flexural strain amplitude in micro-strain, and

K1, K2 = regression constants.

3.5.1.3. Dynamic modulus and flow number

Dynamic modulus testing was conducted on four or five specimens within each subgroup. All specimens were laboratory-compacted to 7% air voids and nominal dimensions of 150-mm in height by 100-mm in diameter using a gyratory compactor. Testing followed AASHTO TP 79

www.manaraa.com

standards using a universal testing machine (UTM) [26]. Eight loading frequencies (25, 10, 5, 2, 1, 0.5, 0.2, and 0.1 Hz) at three temperatures (4, 21, and 37°C) were used to assess each mix subset's stress-strain behavior in the linear viscoelastic domain. Linear variable differential transformers (LVDTs) were used to measure axial strain changes with each load-unload cycle.

Load and strain data were used to auto-calculate dynamic moduli (E*) and phase angles (δ) of each specimen at each temperature-frequency test condition. The full set of data points for each specimen was then averaged amongst the respective mix subset under consideration to construct sigmoidal master curves. Master curves use shifted raw data to predict stress-strain behavior over a wide range of loading frequencies within the linear viscoelastic domain of the mix.

Master curves for each mix subset at 7% air voids were plotted using dynamic modulus test results shifted to an intermediate standard reference temperature of 21°C. Subsequent sigmoidal curves were formed from the shifted raw test data as well as prediction extrapolated curves based on test trends to minimize squared error differences between predicted dynamic moduli and measured dynamic moduli in the test zone. The sigmoidal function used to create all mix master curves is shown in Equation 3.3.

$$Log|E^*| = a + \frac{b}{1+e^{\beta+\gamma(log f_R)}} \qquad \text{[Eq. 3.3]}$$

where:

f_R = reduced frequency at reference temperature in Hz,

a = minimum value of E* in MPa,

a + b = maximum value of E* in MPa, and

β, γ = fitting coefficients.

www.manaraa.com

Flow number testing was performed on specimens previously used to conduct non-destructive dynamic modulus testing in accordance with AASHTO T 378 specifications [27]. A UTM 25 asphalt mixture performance tester (AMPT) was used to conduct all flow number testing under unconfined conditions and a standard temperature of 54°C. The failure criterion was the point at which a specimen attained 5% permanent axial strain or 10,000 load cycles, whichever occurred first.

The reported flow number (FN) for each specimen is defined as the load cycle number corresponding to the minimum permanent strain rate exhibited at that cycle. This is considered the point at which a specimen begins tertiary flow, or creep, within the mix matrix where shearing deformations are no longer recoverable.

3.5.1.4. Hamburg wheel-track testing (HWTT)

Hamburg wheel-track testing was performed in accordance with AASHTO T 324 specifications [28]. Specimens were prepared at Iowa State University and were subsequently tested by the Iowa Department of Transportation (IDOT). Each testing subset consisted of six individual specimens, or three test pairs. Lab-mixed specimens were mixed and compacted to a standard 7% air voids using a gyratory compactor and meeting nominal dimensions of 60-mm in height by 150-mm in diameter. Plant-mixed specimens were lab-compacted from loose bulk mix to a standard 7% air voids using a gyratory compactor and meeting nominal dimensions of 64-mm in height by 150-mm in diameter. After volumetric verifications were completed, specimens were sent to the IDOT for testing. Testing consisted of utilizing a temperature-controlled water bath to normalize all specimens to a standard test temperature of 50°C and loading pairs of specimens with a 47-mm (1.85 in.) wide steel wheel under a 705 N compressive load moving at 0.305 m/s (1 ft/s) to completion. Completion in this case was the point at which specimens failed when

www.manaraa.com

maximum rut depth reached 12-mm or 20,000 passes, whichever occurred first. Recorded data for analysis included maximum average rut depth, stripping inflection point (SIP), and stripping ratio for each pair of specimens. Figure 3.4 shows a picture of specimens being tested in the HWTT apparatus.

Figure 3.14: Hamburg Wheel-Track Testing Apparatus

3.5.2. Testing results

This section provides the results gained from used the testing procedures outlined in subsection 2.5.1. Performance results are summarized graphically and in tables and are accompanied by appropriate statistical analyses.

3.5.2.1. Disc-shaped compact tension (DCT)

Prior studies have shown that specimen fracture energies, G_f, in excess of 400 J/m^2 indicates an acceptable resistance to any widespread low-temperature thermal cracking in the field [29]. Figure 3.5 shows a summary of mean fracture energies for each mix at each mix scale evaluated. Two significant outliers were eliminated from the total data set comprised of three data points for each lab-produced mix and five data points for each plant-produced mix. Bars are shown with statistical means and standard error bars for the means. Mean fracture energies shown correspond to a uniform test temperature of -12°C and air void content of 7%.

www.manaraa.com

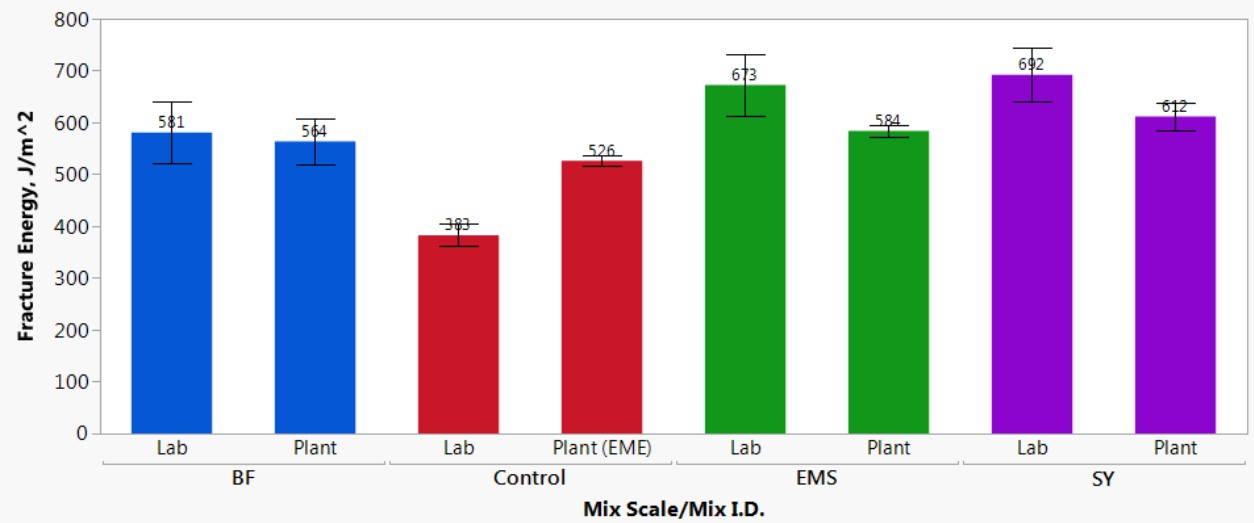

Figure 3.15: Mean Fracture Energy Summary

Figure 3.5 shows that at the lab-produced scale, the control mix with 50% RAP has the lowest mean fracture of 393 J/m^2. This is expected due to the test temperature relative to the blended binder low temperature grade. The three mixes with bio-additives (BF, EMS, and SY) all have mean fracture energies well above the recommended minimum 400 J/m^2 at both mix scales. A one-way analysis of variance (ANOVA) statistical analysis of the plant-produced mixes shows that the mixes with bio-additives have statistically similar thermal cracking resistance to the high performance EME control mix with 20% RAP. These findings show the effectiveness of the bio-additives at sufficiently balancing the stiff RAP content within the mix at low temperatures. Although RAP contents in excess of 30% have been known to cause an increase in thermal and brittle cracking in mixes, these results show that bio-additives can be used to effectively increase the thermal cracking resistance of mixes incorporating up to 50% RAP by mix weight.

When comparing each mix with bio-additives between mix scales, one can see that the BF mix was the most consistent in performance while the EMS and SY mixes had slight decreases in mean fracture energies, though not statistically significant at a confidence level above 85%. These

www.manaraa.com

trends indicate that the BF mix resistance to thermal cracking and associated relative stiffness at low temperatures was not impacted by the change in mixing temperature and other process control and aggregate variations experienced at the plant-produced mix scale. The lower thermal cracking resistance and increased stiffness at low temperatures shown by the EMS and SY mixes at the plant-produced scale indicates that these rejuvenators may be more sensitive to increasing mixing temperature and process control variations. Higher mixing temperatures in addition to a greater fines content may have led to slightly stiffer mixes at the plant relative to the lab-produced mixes. However, these slight increases in stiffness are not significant and all three mixes with bio-additives still provided thermal cracking resistance metrics well above the recommended minimum.

3.5.2.2. Beam fatigue

For each set of beams tested at various micro-strains, data points (inverse of micro-strain vs. cycles to failure) were plotted on a log-log scale and fitted with best-fit power law relationships. Each corresponding power law relationship provides K1 and K2 regression coefficients which can be used to assess the fatigue behavior of each mix at each mix scale. Figure 3.6 shows these relationships for lab-produced mixes. Due to the limited quantity of plant-produced beams, beam fatigue data is provided but is not sufficient to be statistically-founded.

www.manaraa.com

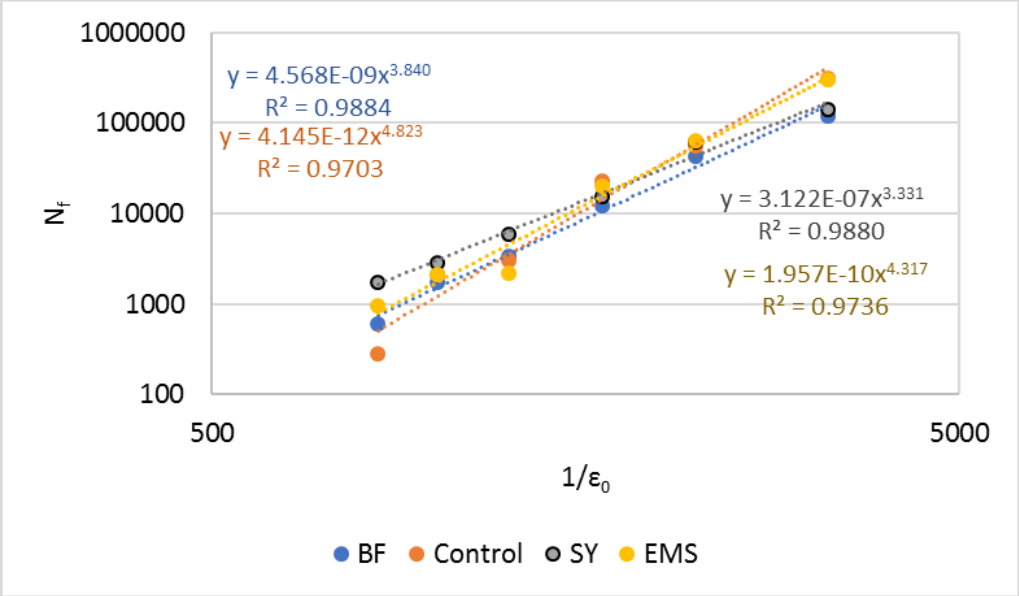

Figure 3.16: Fatigue Coefficient Determination for Small-Scale Mixes

Fatigue coefficients and accompanying coefficients of determination (R^2) for each best-fit regression line are summarized for both small-scale and large-scale mixes in Table 3.7. Coefficients of determination are not provided for the plant-scale mixes due to the low number of beams tested.

Table 3.7: Fatigue Coefficients Summary

Mix I.D.	Mix Scale	K1	K2	R^2
Control	Lab	4.15E-12	4.823	0.970
	Plant	4.16E-07	3.515	-
BF	Lab	4.57E-09	3.840	0.988
	Plant	1.26E-10	4.282	-
SY	Lab	3.12E-07	3.331	0.988
	Plant	3.69E-11	4.624	-
EMS	Lab	1.96E-10	4.317	0.974
	Plant	1.93E-05	2.680	-

As shown in Table 3.7, the fatigue coefficient, K1, is very small for each mix at each mix scale and few conclusions can be drawn from it concerning fatigue behavior. The other fatigue coefficient, K2 provides information about the rate of damage accumulation for each mix subgroup

www.manaraa.com

with lower K2 values indicating a more rapid rate of damage accumulation [30]. The Transport and Road Research Laboratory recommends a K2 value of around 4.32, while the Belgian Road Research Center recommends a value near 4.76 [12]. Carpenter provided a wider K2 range of 3.5 to 4.5 to the Illinois Department of Transportation [31]. With these recommendations in mind, it is reasonable to assume a K2 value between 3.5 and 4.8 is indicative of reasonable fatigue cracking resistance of a conventional bituminous binder mix with no RAP. Research has shown that due to the increased initial stiffness and unconventional mix load-cycling stability often associated with high RAP content mixes, the 50% stiffness reduction as a failure criterion may be somewhat misleading to solely rely on the cycles to failure (N_f) to predict field fatigue performance [32]. Because the K2 fatigue coefficient is derived from cycles to failure, the analysis of fatigue coefficients alone is not likely enough in describing the fatigue performance of high RAP asphalt mixes although it does provide one aspect of fatigue analysis.

Table 3.7 shows that at the lab-mixed scale the control and EMS mixes provide the lowest rates of damage accumulation. The BF mix indicates a more rapid rate of damage accumulation which is likely attributable to the relative “softness” of the virgin binder and self-heating phenomena with successive load cycles. However, the BF mix K2 coefficient is still well within the recommended range indicating good resistance to fatigue cracking. The SY lab-mixed subgroup has a K2 coefficient below 3.5 indicating a more rapid rate of damage accumulation than the BF, control, and EMS mixes. Lower K2 coefficients also indicate a less rigid mix at intermediate temperatures. Therefore, mixes with lower K2 coefficients may potentially indicate more effective rejuvenating properties on the RAP content.

Table 3.7 also shows that at the plant-mixed scale the control (EME), BF, and SY mixes all have K2 coefficients within the suggested range of 3.5 to 4.8 based on conventional mixes. The

www.manaraa.com

decrease in the K2 value for the EMS plant-scale mix below 3.0 indicates a faster rate of damage accumulation with increasing mix scale and accompanying process control variations. However, the limitation in collected data at the plant-produced scale means that significant conclusions should not be made solely on these large-scale data trends.

To help explain the differences in fatigue coefficients summarized in Table 3.7 flexural stiffness dissipation with load cycles was analyzed at a high strain amplitude. Plots showing flexural stiffness dissipation over accumulating load cycles at 1000 micro-strain can be seen in Figures 3.7 and 3.8 for small-scale and large-scale mixes, respectively.

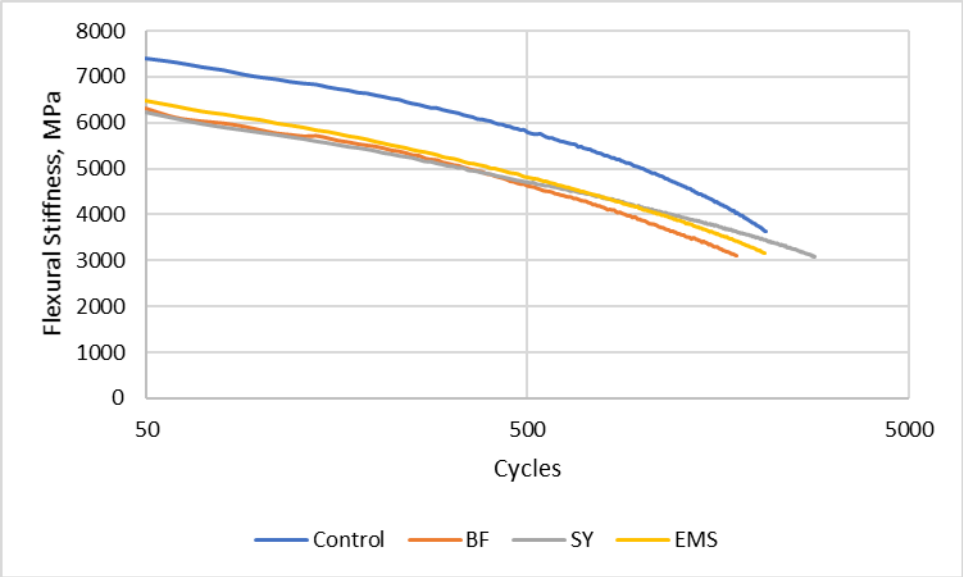

Figure 3.7: Flexural Stiffness Dissipation in Small-Scale Mixes; 1000 micro-strain

www.manaraa.com

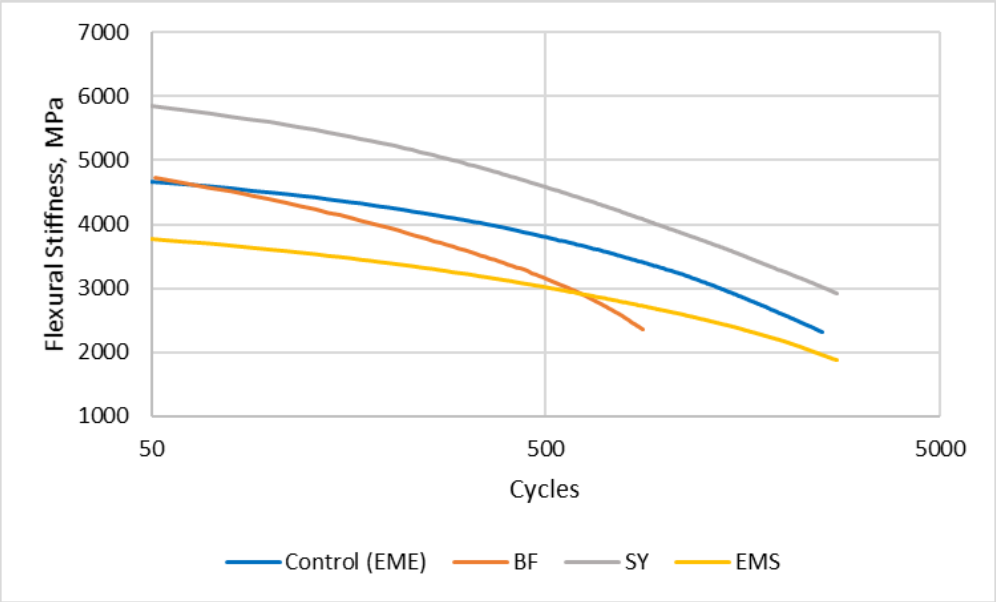

Figure 3.17: Flexural Stiffness Dissipation in Large-Scale Mixes; 1000 micro-strain

Figure 3.7 shows that at 1000 micro-strain, the control mix with 50% RAP has the greatest initial stiffness of the lab-produced mixes as would be expected. The SY mix shows the slowest rate of damage accumulation while the BF, EMS, and control mix rates appear to be quite similar in general trend. Figure 3.8 shows that at the same 1000 micro-strain, the SY mix starts with the highest flexural stiffness of the plant-mixed group. The control (EME) and BF begin at essentially the same flexural stiffness even though the BF mix contains 30% more RAP than the EME control mix. The BF mix dissipation curve has a more rapid rate of stiffness dissipation than the control (EME), SY, and EMS mixes indicating a faster rate of damage accumulation. For plant-produced mixes, EMS shows the lowest slope for the dissipation curve of the subgroup, despite the K2 analysis predicting the EMS mix has the greatest potential for rapid damage accumulation of the plant-produced mixes.

Among the three mixes with bio-additives, the SY mix shows the least sensitivity to mix scale variability considering initial flexural stiffness and dissipation curve behavior at 1000 micro-

www.manaraa.com

strain. While the EMS mix has a lower starting flexural stiffness at the plant-mixed scale as compared to the lab-mixed scale, the dissipation curve shapes and slopes at both scales are relatively the same. The BF mix; however, appears to not only show a lower initial flexural stiffness at the plant-mixed scale but also exhibits a faster rate of stiffness dissipation with successive loading cycles.

Conflicting trends between high-strain flexural stiffness dissipation and K2 coefficient trends show the difficulty in using conventional fatigue analysis methods with assessing unconventional mixes incorporating high RAP contents and bio-additives. Additionally, the variability in process controls between the two scales can have significant impacts on fatigue performance indicators on these types of mixes.

As another way of analyzing mix fatigue behavior, mix phase angle increases with accumulating flexural load cycles at the plant-mixed scale were plotted at the strain level of 1000 micro-strain. Mix phase angles and rate of increase are indicative of the degree of viscous or rigid response to fatigue cycles over time. Figure 3.9 shows plant-produced mix phase angle changes with accumulated flexural load cycles.

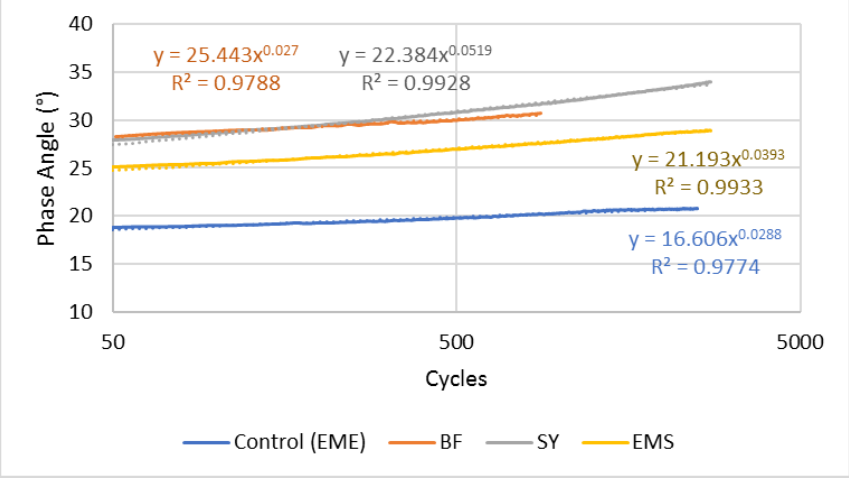

Figure 3.18: Plant-Scale Mix Phase Angles vs. Flexural Load Cycles; 1000 micro-strain

www.manaraa.com

Figure 3.9 shows that the control (EME) mix has the lowest phase angle among the plant-produced mixes throughout fatigue testing indicating that this mix has the least viscous, most rigid response of the group at 1000 micro-strain. A more rigid response by the EME control is expected due to the harder bituminous binder and no rejuvenating agents with the 20% RAP content. The BF and SY mixes show the most viscous, least rigid responses of the group at 1000 micro-strain which is indicative of the effectiveness of the rejuvenating additives to balance the stiffness of the RAP. Exponential best-fit curves can help predict the rate at which mixes increase their viscous response which may in part be caused to self-heating through successive flexural straining. When comparing the exponential rate of mix phase angle increase, the BF mix and control (EME) mixes have very similar rates of increase. The rejuvenated mixes (SY and EMS) have greater rates of mix phase angle increase than the BF and EME control mixes. These results show that the rejuvenators (SY and EMS) have visible effects on fatigue performance of high RAP content mixes when comparing phase angle trends as an indicator of viscous response and reduced mix stiffness at intermediate temperatures.

Research on the impact of aggregate gradation changes on conventional HMA mix performance has shown that fatigue performance is significantly affected by an increase in aggregate fine fractions [33]. A decrease in fatigue performance with an increase in aggregate fines content can be largely attributed to an associated decrease in effective binder content available within the mix matrix. Research on plant-mixed HMA mixes incorporating up to 40% RAP has also shown that plant operations can have a significant impact on the fatigue behavior of mixes in addition to a varying aggregate gradation from design to implementation [34]. The key operations center around heating intensity and time duration variations such as how long the loose mix is held in a silo or transport times. The increase in fines from lab mixes to plant mixes found in the

www.manaraa.com

volumetrics section along with the variability in mixing temperatures, short-term aging phenomena, and other process control differences between mix scales all point to the need for a very thorough investigation of fatigue behavior in the laboratory in order to predict field behavior.

3.5.2.3. Dynamic modulus and flow number

Dynamic modulus test results can be used to assess a mix's response over a wide range of loading rates within the linear viscoelastic range. Results analyzed include both the dynamic modulus (E*), or effective stiffness, and phase angle (δ) which shows the degree to which the mix's response is viscous in nature. Figures 3.10 and 3.11 show the mix master curves with phase angle trends at the lab-mixed scale and plant-mixed scale, respectively.

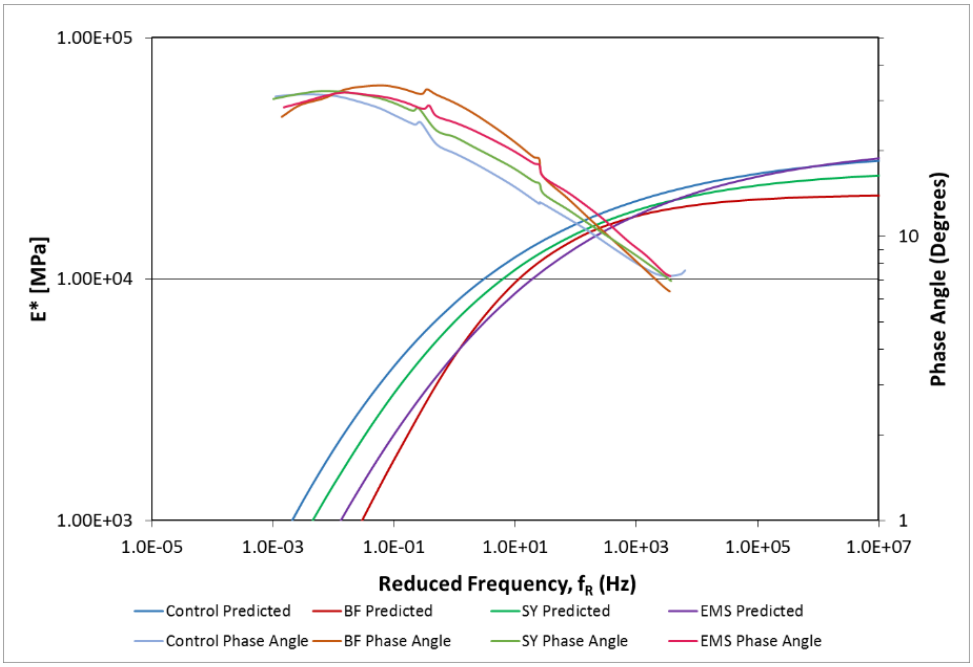

Figure 3.10: Lab-Mixed Specimen Master Curves

www.manaraa.com

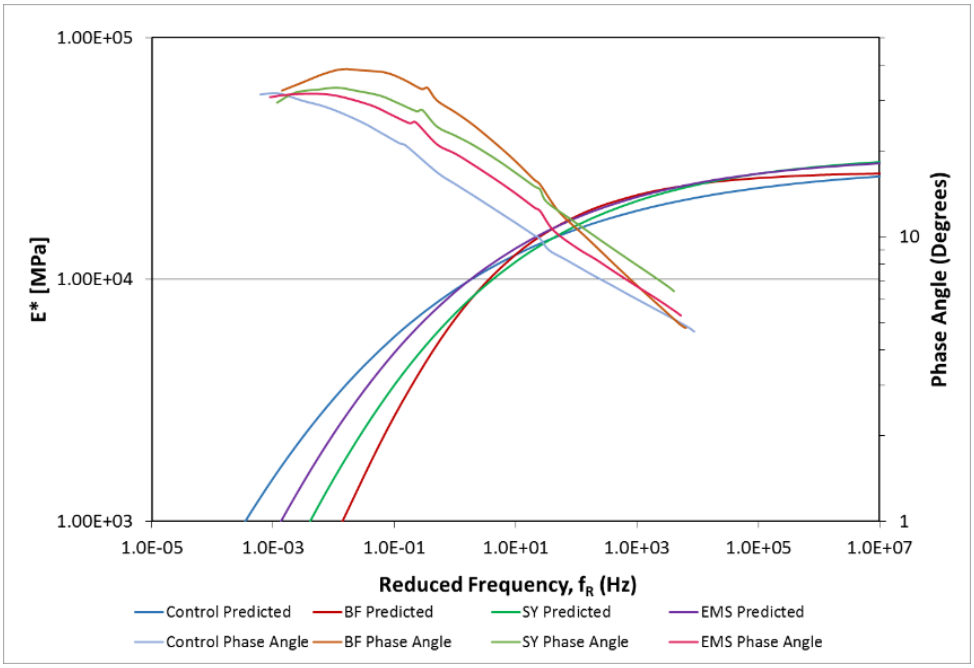

Figure 3.19: Plant-Mixed Specimen Master Curves

To more easily assess statistical trends and differences shown in Figures 3.10 and 3.11, Tables 3.8 and 3.9 provide statistical summaries at critical temperature-frequency pairs that are pertinent to predicting mix performance against common distresses. Low temperatures and high frequencies (corresponding to high reduced frequencies in the master curve plots) is where lower stiffnesses are preferred to resist brittle thermal cracking. Intermediate working temperatures and frequencies is a range where a balanced stiffness is preferred to provide enough viscous dampening of incurred loading cycles to prevent brittle failures, but enough stiffness to elastically-recover much of the imposed load-induced deformation between cycles. Because the measured moduli values at high temperature (37°C) and low frequency (0.1 Hz) are beyond the range of linear viscoelastic response, these data points are not shown in the tables. At high temperatures and low frequency, the measured moduli are significantly influenced by the aggregate skeleton.

www.manaraa.com

Table 3.8: Lab-Mixed Specimen Dynamic Modulus Summary

Mix I.D.	Temp. (°C)	Freq. (Hz)	Mean E* (MPa)	CV (%)	p-value (ANOVA)	Tukey HSD
Control	4	10	22792	6.8%	0.0849	A
BF			18991	8.9%		A
SY			20277	7.0%		A
EMS			19511	18.3%		A
Control	21	1	7910	4.7%	<0.0001	A
BF			4799	14.6%		C
SY			6623	5.7%		B
EMS			4886	10.1%		C

Table 3.8 shows that, while not statistically significant to a 95% degree of confidence, the BF mix shows the lowest stiffness at low temperature and high frequency while the control has the greatest stiffness under the same conditions. These results agree with those from DCT low temperature testing results. The lower stiffnesses at low and intermediate temperatures of the BF, SY, and EMS mixes as compared to the control mix with 50% RAP and no bio-additives shows the effectiveness of the rejuvenating properties of all three bio-additives tested.

Table 3.9: Plant-Mixed Specimen Dynamic Modulus Summary

Mix I.D.	Temp. (°C)	Freq. (Hz)	Mean E* (MPa)	CV (%)	p-value (ANOVA)	Tukey HSD
Control	4	10	20806	4.3%	0.0017	B
BF			24042	2.6%		A
SY			22139	7.2%		A B
EMS			23294	4.8%		A
Control	21	1	9084	3.6%	<0.0001	A
BF			6928	5.8%		B
SY			7194	7.3%		B
EMS			8817	2.6%		A

Table 3.9 shows that at the plant-produced scale, the SY mix has a lower stiffness than the EMS mix at both low and intermediate temperatures which is the reverse of the trend observed in

www.manaraa.com

the lab-produced mixes shown in Table 3.8. The reversal of trends at mix scale may indicate a greater amount of rejuvenator was applied at the plant for the SY mix, or that the direct application method of treatment of the SY rejuvenator is more effective than the application method of the EMS rejuvenator when used a plant-production scale.

The influence of mix scale on the DM testing results are summarized in Table 3.10. The control group was not compared because the lab-mixed and plant-mixed scale control mixes are significantly different in composition Therefore, only the BF, SY, and EMS mixes were statistically analyzed for mix scale influence.

Table 3.10: Influence of Mix Scale on Dynamic Modulus Summary

Mix I.D.	Mix Scale	Temp. (°C)	Freq. (Hz)	Mean E* (MPa)	CV (%)	$\mu_{Lab} - \mu_{Plant}$	p-value (ANOVA)
BF	Lab	4	10	18991	8.9%	-5052	0.0004
	Plant			24042	2.6%		
	Lab	21	1	4799	14.6%	-2129	0.0007
	Plant			6928	5.8%		
SY	Lab	4	10	20277	7.0%	-1863	0.1105
	Plant			22139	7.2%		
	Lab	21	1	6623	5.7%	-571	0.1125
	Plant			7194	7.3%		
EMS	Lab	4	10	19511	18.3%	-3784	0.0571
	Plant			23294	4.8%		
	Lab	21	1	4886	10.1%	-3931	<0.0001
	Plant			8817	2.6%		

As seen in Table 3.10, the BF mix shows statistically significant (at an α=0.05 level) dynamic modulus increases at both low temperature, high frequency and intermediate temperature, intermediate frequency critical points with the increase in mix scale. While an increase in stiffness at low temperature is not necessarily advantageous, the DCT performance results show that this stiffness increase is not enough to degrade thermal cracking resistance to any significant degree.

www.manaraa.com

While the SY mix exhibits greater mean dynamic moduli at each critical point, none of the increases are statistically significant beyond a 90% reliability. The EMS mix had statistically significant dynamic modulus increases at each critical point with a degree of reliability greater than 94% when increasing mix scale. An overarching trend observed within each subgroup is an increase in mean dynamic modulus at each temperature and frequency analyzed with increasing mix scale. The increase in stiffness may be due to a combination of the difference in fines contents at the different scales, greater heating temperatures at the mixing plant which would increase rejuvenator volatilization and aging, and other process control variation phenomena.

In addition to analyzing dynamic modulus values, phase angles were also statistically compared at the intermediate temperature of 21°C and load frequency of 1 Hz. The intermediate critical condition is where mix phase angle will have the greatest variability and impact on performance. Greater phase angles indicate a more viscous response with less recoverable energy under load. Figure 3.12 shows a box and whisker plot summary of measured mix phase angles found through DM testing.

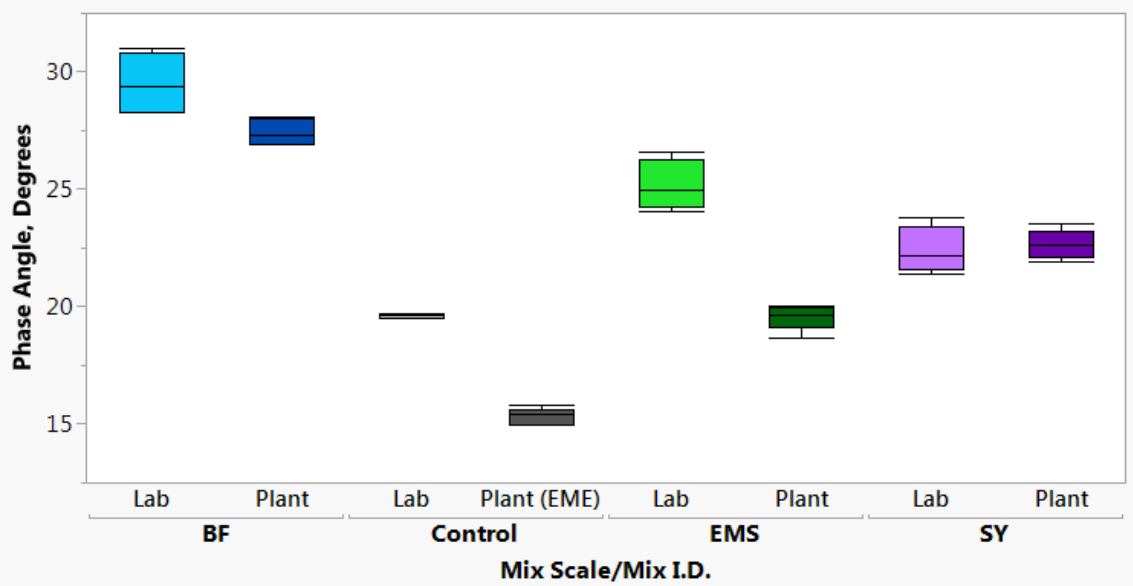

Figure 3.20: Mix Phase Angles, 21°C and 1 Hz

www.manaraa.com

Figure 3.12 shows that at the lab-mixed scale the BF mix had the most viscous response followed by the EMS mix, the SY mix, and the lab control mix having the least viscous response. At the plant-produced scale, the BF mix again exhibited the most viscous behavior while the control EME mix with 20% RAP and no bio-additives had the least viscous behavior. The SY mix had a more viscous response at the plant-produced than the EMS mix which is the opposite trend of the lab-produced mix results. The stiffer responses of the control mixes are expected while the more viscous responses of the mixes with bio-additives showcases the rejuvenation effectiveness in balancing the stiffness induced by the RAP content. While a more viscous response to repetitive loading may explain the lower K2 coefficients found in the beam fatigue analysis, this property is not detrimental to mix performance but rather shows an increased resistance to brittle failure and micro-cracking initiation and propagation.

Comparing differences between mix scales, the BF and EMS mixes had a statistically significant phase angle decrease at the intermediate temperature when increasing mix scale. The SY mix phase angles remained statistically very similar at the intermediate temperature and load frequency. These trends show that a rejuvenator applied directly to the RAP material prior to mixing as is the case with the SY mix may be less sensitive to the process control variabilities experienced with the increase in mix scale from lab to an asphalt plant. Higher mixing temperatures at the plant along with other process control variables significantly increased the stiffness of the EMS mix at intermediate temperatures based on these results while only slightly increasing the stiffness of the BF mix and not affecting the SY mix. The relative softness of the BF binder potentially makes the BF mix less sensitive to such process control variances while the EMS rejuvenator may not have been able to influence the RAP material under the higher temperature conditions of the plant as compared to the lab.

www.manaraa.com

Figure 3.13 shows a summary of mean flow numbers for each mix subgroup at both the lab-produced and plant-produced scales. One significant outlier was removed from the SY mix plant-produced group to make the mean values shown to be representative given the small number of samples tested (4 each for lab-produced and 3 each for plant-produced).

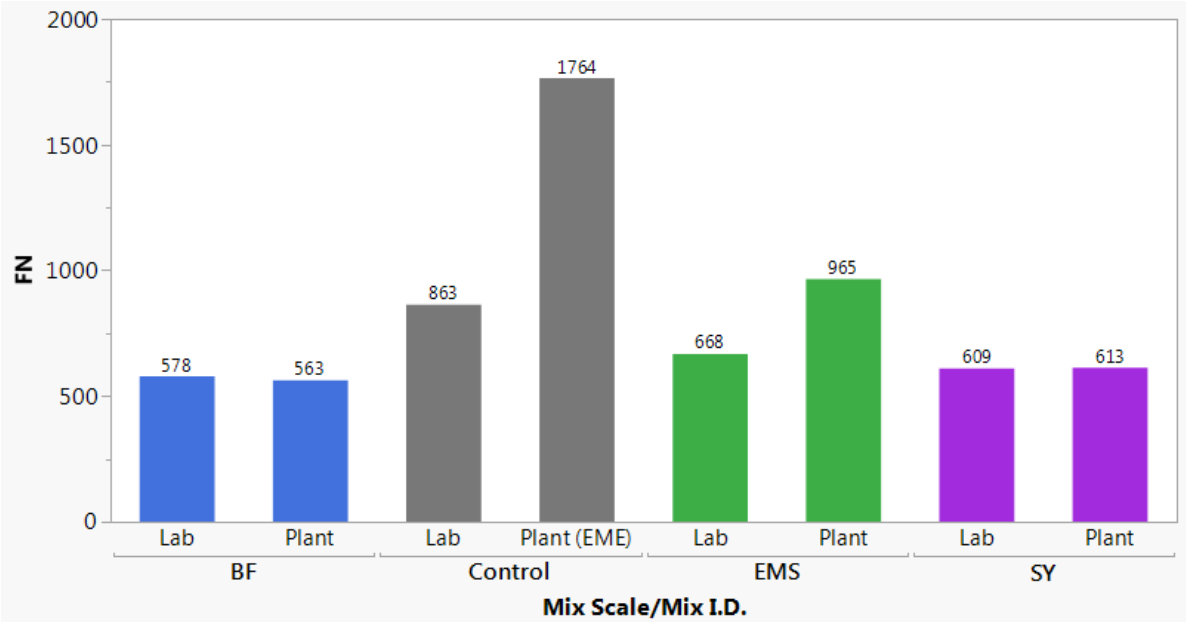

Figure 3.21: Flow Number Summary

Figure 3.13 shows that the control mixes had the greatest flow number within each mix scale category. When a one-way ANOVA test was conducted, the control mixes were the only statistically significant outlier within each mix scale subgroup at an α=0.10 level. At the lab-produced scale, the three mixes with bio-additives have very similar mean flow numbers within a range of 578 (BF) to 668 (EMS). At the plant-mixed scale, the BF and SY mixes have almost identical mean flow numbers as at the lab-mixed scale. The EMS mix; however, shows a somewhat significant increase in flow number at the larger plant-produced scale. These trends mirror the findings of the dynamic modulus testing which showed an increase in stiffness of the EMS mix with at the plant-produced scale. Again, this may indicate the rejuvenator application method of

www.manaraa.com

the EMS mix to be slightly less effective at the larger plant-production scale with higher mixing temperatures, greater fines content, and other associated process control variations. While the mixes with rejuvenating bio-additives (BF, SY, and EMS) had effective performance in reducing the stiffness of the incorporated RAP, the mixes still retained adequate stiffness at high temperatures to resist rutting. Superpave standards in the U.S. recommends a minimum FN of 190 for pavements with 20-year design loads of greater than 10 but less than 30 million ESALs [35].

3.5.2.4. Hamburg wheel-track testing (HWTT)

Hamburg wheel-track testing results provide valuable information about a mix's high-temperature rutting resistance as well as indication of potential stripping issues. The importance of evaluating a mix's rutting resistance at high temperatures was already discussed in the FN results section and the HWTT rutting results will be used a cross-check on FN trends previously analyzed. A mix's stripping inflection point (SIP) is the point at which rutting deflection slopes with consecutive load cycles increase negatively or "hinge". This point indicates when the adhesive matrix bond between binder film and aggregates becomes compromised and individual aggregate particles begin to translate, rotate, and dislocate. Early stripping or a drastic change in accumulated rutting slopes can indicate potential for aggregate loss and moisture intrusion in the pavement structure. Such conditions increase a pavement's susceptibility to freeze-thaw damage and raveling potential [19]. Figure 3.14 shows an example of rut depth increase with consecutive load cycles. The SIP in this example is around 16,000 passes where the inflection slopes change.

www.manaraa.com

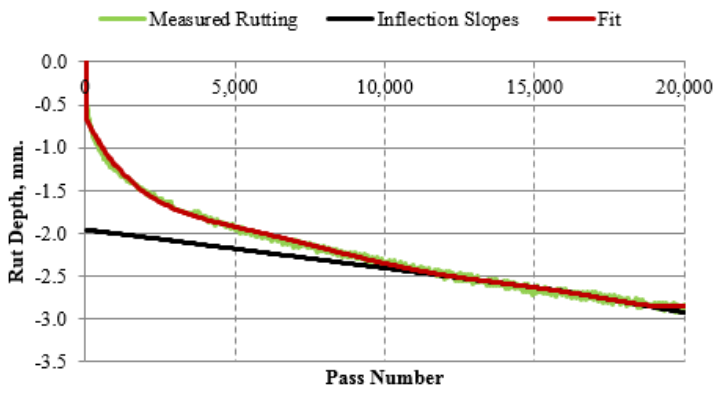

Figure 3.22: Example of HWTT Rut Depth Curve and SIP

Figure 3.15 shows box and whisker plot summaries of mean maximum rut depth at 20,000 passes of the HWTT wheels which marked the end of testing if specimen failure was not reached prior to 20,000 passes. Failure criteria for HWTT rutting was ≥12 mm which is a point where significant wheel-track ponding will begin to occur.

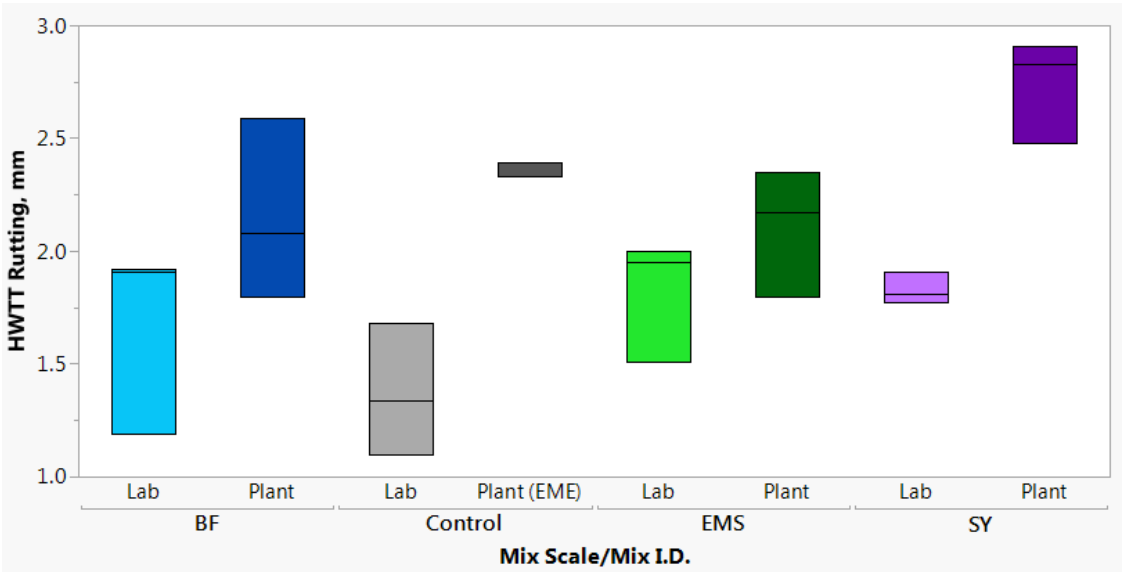

Figure 3.23: HWTT Rutting Summary

Figure 3.15 shows that among the lab-produced mixes, each mix had similar mean maximum rut depths. An ANOVA statistical analysis further showed that all four lab-produced are statistically similar in mean rut maximum rut depths. This finding shows that although the three

www.manaraa.com

mixes with rejuvenating bio-additives effectively reduced the stiffness of the RAP at low and intermediate temperatures, the mixes with bio-additives still have similar rutting resistance at high temperatures as the control mix with 50% RAP. Each mix subgroup experienced an increase in mean maximum rut depth with an increase in mix scale. However, a statistical analysis at the plant-produced scale again showed no significant differences among the mixes including the EME control pertaining to rut depth. When comparing maximum mean rut depths within each mix I.D., the only mix with a statistically significant increase in rut depth was the SY mix. The control mixes were not analyzed due to the differing mix designs. The increase in mean rut depth for the SY mix at the plant-produced scale may be indicative of sensitivity to process control variable differences or a simple overdosing of the rejuvenator at the plant in comparison to the lab mixing operations.

Table 3.11 shows a summary of HWTT stripping performance parameters from the various mix groups. Because the plant-mixed mixes showed greater maximum rut depths, only plant-mixed stripping data was analyzed. The stripping inflection point (SIP) has no criteria but it is favorable to have a SIP at a maximized number of passes to ensure no early stripping will occur. The stripping slope ratio (SR) is simply a ratio of the two slopes that intersect at the SIP. A SR of less than 2.0 indicates that no significant stripping has occurred during the HWTT.

Table 3.11: HWTT Stripping Performance Summary

Mix I.D.	Mean SIP (Passes)	CV, SIP (%)	Tukey HSD, SIP	p-value (ANOVA), SIP	Slope Ratio	CV, SR (%)	Tukey HSD, SR	p-value (ANOVA), SR
Control (EME)	15,685	1.2%	A	0.5137	1.6	21.7%	A	0.1107
Control (Lab)	15,592	1.1%	A		2.1	14.3%	A	
BF	15,695	1.2%	A		1.8	16.7%	A	
SY	15,630	0.9%	A		1.6	12.5%	A	
EMS	15,863	1.6%	A		1.5	10.0%	A	

www.manaraa.com

Table 3.11 shows that each mix subgroup has a statistically-similar mean SIP of over 15,000 passes. When considering SR, the lab-mixed control group has a mean ratio greater than 2.0 indicating that this mix is potentially susceptible to stripping damage. While the other mix subgroups all have mean slope ratios less than 2.0 indicating no stripping potential, the rejuvenated EMS and SY groups have very similar slope ratios to the high-performance control group (EME). The lack of stripping indicators found within the BF, SY, and EMS mixes which contain 50% RAP by mix weight signifies that there are no significant problems with binder blending as they pertain to "black rock" and corresponding adhesive blended matrix interface issues. It also shows the effectiveness of the rejuvenating properties of the BF, SY, and EMS mixes at the plant-production scale even with the process control variations as compared to small-scale laboratory mixing.

3.6. Summary and Conclusions

This research investigated the viability of a novel bio-binder and two rejuvenators in mixes consisting of 50% RAP by mix weight against two controls based on a range of performance tests. The research also focused on a cross-examination of the influence of mix scale and associated process control variations as it pertains to a range of performance tests and volumetrics. Analyzing the effect of mix performance against control mixes at each scale as well as analyzing mix performance across mix scales allows for a more complete understanding of these mixes and better prediction of mix performance in the field. Because most standards and testing guidelines referenced were originally developed for conventional mixes with conventional neat bitumen and no RAP content, a more thorough investigation was deemed necessary.

Low temperature DCT testing showed that the BF, SY, and EMS all had mean fracture energies greater than 400 J/m^2 at -12°C and 7% air voids indicating favorable rejuvenating behavior versus the control with 50% RAP. At the plant-produced scale the BF, SY, and EMS

www.manaraa.com

mixes all had mean fracture in excess of 400 J/m^2 as well as having mean fracture energies greater than the EME high performance control at -12°C and 7% air voids further showing the extent of the rejuvenation effects at improving the resistance to thermal cracking even with a significant RAP binder content. The analysis of mix scale influence on DCT results showed that the BF mix had little sensitivity to the change in process control variables regarding resistance to thermal cracking. The SY and EMS mixes both experienced a slight decrease in thermal cracking resistance with the increase in mix scale; however, the decreases were not statistically significant nor were the lowered results below the minimum recommended fracture energy.

Intermediate temperature beam fatigue testing showed that while the BF, SY, and EMS mixes had K2 fatigue coefficient values within a similar range as the control mixes at the smaller lab-mixed scale, the influence of mix scale was quite pronounced on the K2 coefficients at the larger plant-mixed scale. Because K2 value suggestions are based on conventional mixes, further analyses such as flexural stiffness dissipation with load cycles, mix phase angle rates of increase with load cycles, and dynamic modulus results are all important in predicting field performance of high RAP content mixes with bio-additives. The increase in mix scale with varying heating applications, mix processing, and other process control variances had varied effects on the BF, SY, and EMS mix flexural stiffnesses and stiffness dissipation at different strain levels. Changes in flexural stiffness among mixes at the two mix scales is likely most attributable to rejuvenator volatilization and application rate variation at the two scales and potentially an increase in fines content reducing the effective neat binder content within the mix matrices and increasing the initial stiffness. Therefore, aggregate gradations and rejuvenator application and heating times must be carefully monitored to ensure the accuracy of lab-mixed test results to predicting field performance when addressing fatigue.

www.manaraa.com

Flow number and HWTT results were used to assess the mixes' resistance to rutting and stripping. Flow number results showed that at both scales, the control mixes had the statistically-greatest flow number indicating their relative greater stiffnesses at high temperatures. The BF, SY, and EMS mixes all had stiffness reductions due to rejuvenating effects; however, all three mixes still provided flow numbers well above the U.S. standard recommended minimum for pavements with 20-year design loads of greater than 10 million but less than 30 million ESALs. Mix scale influence analyses on flow number results showed little influence on the BF mix results and mean flow number increases with increasing mix scale for the rejuvenated SY and EMS mixes. The increase in flow number is a result of increasing mix stiffness due to process control variations such as increased mixing temperatures at the plant-production scale. The HWTT results showed excellent rutting resistance for all mixes tested at each mix scale. Small-scale mixes had less rutting than the large-scale mixes despite the flow number result trends. The only mix with a statistically significant increase in rutting was the SY mix when increasing mix scale which indicates a potentially greater dosage of rejuvenator being applied at the plant or simply more time was allowed for the rejuvenator to activate the RAP binder content. Results further showed no stripping is predicted for the BF, SY, and EMS mixes while stripping is predicted for the 50% RAP control mix. These findings point to the conclusion that the rejuvenating effects of the bio-additives improve the binder diffusibility of the RAP and virgin binders which potentially increases the degree of binder blending.

Some significant broad conclusions can be made from the analyses and results found within this research. In an age where fossil fuels become scarce or economically unfeasible to use in production of virgin flexible pavement mixes, bio-additives can be used successfully with 50% RAP by mix weight to develop pavements that pass all performance criteria for conventional mixes

www.manaraa.com

with conventional bitumen for design loads of greater than 10 million but less than 30 million ESALs based on laboratory evaluations. Mixes with high RAP contents and bio-additives or rejuvenators are potentially more sensitive to mix scale changes and process control variations than conventional mixes. Aggregate gradation changes and plant conditions must be carefully considered before using lab-mixed pavement performance test results to predict field performance. High RAP content mixes incorporating bio-additives should address fatigue performance using a multi-faceted approach as different analyses produce variable results. Finally, current standards and specifications for mix performance analysis should be used as a starting guideline when considering high RAP content mixes with bio-additives because such standards and specifications may not fully realize the benefits of these particular kinds of mixes.

References

1. FHWA, U.S. Department of Transportation Federal Highway Administration. "Reclaimed Asphalt Pavement in Asphalt Mixtures: State of the Practice." *FHWA Publication No. FHWA-HRT-11-021*. April 2011.

2. National Center for Asphalt Technology (NCAT): *Hot Mix Asphalt Materials, Mixture Design and Construction, 3rd ed.*, NCAT. 1991.

3. EAPA (European industry association), Asphalt in Figures, 2016. [www.eapa.org]

4. Ali, Hesham. "Long-Term Aging of Recycled Binders." Florida International University: Civil and Environmental Engineering Department; submitted to the Florida Department of Transportation. July 2015.

5. Haghshenas et al. "Research on High-RAP Asphalt Mixtures with Rejuvenators and WMA Additives." University of Nebraska-Lincoln: Nebraska Department of Roads Research Reports. September 2016.

6. Kowalski et al. "Thermal and Fatigue Evaluation of Asphalt Mixtures Containing RAP Treated with a Bio-Agent." *Applied Sciences, Vol. 7, Issue 3*. February 2017.

www.manaraa.com

7. Mogawer, Walaa & Booshehrian, Abbas & Vahidi, Siavash & Austerman, Alexander. (2013). "Evaluating the effect of rejuvenators on the degree of blending and performance of high RAP, RAS, RAP/RAS mixtures." *Road Materials and Pavement Design*. 14. 10.1080/14680629.2013.812836.

8. P. Turner, A. Taylor, N. Tran. "Laboratory evaluation of SYLVAROAD™ RP1000 Rejuvenator." NCAT report 15-03, June 2015. https://eng.auburn.edu/research/centers/ncat/files/technical-reports/rep15-03.pdf

9. Zaumanis et al. "Influence of Six Rejuvenators on the Performance Properties of Reclaimed Asphalt Pavement (RAP) Binder and 100% Recycled Asphalt Mixtures." *Construction and Building Materials.* November 2014.

10. Jiménez del Barco Carrión, A., Pérez-Martínez, M., Themeli, A., Lo Presti, D., Marsac, P., Pouget, S., Chailleux, E., Airey, G. D. (2017). Evaluation of bio-materials' rejuvenating effect on binders for high-reclaimed asphalt content mixtures. *Materiales de Construcción*, *67*(327), 1–11.

11. Jiménez del Barco Carrión, A., Lo Presti, D., Pouget, S., Airey, G., & Chailleux, E. (2017). Linear viscoelastic properties of high reclaimed asphalt content mixes with biobinders. *Road Materials and Pavement Design*, 1–11.

12. Y.H. Huang. *Pavement Analysis and Design*. Second Edition, Prentice Hall, New Jersey, 2004.

13. Andrew Hanz, Ervin Dukatz & Gerald Reinke (2017). "Use of performance-based testing for high RAP mix design and production monitoring." *Road Materials and Pavement Design*, 18:sup1, 284-310.

14. Biophalt patent US 8,652,246 B2

15. Pouget S. & Loup L. "Thermo-mechanical behaviour of mixtures containing bio-binders." *Road Materials and Pavement Design*, vol.14, Special Issue EATA, pp. 212-226, 2013.

16. ASTM D2172. "Standard Test Methods for Quantitative Extraction of Asphalt Binder from Asphalt Mixes." Standard Specifications for Transportation Materials and Methods of Sampling and Testing, Washington D.C., 2007.

www.manaraa.com

17. ASTM D7906. “Standard Practice for Recovery of Asphalt from Solution Using Toluene and the Rotary Evaporator.” Standard Specifications for Transportation Materials and Methods of Sampling and Testing, Washington D.C., 2007.

18. Porot, L. and W. Grady. “Effectiveness of a bio-based additive to restore properties of aged asphalt binder”. Proc., International Society for Asphalt Pavements (ISAP) Symposium. 2016.

19. Elkashef, Mohamed Elsayed, "Using soybean-derived materials to rejuvenate reclaimed asphalt pavement (RAP) binders and mixtures" (2017). Graduate Theses and Dissertations. 15514. https://lib.dr.iastate.edu/etd/15514

20. Vavrik et al. *Bailey Method for Gradation Selection in Hot-Mix Asphalt Design*. Transportation Research Circular No. E-C044. October 2002.

21. Asphalt Institute. Asphalt Mix Design Methods, 7th Edition. MS-2. 2014.

22. AASHTO T 331-13. “Standard Method of Test for Bulk Specific Gravity (Gmb) and Density of Compacted Hot Mix Asphalt (HMA) Using Automatic Vacuum Sealing Method.” Standard Specifications for Transportation Materials and Methods of Sampling and Testing, Washington D.C., 2015.

23. AASHTO T 209. “Theoretical Maximum Specific Gravity and Density of Hot Mix Asphalt (HMA).” Standard Specifications for Transportation Materials and Methods of Sampling and Testing, Washington D.C., 2015.

24. ASTM D7313. “Standard Test Method for Determining Fracture Energy of Asphalt-Aggregate Mixtures Using the Disk-Shaped Compact Tension Geometry.” Standard Specifications for Transportation Materials and Methods of Sampling and Testing, Washington D.C., 2007.

25. AASHTO T 321. “Determining the Fatigue Life of Compacted Asphalt Mixtures Subjected to Repeated Flexural Bending.” Standard Specifications for Transportation Materials and Methods of Sampling and Testing, Washington D.C., 2017.

26. AASHTO TP 79-13. “Determining the Dynamic Modulus and Flow Number for Asphalt Mixtures Using the Asphalt Mixture Performance Tester (AMPT).” Standard Specifications for Transportation Materials and Methods of Sampling and Testing, Washington D.C., 2013.

www.manaraa.com

27. AASHTO T 378. “Determining the Dynamic Modulus and Flow Number for Asphalt Mixtures Using the Asphalt Mixture Performance Tester (AMPT).” Standard Specifications for Transportation Materials and Methods of Sampling and Testing, Washington D.C., 2017.

28. AASHTO T 324. “Standard Test Method for Hamburg Wheel-Track Testing of Compacted Asphalt Mixtures.” Standard Specifications for Transportation Materials and Methods of Sampling and Testing, Washington D.C., 2017.

29. W.G. Buttlar, S. Ahmed, E.V. Dave, and A.F. Braham. “Comprehensive Database of Asphalt Concrete Fracture Energy and Links to Field Performance.” Paper presented at the 89th Annual Meeting of the Transportation Research Board, Washington, D.C., January 2010.

30. Cascione et al. “Laboratory Evaluation of Field Produced Hot Mix Asphalt Containing Post-Consumer Recycled Asphalt Shingles and Fractionated Recycled Asphalt Pavement.” Asphalt Paving Technology 2011, Association of Asphalt Paving Technologies, Vol. 80.

31. S.H. Carpenter. “Fatigue Performance of IDOT Mixtures.” Research Report FHWA-ICT-07-007, Illinois Center for Transportation, July 2006.

32. Tang, Sheng, "Evaluate the fracture and fatigue resistances of hot mix asphalt containing high percentage reclaimed asphalt pavement (RAP) materials at low and intermediate temperatures" (2014). Graduate Theses and Dissertations. 13782. https://lib.dr.iastate.edu/etd/13782.

33. Banerjee, Ambarish & de Fortier Smit, Andre & A. Prozzi, Jorge. (2012). “Influence of operational tolerances on HMA performance.” *Construction and Building Materials*. 27. 15–23.

34. Mohammadreza Sabouri, Thomas Bennert, Jo Sias Daniel & Y. Richard Kim. (2015). “A comprehensive evaluation of the fatigue behaviour of plant-produced RAP mixtures.” *Road Materials and Pavement Design*,16:sup2, 29-54.

35. National Cooperative Highway Research Program. “NCHRP Report 673: A Manual for Design of Hot Mix Asphalt with Commentary.” Transportation Research Board, Washington D.C., 2011.

www.manaraa.com

CHAPTER 4: CHARACTERIZATION OF IN-SITU PERFORMANCE OF HMA MIXES INCORPORATING HIGH RAP CONTENTS AND NOVEL BIO-ADDITIVES

Modified from a paper to be submitted to Road Materials and Pavement Design

Nicholas D. Manke[a]*, R. Christopher Williams[a], Zahra Sotoodeh-Nia[a], Eric W. Cochran[b], Laurent Porot[c], Emmanuel Chailleux[d], Simon Pouget[e], Francois Olard[e]

[a] *Department of Civil, Construction, and Environmental Engineering, Iowa State University, Ames, Iowa, 50011*
[b] *Department of Chemical, and Biological Engineering, Iowa State University, Ames, Iowa, 50011*
[c] *Kraton Corporation, Arizona Chemical*
[d]*Department of Materials and Structures, IFSTTAR*
[e]*EIFFAGE Infrastructures,France*
**Corresponding author: nmanke@iastate.edu*

Abstract

As the world population increases and cities continue to grow, the strain on existing aging transportation infrastructure is ever-growing. While the demand for new paved roadway extensions and existing roadway replacement and rehabilitation are on the rise, sources of economical, quality aggregates and funding are decreasing. In order to meet the demand provided the limitations, new ingenuity must be used to increase utilization of recyclable materials and refinable products/industrial co-products. Reclaimed asphalt pavement (RAP) is a readily available material in many nations. While much of the RAP around the world is utilized as granular fill for construction sites or granular base material, these uses often do not most effectively recycle the bitumen content, creating better value. Aged bitumen increases the stiffness of a pavement which is favourable at high temperatures to resist rutting, but generally unfavourable at low and intermediate temperatures where brittle cracking failures are prevalent and increased elastic

www.manaraa.com

recovery potential is preferred. The use of rejuvenating bio-additive agents can effectively balance these properties in high RAP content mixes. However, the unconventional nature of 50% RAP content mixes with novel bio-additives means that laboratory-based test procedures and standards are potentially not well-suited to accurately characterize these mixes' performance in the field. This research investigates the in-situ performance of three 50% RAP content mixes with three novel bio-additives using in-situ accelerated pavement testing (APT) measurements as well as mechanistic-empirical computer predictions. Performance criteria assessed includes rutting resistance and fatigue cracking (bottom-up and top-down) as well as performing sensitivity studies for construction specification and traffic condition impacts on performance. Results showed that computer modelling can be effectively used to project APT data for rutting to greater in-situ loading conditions. The coupling of results also allows for the modelling of performance trends over time with critical temperature and loading relative to the distress under consideration. Two of the mixes incorporating novel bio-additives were predicted to perform as well as the high-performance, 20% RAP control mix with the third mix incorporating a novel bio-additive performing just below the others. For all mixes considered, top-down longitudinal cracking was the critical failure distress limiting the pavement 20-year design.

4.1. Introduction

Rising construction costs, limited funding, and increasing scarcity of economical, quality virgin materials has led many agencies, owners, and engineers to search for alternative methods for rehabilitating and rebuilding aging infrastructures. Many nations rely on transportation infrastructure for both travel and shipping of goods. Therefore, it is often not a possibility to simply let paved roadways continue to degrade without repair and replacement. The increase in demand for pavements with limitations to the supply of quality, economical materials and funding means

www.manaraa.com

that unconventional methods are on the forefront of consideration. By utilizing recycled materials and refined industry byproducts and co-products, material costs and non-renewable material source depletion attributable to asphalt paving can be reduced. Reclaimed asphalt pavement (RAP, or RA in EU convention) is a readily available material in many locales and provides a viable partial solution to the current limitations. Reclaimed pavement is currently the most recycled material by weight in the U.S. with over 80 million tons recycled annually [1,2]. Europe also recycles over 40 million tons of asphalt pavement annually [3]. Much of the reclaimed pavement is used as construction site fill or granular base material instead of incorporation into new mixes where the bitumen content is fully utilized.

Although laboratory testing has shown great success with the use of properly engineered asphalt mixes incorporating high RAP contents and bio-additives, there remains much hesitation to rely on small-scale testing outcomes for mass implementation. Due to the variances in quality control when dealing with larger quantities in the field and the fact that laboratory testing standards were developed based on conventional mix designs with conventional materials, such hesitation is potentially warranted. However, if it can be shown that in-situ accelerated pavement testing (APT) coupled with computer modeling predictions can provide good modeling and predictions for these unconventional mix design performances in the field, such hesitation could be overcome.

As part of the BioRePavation project, this research analyzes in-situ APT measurements for three mix designs incorporating 50% RAP by mix weight and three novel bio-additives with rejuvenating properties. To further build on the in-situ results, computer software was used to develop statistical models for pavement performance based on critical equivalent single axle loads (ESALs) relative to the distress considered. Software predictions were based on measured mix properties from laboratory test results and simulated 20 years of environmental and traffic loading.

www.manaraa.com

Beyond performance verification, the data and modeling were also used to assess mix performances against various traffic conditions as well as construction criteria and tolerances. Full analyses can be used for predicting mix performance in other climate regions as well as provide considerations for construction and design criteria to maximize mix performance at a range of temperatures and distresses.

4.2. Background

In many specifications, "high" RAP contents are defined as those that meet or exceed 30% by mix weight. According to recommendations by the Federal Highway Administration (FHWA), mixes incorporating greater than 30% RAP require more intensive design strategies than simply incorporating a softer bitumen [1]. At RAP contents of greater than 30% by mix weight, the aged binder content of the RAP often begins to significantly alter the performance of the new mix which must be properly balanced. As bitumen ages, it undergoes chemical and physical changes through polycondensation, oxidative processes, and volatilization of maltene fractions [4]. Changes undergone by the bitumen can affect the mechanical characteristics of mixes incorporating significant RAP contents by making them "stiff", or more prone to brittle failure mechanisms under mechanical and environmental loading. Although a "stiffer" mix is typically beneficial to reducing rutting potential, incorporation of RAP can create insufficient blending of the aged and neat binders and lead to "black rock". Inclusions of "black rock" can cause premature moisture damage like stripping, localized rutting, and freeze-thaw-induced crack propagation from weak aggregate-binder interfaces [5,6].

Increasing the degree of blending of recycled and neat binders as well as balancing the stiffness of the blended binder content can be achieved with varying results. The use of rejuvenating agents as well as the use of soft viscoelastic materials as a partial or complete

www.manaraa.com

replacement to conventional neat bitumen are common solutions to overcome some of these challenges. Today's rejuvenators can be used to chemically rebalance the ratios of maltene to asphaltene molecules by breaking polycondensed intermolecular associations [5]. Rejuvenators have been shown to effectively improve the thermal and fatigue cracking resistance of mixes incorporating 40% RAP as well as up to 100% RAP as an aggregate source [7,8]. While some research has shown that rejuvenators can enhance the diffusibility of neat bitumen with the aged bitumen [7], other studies have indicated that some rejuvenators adversely impact a mix's resistance to rutting and stripping at high doses [7,8]. However, anti-stripping agents or polymer modification can be used to enhance resistance to stripping and rutting, respectively. Research conducted on a non-bituminous binder manufactured from polymer-stabilized pine chemistry has been shown to have rejuvenating effects and promising properties for use in low to medium-volume roadways when used with 50% RAP by mix weight [9,10].

There is little published research available using APT results in tandem with mechanistic empirical software predictions to model pavement performance of high RAP content mixes incorporating bio-additives with rejuvenating properties. A study on mechanistic empirical modeling predictions for pavements incorporating reclaimed asphalt shingles (RAS) and recycling agents found that the software does not fully account for the complex nature of mixes incorporating unconventional materials or high concentrations of aged binders [11]. Research on the viability of using mechanistic empirical modeling predictions for warm mix asphalt mixes with rejuvenators has also shown promising results for software modeling use in predicting in-situ pavement performance [12,13].

www.manaraa.com

4.3. Materials and Mix Designs

This section provides a summary of material sources, mix designs, and mix volumetrics. Summaries of mix compositions and characteristics outline the primary material and design differences among the various mixes tested for performance on the APT carrousel as well as the computer modeling.

4.3.1. Materials

Materials used for laboratory testing were provided by the paving contractor EIFFAGE to ensure the representativeness of laboratory and computer modeling results to the in-situ full-scale field testing. Aggregates used were from the same quarry sources and RAP stockpile for all testing at both the laboratory and full-scale levels. The RAP was fractionated into coarse (8/12 mm) and fine (0/8 mm) fractions. Bulk shipments of RAP for the purpose of laboratory testing was oven-dried at low temperature to prevent excessive binder aging and split to ensure statistical uniformity of the materials. Binders used were a neat 50/70 pen grade bitumen and a novel bio-binder called Biophalt® (BF) which were provided by EIFFAGE [14,15]. Two rejuvenators were also used in this research. The first, SYLVAROAD™ RP1000 (SY), is produced from refined pine chemistry which is a co-product of paper production and used to treat RAP through direct application [16]. The second rejuvenator, epoxidized methyl soyate (EMS), is produced from soybean chemistry and is blended with neat bitumen for application rather than direct application to the RAP itself [17].

The binder content of the RAP was separated for binder evaluation and performance grading using toluene-aided dissolving and distillation following the guidelines of ASTM D 2172 [18] and ASTM D 7906 [19]. Neat and blended binder grades were determined following

www.manaraa.com

Superpave performance grading (PG) methodology as well as all applicable ASTM and AASHTO test standards. Table 4.1 provides a summary of neat and blended binder performance grades as well as standard European bitumen properties.

Table 4.1: Neat and Blended Binder Characteristics

Binder I.D.	Performance Grade (PG)	Penetration (x0.1mm)	Softening Point (°C)	Fraass Breaking Point (°C)
Control: 50/70 pen grade bitumen	PG 64-22	55	49.0	-7
RAP binder	PG 94-4	7	81.0	+14
BF virgin binder	N/A	147	73.5	-15
Control + RAP binder	PG 76-16	25	61.8	+1
BF + RAP binder	PG 58-22	80	68.8	-7
Control + RAP binder + SY	PG 76-22	33	57.2	-4
Control+ RAP binder+ EMS	PG 70-22	21	60.8	+1
Control + reduced RAP binder (EME)	PG 82-xx	N/A	N/A	N/A

Due to the unconventionally sticky nature of the neat BF binder, it was unable to be accurately performance graded using the dynamic shear rheometer (DSR). The EME control mix is a standard high-performance French mix design consisting of conventional bitumen and 20% RAP by mix weight so this recovered binder was only tested for high temperature performance.

4.3.2. Mix designs

While most analyses included within this research focus on plant-produced mixes to correspond with in-situ carrousel performance results, laboratory-mixed mix designs and results will also be included as part of a sensitivity analysis. The laboratory control mix design is significantly different from the in-situ plant control mix design (referenced as EME). Table 4.2 provides a summary of mixes used in laboratory analysis and plant-scale mixes used in construction of the pavement sections for the accelerated pavement testing carrousel.

www.manaraa.com

Table 4.6: Mix Design Summary

Mix I.D.	Mix Scale	RAP Content (by mix wt.)	Binder Content (total by mix wt.)	Bio-additive Dosage	NMAS (mm)
Control (bitumen)	Lab	50%	4.49%	0%	19.0 mm
	Plant (EME)	20%	5.26%		12.5 mm
BF	Lab	50%	4.49%	100% by wt. of virgin binder	19.0 mm
	Plant		4.44%		
SY (bitumen + SY)	Lab	50%	4.49%	6% by wt. of RAP binder	19.0 mm
	Plant		4.49%		
EMS (bitumen + EMS)	Lab	50%	4.49%	3% by wt. of virgin binder	19.0 mm
	Plant		4.36%		

In addition to the summary of mix binder and additive compositions, summaries of mix volumetrics are important to help explain performance behaviors. The 19.0 mm NMAS mixes require a minimum pavement lift thickness of 76 mm (3 inches) while the 12.5 mm NMAS EME control mix requires a minimum lift thickness of 50 mm (2 inches) [20].

Table 4.3 provides a summary of mixture volumetrics for the laboratory-mixed control with 50% RAP content and the plant-mixed mixes used in this research. Target binder contents for the mixes with 50% RAP content were 2.8% neat binder and 1.69% RAP binder by mix weight resulting in total target binder contents of around 4.5% by mix weight. Requirements shown follow Superpave standards for dense-graded mixes with a NMAS of 19.0 mm and a 20-year design traffic level of greater than 10 million but less than 30 million ESALs with a final design air void (V_a) content of 4.0%.

www.manaraa.com

Table 4.3: Mixture Volumetrics

Property	Control (Lab)	Control (EME)	BF	SY	EMS	Requirement
P_b (%)	4.49	5.26	4.44	4.49	4.36	-
VMA (%)	13.2	18.9	15.8	15.8	15.0	>13.0
VFA (%)	69.5	71.6	71.9	71.7	70.9	65-78
DP	0.7	1.5	2.4	2.5	2.4	0.6-1.2
G_{mm}	2.63	2.55	2.59	2.60	2.61	-
G_{mb}	2.52	2.37	2.40	2.42	2.43	-

Voids in the mineral aggregate (VMA), voids filled with asphalt (VFA) and dust proportion (DP) values shown in Table 3 were calculated using standard Superpave equations [20]. Reported bulk specific gravities (G_{mb}) and maximum theoretical specific gravities (G_{mm}) were evaluated using the CoreLok® method in the AASHTO T 331 standard [21] and AASHTO T 209 [22] standard, respectively. The Superpave standard requirement for VMA varies by mix NMAS, and a suggested minimum VMA is 14.0 for the EME control mix with the 12.5 mm NMAS. It is also recommended that the VMA should not exceed the minimum requirement by more than 2% to reduce proneness to flushing and rutting [20]. However, these requirements are applicable to dense-graded mixes, so a slightly greater VMA is likely due to the gap-graded nature of the 19.0 NMAS mixes. Further, the high DP values relative to the requirement is more in line with a stone matrix asphalt (SMA) mix which is also gap-graded. These mixes require more fines to fill larger voids; however, they also typically include binder contents (P_b) of around 6%. The lower binder contents coupled with the higher fines content may create a stiffer mix less prone to rutting, but also may require more field compaction energy to achieve the required design density [20].

4.4. Experimental Design and Modeling Inputs

This section provides an overview of the overall experimental design and inputs used to generate the computer modeling predictions. Due to the exhaustive and complex nature of the

www.manaraa.com

totality of modeling inputs, only the inputs used to simulate the APT carrousel sections and laboratory-measured material properties are provided in this research.

4.4.1. Laboratory assessment of materials

Material properties used in computer predictive modeling were assessed using laboratory testing. Properties such as mix moduli and binder complex modulus and phase angles are used by the software to predict pavement response to loading as well as aging.

4.4.1.1. Dynamic modulus testing procedure

Dynamic modulus performance testing allows for the assessment of mix response to a wide range of loading frequencies within the linear viscoelastic domain. Test results include both the dynamic moduli (E*) and phase angle (δ) which are valuable in predicting changes in stiffness and viscous/elastic response, respectively over a wide range of critical temperature-frequency scenarios. Testing was conducted on five specimens of each mix subgroup with respective mean values constituting master curve inputs. Each specimen tested was laboratory-compacted using a gyratory compactor to the target air void content (4% or 7%) and dimensions (150 mm in height by 100 mm in diameter). Although the air void contents for dynamic modulus testing differ from those measured on the in-situ carrousel, a sensitivity analysis was conducted with results presented later in this research. Compacted specimens were loaded individually into a universal testing machine (UTM) and tested following AASHTO TP 79 standards at various temperatures and a range of frequencies [23]. Each specimen was subjected to sinusoidal axial compressive loading at three temperatures (4, 21, and 37°C) and eight frequencies (25, 10, 5, 2, 1, 0.5, 0.2, and 0.1 Hz) to obtain a dataset of auto-calculated dynamic moduli and phase angles. These datasets were then

www.manaraa.com

used to construct sigmoidal master curves. The sigmoidal function used to shift the raw data is shown in Eq. 4.1.

$$Log|E^*| = a + \frac{b}{1+e^{\beta+\gamma(log f_R)}} \quad \text{[Eq. 4.1]}$$

where:

f_R = reduced frequency at reference temperature in Hz,

a = minimum value of E* in MPa,

a + b = maximum value of E* in MPa, and

β, γ = fitting coefficients.

4.4.1.2. Mix master curves

Predicted master curves within the linear viscoelastic range were developed for three main categories: laboratory-mixed specimens at 7% air voids, laboratory-mixed specimens at 4% air voids, and plant-mixed, laboratory-compacted specimens at 7% air voids. Both mix complex modulus (E*) and phase angle (δ) are shown although the mix phase angles were not used as inputs into the computer modeling analyses. Figure 4.1 shows the master curves (E*) and phase angles (δ) for the four plant-mixed mixes at 7% AV. Master curves for laboratory-mixed specimens at 4% and 7% AV are not shown here because they were only used for the sensitivity analyses.

www.manaraa.com

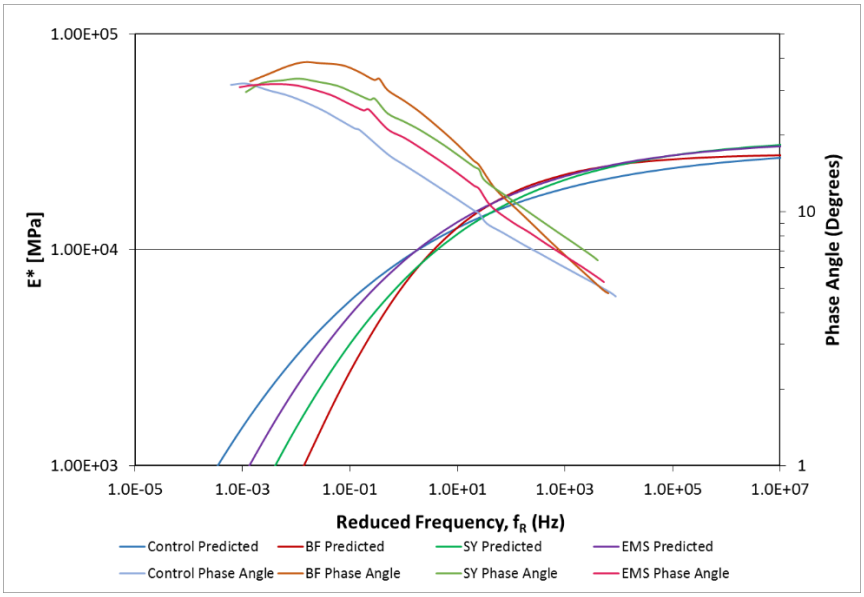

Figure 4.1: Plant-Mixed Specimen Master Curves, 7% AV

4.4.1.3. Binder testing procedures

Blended binder contents (neat binders with RAP binder content and/or any additives) were laboratory-tested to assess required material properties for inputs in the computer modeling analyses. Binders were laboratory-blended using a shear-mill based on design binder and additive contents except for the EME binder which was extracted and recovered for testing. It should be noted that neat and aged binders and additives are not assumed to be fully blended within the mix matrix. This reason is why both blended binder as well as mix properties are used in simulation modeling analyses. Because the in-situ pavement sections underwent short-term aging through the mixing and construction processes, rolling thin film oven (RTFO)-aged blended binders were used for analysis to offer a more direct comparison with the in-situ pavement test results.

After the respective binders were fully blended using a shear mill, they were short-term aged using a rolling thin film oven (RTFO) in accordance with ASTM D 2872 standards [24]. Representative aging is important when using unconventional binders and rejuvenating agents because a portion of those additives volatilize during the mixing and construction processes.

www.manaraa.com

Blended binders' complex moduli (G*) and phase angles (δ) were measured at varying temperatures using a DSR. Testing followed ASTM D 7175 standard procedures [25] and collected data (G*, δ, test temperature) were used as computer modeling inputs to characterize binder behavior under mechanical and environmental loading.

4.4.2. In-situ carrousel design and implementation

The in-situ accelerated pavement testing on the carrousel was conducted near Nantes, France using the IFSTTAR facilities and an EIFFAGE asphalt plant for mix production. This carrousel consists of a 120-meter long test track with a concentrically-located motor and four protruding arms. Each arm has loaded axle configurations which constitute successive load passes and the accelerated accumulation of ESALs. Figure 4.2 shows the IFSTTAR carrousel configuration along with layer construction cross-section for reference.

Figure 4.2: IFSTTAR Accelerated Pavement Test Track

The inner pavement sections (radius of about 17m) in Figure 4.2 are for rutting testing while the outer pavement sections (radius of about 19m) are for fatigue testing. Each pavement section was constructed on compacted granular base layers with base layer bearing capacities measured using dynamic plate load testing. Pavement sections were also installed with embedded instrumentation to measure strains as well as pavement temperatures throughout the loading

www.manaraa.com

sequences. Subsequently-compacted asphalt layers averaging about 100-mm thick were measured for air void content using a Troxler device. Each section was also cored for volumetric air void measurements at a different university. Table 4.4 provides a summary of pertinent carrousel pavement section characteristics upon construction. The cross-section shown in Figure 4.2 can be referenced for layer designations pertaining to bearing capacities.

Table 4.4: Accelerated Pavement Test Carrousel Section Summary

Mix I.D.	Mean Bearing Capacity (MPa)			Mean Air Voids (%)		Mean Pavement Thickness (mm)
	Subgrade	Base 2	Base 1	Troxler	Cores	
EME	82	80	94	4.3	3.4	102
BF	81	88	93	3.3	1.6	95
SY	63	83	103	2.9	3.3	86
EMS	85	88	102	4.5	2.0	91

As seen in Table 4.4, the measured bearing capacities of the base and subgrade layers are appreciably uniform amongst the pavement sections except for the lower subgrade layer mean bearing capacity for the SY section. Mean air voids measured deviated slightly from target air voids for the SY and BF pavements according to Troxler measurements and core air void measurements were significantly lower than expected target values of around 4.0-4.5% based on design predictions. There is also some slight variability in mean pavement thickness. Although these variabilities do not appear to be significant, they indicate the need for careful analysis of the raw performance data to be able to attribute performance differences to the materials themselves rather than on construction variables. Computer modeling sensitivity analyses were conducted to similarly help understand the impact that such construction variables may have on pavement performance measured at the carrousel.

www.manaraa.com

4.4.3. Computer modeling inputs

Computer modeling was performed using AASHTOWare® Pavement M-E Design software of the latest 2018 version. The software allows one to simulate and predict various pavement distress progressions over the design life of the pavement accounting for both mechanical and environmental loading as well as seasonal variables such as freeze-thaw cycle impacts on subgrade modulus, etc. Pavement M-E Design software does not; however, accurately account for pavement aging when predicting distresses over time. Computer modeling inputs were used to reflect both the carrousel site conditions as well as several sensitivity analyses. Table 4.5 provides a summary of model run configuration designs used in this research.

Table 4.5: Computer Modeling Run Summary

Mix I.D.	Mix Scale (s)		AV (%)		ADTT (trucks/day)		Speed (mph/km/h)	
Input Levels	Lab	Plant	4%	7%	150	1250	30/48	55/89
Control (Lab)	X		X	X	X	X	X	X
Control (EME)		X		X	X	X	X	X
BF	X	X	X	X	X	X	X	X
SY	X	X	X	X	X	X	X	X
EMS	X	X	X	X	X	X	X	X

Table 4.5 shows a hierarchy from left to right. For instance, plant mixes were only laboratory-tested for properties at 7% air voids (AV), so thus the EME control does not include a sensitivity analysis for air void content. Similarly, average daily truck traffic (ADTT) in the design lane and traffic speed were both conducted as sensitivity analyses on the applicable air mix scale and/or air void contents indicated for each mix i.d. An ADTT of 150 trucks/day in the design lane and a traffic speed of 30 mph (48 km/h) are analogous to carrousel loading conditions for reference.

A location input was required to characterize weather conditions and environmental effects on both the pavement structure and sub-structures. A location near Coos Bay, Oregon, U.S., was determined to be similar in temperatures and rainfall to Nantes, France where the carrousel is

www.manaraa.com

located. A uniform pavement thickness of 4-inches (101 mm) was used to reflect the target design pavement thickness of the carrousel pavement sections. Moduli data inputs included measured and sigmoidal-predicted dynamic moduli based on the developed master curves with data points at five temperatures (-10, 4, 21, 37, and 54°C) and six frequencies (0.1, 1, 5, 10, 20, and 25 Hz). Dynamic moduli inputs at the five temperatures and six frequencies were calculated from the sigmoidal master curves which were determined using the dynamic modulus test data from laboratory testing. Dynamic moduli inputs were used by the software to construct mix master curves based on the software pre-set Witczak model instead of the sigmoidal model [26]. Binder inputs included complex moduli (G*) and phase angles (δ) of the RTFO-aged blended binders at various test temperatures above and below their respective failure points to create binder master curves for the software to use for performance modeling. Finally, base layer gradations and relative bearing capacities for each layer were input with corresponding layer thicknesses and failure criterion were set for performance standards. Bearing capacities were estimated using the California bearing ratio (CBR) values of representative materials while still being sufficiently conservative. Research comparing the dynamic modulus of deformation (E_{vd}) as measured by a dynamic plate load test to CBR values of common materials shows conflicting trends when back-calculating measured moduli values on the APT carrousel and estimated CBR values [27]. Based on the trends, for an A-4 class material with an E_{vd} of 80 MPa, the corresponding CBR value would be 61% which is significantly greater than would be expected [27]. Tables 4.6 and 4.7 summarize the base and subgrade layer inputs and performance failure criterion, respectively.

www.manaraa.com

Table 4.6: Pavement Substructure Input Summary

Layer I.D.	Layer Thickness		CBR (%)	Resilient Modulus (M_R)	
	(inches)	(cm)		(psi)	(MPa)
Base Layer 1	8.0	20.3	20.0	17,380	120
Base Layer 2	10.0	25.4	20.0	17,380	120
Base Layer 3	12.0	31.5	18.0	16,247	112
Subgrade	Semi-Infinite	Semi-Infinite	-	18,000	124

Table 4.7: Performance Failure Criterion Summary

Performance Criterion	Failure Limit (Imperial)	Failure Limit (Metric)
Rutting (AC only)	≤ 0.4 inches	≤ 10 mm
Rutting (Total)	≤ 0.75 inches	≤ 19 mm
Bottom-up Fatigue Cracking	≤ 25% lane area	≤ 25% lane area
Top-down Longitudinal Cracking	≤ 2,000 ft./lane-mile	≤ 380 m/lane-km

4.5. Rutting Characterization

This section provides rutting performance results from the in-situ APT carrousel in France as well as the predictive computer modeling results for pavement sections under similar loading and traffic speeds as the APT carrousel. While the climate conditions selected for the computer models were chosen to reflect the climate near the APT carrousel, rutting results were further analyzed to reflect both the total ESALs (total temperature range) as well as high temperature ESALs (temperature range with a predicted pavement surface temperature greater than or equal to 30°C). This further analysis not only more accurately reflects critical high temperature loads generating the greatest amount of rutting in the pavement sections, but also allows for the prediction of pavement performances regarding pavement life span in other climate areas. Carrousel results were also statistically fitted with computer simulation predictions to determine fitted models for rutting progression over a greater range of ESAL loading.

www.manaraa.com

4.5.1. In-situ carrousel results

The APT carrousel was designed to represent 150 trucks/day over a 20-year span based on EU standards with a 65-kN dual-wheel axle load moving at a rate of 43 km/h for 200,000 cycles. Loading of the pavement sections took place during summer months where the greatest fraction of loads would occur when pavement surface temperatures were greater than or equal to 30°C which was considered to be the point at which pavement sections would be most vulnerable to rutting. Each load cycle on the APT carrousel is estimated to equal 0.432 U.S. standard ESALs [28]. Based on the conversion factor, the 200,000 loads applied equal an equivalent 86,400 total ESALs, of which 73,440 ESALs were applied when pavement surface temperatures exceeded 30°C. Mean rut depths are from four measurements for each pavement section except for the EME section which had five measurements at each load increment. Figure 4.3 shows a summary of total rut depth progression taken as a percentage of respective mean pavement section thickness in mm. Figure 4.3 does not attempt to isolate base and subgrade deformations from pavement section rutting but is rather a summary of raw data and total cumulative ESALs.

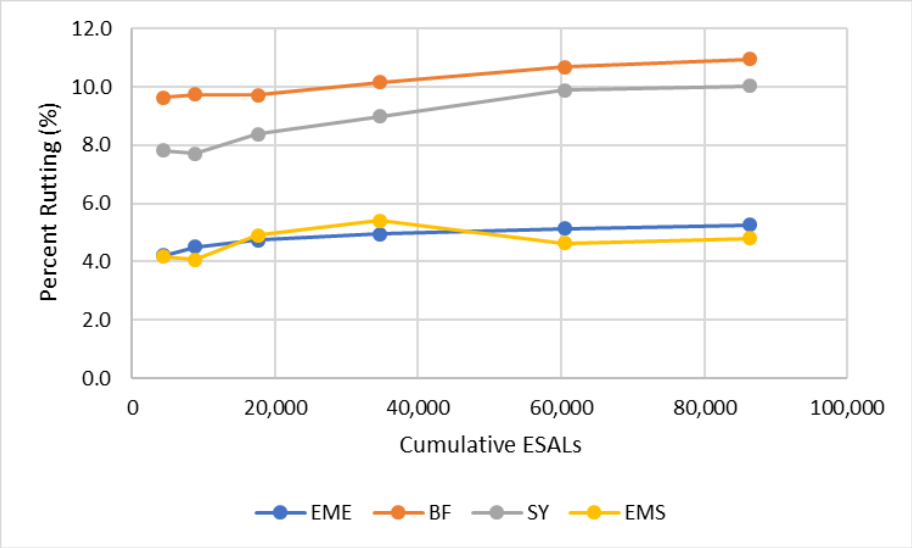

Figure 4.3: Percent Rutting Trends with Total Cumulative ESALs

www.manaraa.com

As seen in Figure 4.3, the control (EME) and EMS mixes had very similar trends based on raw percentage of rutting of pavement thickness. The SY and BF mixes had roughly double the percentage of rutting as EME and EMS. All mixes have relatively slow progressions of rutting as shown in Figure 4.3, with a point of interest being the EMS mix rutting percentage decreasing between about 37,000 and 60,000 ESALs indicating rebound. However, these trends are subject to a relatively high degree of profilometer measurement error relative to the total incremental rutting measured. Additionally, Figure 4.3 trends are subject to any initial primary base and subgrade consolidation and/or deformations.

Figure 4.4 shows pavement layer isolation rutting trends over time/critical loading as opposed to raw data trends shown in Figure 4.3. The first load increment measurements (4,425 ESALs) were not considered in Figure 4.4 to decrease the trend subjectivity to any primary base/subgrade consolidation. Additionally, successive rutting measurements indicative of rebound were considered as incremental rutting of 0.0mm/ESAL for that load increment due to the level of precision of the profilometer used to measure the maximum rut depth (±0.5mm). Adjusted incremental rutting was then divided by equivalent high-temperature incremental ESALs to calculate the equivalent mm/ESAL incremental rutting shown in Figure 4.4.

www.manaraa.com

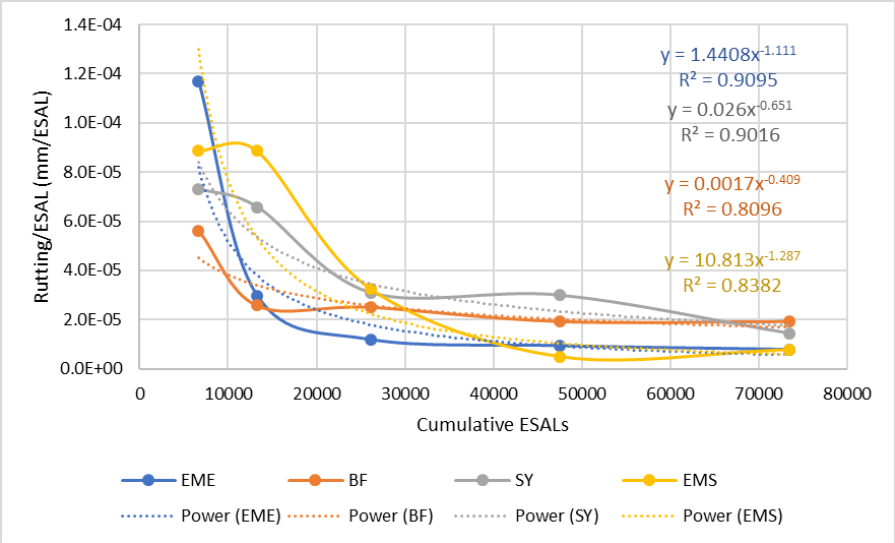

Figure 4.4: Incremental Rutting Trends

The best fit power functions shown in Figure 4.4 were used to interpolate rutting in 1,000 ESAL increments over a wide range of ESALs in order to create power functions describing cumulative rutting in mm with cumulative high temperature ESALs. The results of this fitting can be seen in Figure 4.5.

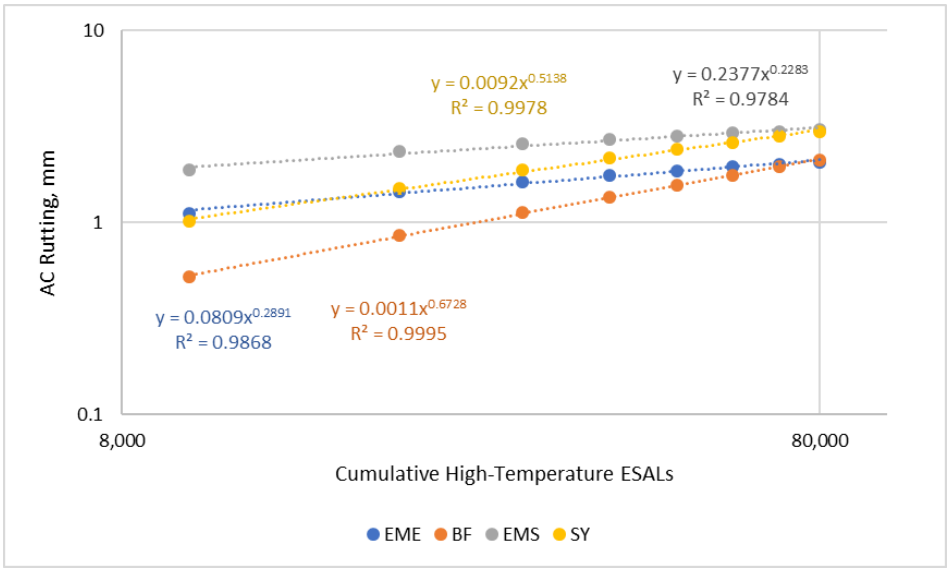

Figure 4.5: AC Layer Rutting vs. Cumulative High-Temperature ESALs

www.manaraa.com

Initial rutting in Figure 4.5 is still somewhat susceptible to the initial primary consolidation phenomena of the base, subgrade, and asphaltic layer. Therefore, the trends (AC rutting rate power variable) are of most interest. The BF and SY mixes showed the greatest rates of rutting increase with cumulative high-temperature ESALs with exponents of 0.51 and 0.67, respectively. The control (EME) and EMS mixes had the lowest rates of rutting increase with cumulative high-temperature ESALs with exponents of 0.29 and 0.23, respectively which are roughly half that of the BF and SY mixes. Trends shown in Figure 4.5 were used to form the fitted AC rutting models incorporating computer modeling extrapolations discussed in the following sections.

4.5.2. Computer simulation results

Using the inputs described in the prior-designated carrousel results section, rutting predictions for each pavement section under similar conditions as the APT carrousel were analyzed. The software provides outputs for total rutting (AC layer and base/subgrade), AC rutting (AC layer only), and total cumulative ESALs over the selected 20-year design life of the pavements. For 150 ADTT in the design lane at 30 mph (48 km/h), the 20-year design total cumulative ESALs was 1.17 million. A 256-month summary of hourly air temperatures was analyzed to determine the quantity of critical high temperature ESALs corresponding to mean pavement surface temperatures of 30°C or greater. Based on prior studies correlating pavement surface temperatures to air temperatures, air temperatures greater than or equal to 24°C were chosen to determine high temperature ESALs [29,30]. Further, the hourly traffic data was analyzed to determine the average number of ESALs/hour at times when high temperatures were most prone to occur (10 a.m. to 6 p.m.). Traffic percentages per hour were converted to ESALs per hour using equivalent ESAL conversion factors based on vehicle types and software default traffic percentages by vehicle type [31]. High temperature ESALs/hour were multiplied by the average

www.manaraa.com

high temperature hours/month and then by 12 months/year to calculate the high temperature ESALs/year and subsequently determine cumulative high temperature ESALs with time.

Table 4.8 provides a summary of computer modeling rutting results for the four plant-produced mixes at 7% air voids and traffic loadings representative of the APT carrousel (150 ADTT, 30 mph/48 km/h).

Table 4.8: Computer Software Prediction Results Summary

Mix I.D.	Rutting (mm)		20-year Cumulative ESALs		% Rutting (of Pavement Thickness)	
	Total	AC Only	Total	High Temp.	Total	AC Only
Control (EME)	7.11	0.25	1,170,000	76,424	7.1%	0.3%
BF	10.92	2.79	1,170,000	76,424	10.9%	2.8%
SY	12.45	3.81	1,170,000	76,424	12.4%	3.8%
EMS	11.18	2.79	1,170,000	76,424	11.2%	2.8%

As seen in Table 4.8, the high-performance control base mix, EME, had superior rutting resistance based on the computer model predictions. The BF and EMS mixes performed very similar with just 2.79 mm of total AC rutting, and the SY mix exhibited the most rutting with 3.81 mm of AC rutting. Table 4.8 also shows that the AC layer rutting accounted for only about one-third of the total rutting which further shows the importance of isolating the pavement AC layer rutting from the total rutting measurements in the previous APT carrousel analyses. Modifications to the base and subgrade layers can be made to decrease the total rutting and should not be taken as representative of the AC layer mix performance.

Computer predictions were made at both low (150 ADTT) and moderate (1,250 ADTT) traffic levels for each mix in order to extrapolate rutting predictions up to 640,000 high-temperature ESALs. Figure 4.6 shows these rutting predictions plotted with accompanying best-fit trend lines. Figure 4.6 analyzes AC layer rutting only, disregarding base and subgrade rutting deformations. Additionally, modeling was done for plant-produced mixes at 7% air voids.

www.manaraa.com

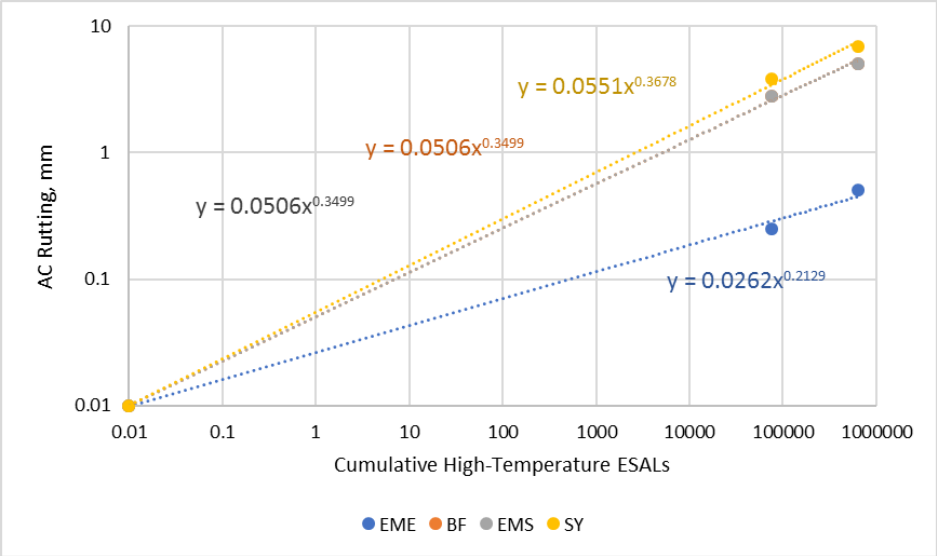

Figure 4.6: Computer Predictions for AC Layer Rutting Trends

Figure 4.6 shows that the high-performance control EME mix has the least predicted AC layer rutting at less than 1.0 mm with cumulative high-temperature ESALs of 640,000. The BF, SY, and EMS mixes are predicted to have very similar rutting of about 8-9 mm by 640,000 high-temperature ESALs which is still very good performance. Because the computer software does not account for pavement aging phenomena, it is expected that these trends are conservative with the accrual of time. As pavements age, they become stiffer and less prone to rutting and therefore these trends are most useful for performance comparisons among the mixes at various traffic levels only as the effects of long-term aging are not considered.

4.5.3. Fitted model results

Adjusted trends shown in Figures 4.5 and 4.6 were used to generate fitted models predicting AC layer rutting up to 640,000 cumulative high-temperature ESALs. The APT carrousel rutting trends and computer M-E predictive trends were fitted using a least squares error methodology. This methodology allowed for the extrapolation of APT carrousel results beyond the tested 73,440 high-temperature ESALs and simultaneous fitting of the M-E predictions to

www.manaraa.com

measured results from the APT carrousel. Table 4.9 provides a comparative summary of the carrousel (APT) and computer (M-E) results for the same loading conditions. It should be noted that the air void contents of the two are different.

Table 4.9: APT Carrousel vs. Pavement M-E Predictions Comparison

Mix I.D.	Rutting (AC Only), mm		% Rutting (Total)		High Temp. ESALs		Incremental Rutting, High Temp. (mm/ESAL)	
	APT	M-E	APT	M-E	APT	M-E	APT	M-E
EME	2.00	0.25	5.3%	7.1%	73,440	76,424	4.54E-05	1.31E-07
BF	1.95	2.79	10.9%	10.9%	73,440	76,424	4.12E-05	1.44E-06
SY	2.80	3.81	10.0%	12.4%	73,440	76,424	4.91E-05	1.96E-06
EMS	2.99	2.79	4.8%	11.2%	73,440	76,424	5.36E-05	1.31E-07

Table 4.9 shows that the predicted AC rutting is within 1.0 mm for the BF, SY, and EMS mixes for the two predictive analyses while the M-E predictions for EME AC rutting is significantly less than that of the APT carrousel analysis predictions. Research has shown that vehicle wander limits can have significant impacts on rutting of conventional pavements with less wander resulting in a more rapid accumulation of rutting [32]. However, the APT carrousel wander criteria for rutting testing was ±26 cm while the Pavement M-E software wander was similarly ±25.4 cm so wander should not have a significant impact on the comparison of these results. High temperature ESALs and total rutting as a percentage of pavement thickness were also very similar for the two predictive methods. The incremental rutting predictions for the APT carrousel analyses were one to two orders of magnitude greater than those of the M-E predictions overall. However, the similarity of the results indicates that the fitted model can closely predict extrapolated trends using APT low-ESAL corrections and M-E high-ESAL extrapolations. Figure 4.7 shows the fitted model AC layer rutting trends for the four plant-produced mixes.

www.manaraa.com

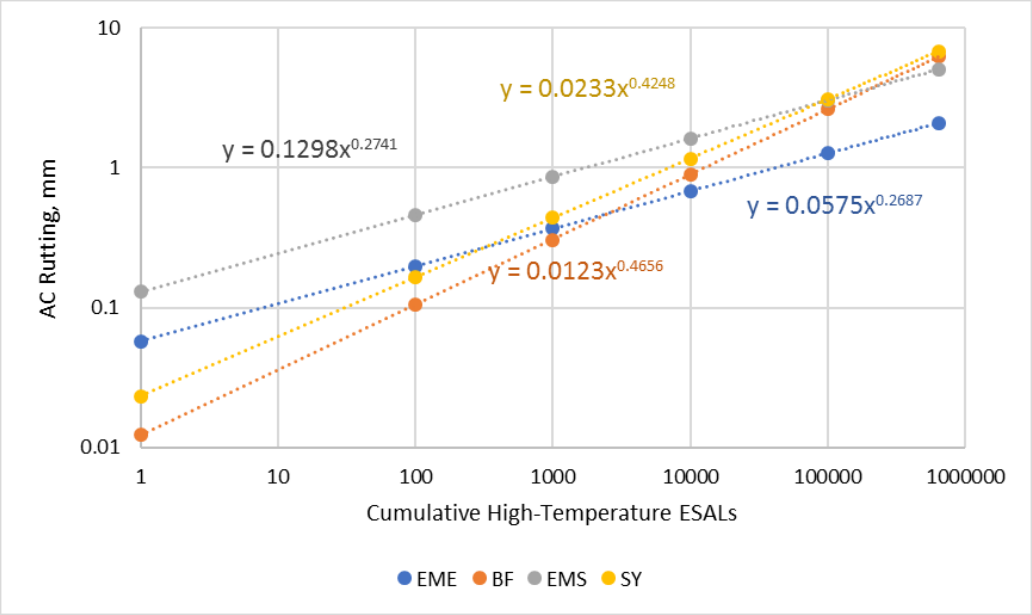

Figure 4.7: Fitted Model AC Layer Rutting Trends

Figure 4.7 shows adjusted fitted AC layer rutting trends up to 640,000 high-temperature ESALs. These trends can thus be used to predict rutting performance of these mixes in various climates. The control EME and EMS mixes had the slowest rates of rutting progression with exponents of 0.269 and 0.274, respectively. The SY and BF mixes had slightly greater rates of rutting progression with exponents of 0.425 and 0.466, respectively. At 640,000 high-temperature ESALs, the EME control mix had the least predictive rutting of just 2.1 mm. The BF, SY, and EMS mixes all had similar predicted rutting at 640,000 high-temperature ESALs with 5.1 to 6.8 mm. At a standard performance criteria of AC rutting of less than 10.0 mm, all four mixes exhibited good rutting resistance up to 640,000 high-temperature ESALs which in the applied climate conditions corresponds to a 20-year design ESAL rating of 9.75 million total ESALs.

4.6. Fatigue Characterization

In addition to rutting measurements, fatigue performance was also measured and analyzed for both the in-situ APT carrousel testing as well as the computer simulations. The APT carrousel

www.manaraa.com

fatigue performance focused primarily on percentage of total cracking while the computer simulation outputs provided both percentage of bottom-up fatigue cracking as well as lengths of top-down longitudinal fatigue cracking. Longitudinal fatigue cracking is exacerbated by thermal fluctuations and environmental loading whereas bottom-up fatigue cracking is primarily attributable to pavement performance under repetitive mechanical traffic loading. Both will be addressed in this section as indicators of mix fatigue performance.

4.6.1. In-situ carrousel results

The APT carrousel fatigue testing took place at critical low to moderate temperatures (0 to 20°C) where fatigue cracking is most likely to occur. An initial 1 million 65-kN axle loads travelling at 70 km/h were applied to the pavement sections with little surface cracking apparent. An additional 400,000 75-kN axle loads were then applied to the pavement sections to increase the degree of cumulative loading and gather data on fatigue cracking growth of the pavement sections. Figure 4.8 shows a summary of measured fatigue cracking as a percentage of respective pavement area with cumulative equivalent ESALs.

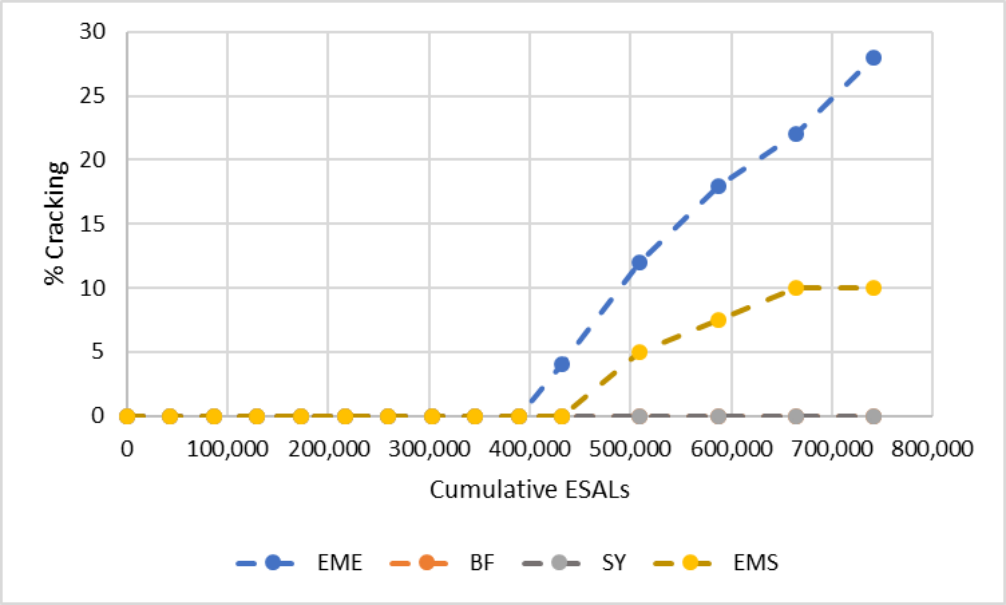

Figure 4.8: Percent Cracking with Cumulative ESALs

www.manaraa.com

Figure 4.8 shows that the APT carrousel showed no surface cracking for the BF and SY sections through 742,000 equivalent ESALs [28]. The high-performance control EME section had the greatest percentage of surface cracking (28%) after 742,000 ESALs. At 10% cracking, the EMS mix exhibited fatigue performance between EME and the BF and SY mixes. However, these results do not show potential bottom-up fatigue cracking that has not propagated through to the surface. Additionally, measurements were made visually so only large enough cracks to be seen were measured and accounted for. Carrousel fatigue testing is ongoing at the APT test facility.

4.6.2. Computer simulation results

Pavement M-E software simulations had fatigue performance outputs of bottom-up (alligator) fatigue cracking and top-down longitudinal (wheel path) cracking. Criteria of 25% of pavement surface and 2,000 ft./lane-mile (380 m/lane-km) were selected as failure points for bottom-up and top-down cracking, respectively. Critical ESALs were calculated similarly to the critical high-temperature ESALs for the rutting analyses. For fatigue cracking, air temperatures of -5 to 20°C were chosen to be critical representative air temperatures corresponding to pavement surface temperatures of 0 to 20°C. Table 4.10 provides performance results for plant-produced mixes at 7% air voids and 30 mph (km/h) traffic speeds. Simulations at high traffic levels were conducted to determine failure points for each mix which are reflected in Table 4.10.

Table 4.10: Computer Simulation Fatigue Performance Summary

Mix I.D.	Bottom-Up Fatigue Cracking		Top-Down Longitudinal Cracking	
	Total ESALs to Failure	Critical ESALs to Failure	Total ESALs to Failure	Critical ESALs to Failure
Control (EME)	9,346,000	7,921,000	1,401,000	1,117,000
BF	1,185,000	939,000	239,000	186,000
SY	1,019,000	831,000	254,000	198,000
EMS	1,074,000	880,000	234,000	181,000

www.manaraa.com

Table 4.10 shows that the computer modeling predicts the control (EME) mix to have superior cracking resistance to the BF, SY, and EMS mixes contrary to the APT carrousel results. However, these results had inputs relative to mix properties at 7% air voids whereas the carrousel sections had significantly lower air void contents. The BF, SY, and EMS mixes are predicted to perform very similarly at 7% air voids based on these results. All four mixes are governed by top-down longitudinal cracking failure criterion while not reaching 25% bottom-up cracking until surpassing 1 million total ESALs. These results show that top-down longitudinal cracking performance should be carefully considered and addressed when using these types of mixes. Research conducted in coordination with the Oregon DOT similarly found that top-down cracking is often an early critical distress which is exacerbated by the incorporation of RAP or other materials which lead to stiff mixes [33]. The APT carrousel results may have shown varying cracking results than the computer results due in part to varying wander tolerances (±52 cm for the APT and ±26 cm for computer modeling) [32]. As is the case for rutting predictions, the computer modeling performance predictions do not account for aging phenomena and their impact on performance regarding distresses. It is expected that pavement sections will be more prone to cracking as they age, and initial micro-cracks continue to propagate.

4.7. Sensitivity Analyses

Pavement M-E software analyses were conducted for sensitivity analyses. These analyses were conducted to investigate how rutting and fatigue performance are influenced by the input values and potentially APT carrousel construction and loading variables. Performance sensitivity to traffic speed, air void content, traffic levels, and mix scales were all considered. The lab control mix containing 50% RAP was also analyzed for sensitivity to provide another benchmark of

www.manaraa.com

comparison because the EME control mix passed all criteria simulated up to 9.75 million total ESALs which meant that accurate sensitivities could not be analyzed for the EME mix.

4.7.1. Sensitivity effects on rutting

Mix performance rutting sensitivity to mix scale, air void content, average daily truck traffic, and traffic speed is summarized in Table 4.11. The investigated rutting performance indicator was AC pavement layer rutting in mm. Statistical analysis of variance (ANOVA) least squares models were analyzed for each mix to assess individual variable influence on AC rutting. Associated p-values less than α=0.05 are shown in red and correspond to significant sensitivity at a 95% confidence level.

Table 4.11: Sensitivity Effects on Rutting Summary

Mix I.D.	Scale		% AV		ADTT		Traffic Speed	
	p-value	+/-*	p-value	+/-**	p-value	+/-***	p-value	+/-***
BF	0.0029	- (P)	0.0048	+	<0.0001	+	0.0006	-
SY	0.0572	- (P)	0.0021	-	<0.0001	+	0.0016	-
EMS	0.0025	- (P)	<0.0001	+	0.0010	+	0.1410	-
Control (Lab)	N/A	N/A	0.0074	+	0.0020	+	0.0740	-

*Scale: "- (P)" indicates a decrease in rutting with increase in mix scale, i.e. lab to plant
**%AV: sign indicates increase/decrease in rutting with increasing air void content
***ADTT: sign indicates increase/decrease in rutting with increasing ADTT
****Traffic Speed: sign indicates increase/decrease in rutting with increasing traffic speed

Table 4.11 shows that the BF mix rutting performance was significantly sensitive to each variable tested. The SY and EMS mixes were sensitive to all but one variable. Each mix showed similar sensitivity reactions in terms of rutting increase/decrease with increasing variables except for the SY mix displaying less rutting with increasing air void content. These results help explain the differences between the low air void content (2-4%) carrousel section rutting results with the 7% air void content computer modeling results for comparison.

www.manaraa.com

4.7.2. Sensitivity effects on bottom-up cracking

Mix bottom-up cracking performance sensitivity on mix scale, air void content, average daily truck traffic, and traffic speed are summarized in Table 4.12. Statistical modeling for bottom-up cracking focused on predicted critical temperature ESALs sections would support before reaching 25% cracking. Highlighted in red are the variables shown to be statistically significant at an α=0.05 level.

Table 4.12: Sensitivity Effects on Bottom-Up Cracking Summary

Mix I.D.	Scale		% AV		ADTT		Traffic Speed	
	p-value	+/-*	p-value	+/-**	p-value	+/-***	p-value	+/-***
BF	0.8377	- (P)	0.0484	+	0.1039	+	0.6786	-
SY	0.8536	- (P)	0.0315	+	0.0825	-	0.6528	-
EMS	0.8264	- (P)	0.0413	+	0.1064	+	0.8248	-
Control (Lab)	N/A	N/A	0.1092	+	0.1145	-	0.8188	-

*Scale: "- (P)" indicates a decrease in cracking with increase in mix scale, i.e. lab to plant
**%AV: sign indicates increase/decrease in cracking with increasing air void content
***ADTT: sign indicates increase/decrease in cracking with increasing ADTT
****Traffic Speed: sign indicates increase/decrease in cracking with increasing traffic speed

Table 4.12 shows that none of the mixes were sensitive to mix scale for bottom-up cracking resistance. The BF, SY, and EMS mixes were all significantly sensitive to air void content with greater air voids corresponding to earlier cracking failure. This finding is likely why the APT carrousel fatigue cracking results showed varying cracking performances in relationship to the computer predictions based on 7% air void content mix properties. All mixes were somewhat sensitive to truck traffic with varying responses and none of the mixes were significantly sensitive to traffic speed.

4.7.3. Sensitivity effects on top-down cracking

Mix top-down longitudinal fatigue cracking sensitivity to input and construction variables are summarized in Table 4.13. Variables shown to be statistically significant at an α=0.05 level

www.manaraa.com

are shown in red to distinguish them from statistically insignificant variables at the same level. Statistical modeling was performed on critical temperature ESALs at which pavements were predicted to surpass 380 m/lane-km of longitudinal cracking.

Table 4.13: Sensitivity Effects on Top-Down Cracking Summary

Mix I.D.	Scale		% AV		ADTT		Traffic Speed	
	p-value	+/-*	p-value	+/-**	p-value	+/-***	p-value	+/-***
BF	0.0201	- (P)	<0.0001	+	0.1824	-	0.0190	-
SY	0.0087	- (P)	<0.0001	+	0.0636	-	0.0218	-
EMS	0.0045	- (P)	<0.0001	+	0.0502	-	0.0173	-
Control (Lab)	N/A	N/A	<0.0001	+	0.0167	-	0.0775	-

*Scale: "- (P)" indicates a decrease in cracking with increase in mix scale, i.e. lab to plant
**%AV: sign indicates increase/decrease in cracking with increasing air void content
***ADTT: sign indicates increase/decrease in cracking with increasing ADTT
****Traffic Speed: sign indicates increase/decrease in cracking with increasing traffic speed

Table 4.13 shows that all mixes were statistically significantly sensitive to mix scale with the lab-produced mixes failing earlier than the plant-produced mixes. Each mix was most sensitive to air void content with higher air void contents failing much earlier than mixes compacted at lower air void contents. This finding is similar to that of the bottom-up fatigue cracking and supports the reasoning behind the disparities between APT carrousel cracking observations and computer modeling predictions. All mixes were also sensitive to traffic speed with greater speeds leading to longer pavement lives before failure criteria was met.

4.8. Summary and Conclusions

This research investigated the predictive in-situ performance of three base-layer asphalt mixes incorporating 50% RAP by mix weight and novel bio-additives with rejuvenating characteristics. Two controls were used for comparison: one 20% RAP high-performance French mix design which uses petrol-derived binder (EME) and one 50% RAP mix design with the same aggregate blend and binder content as the BF, SY, and EMS mixes. An accelerated pavement

www.manaraa.com

testing (APT) carrousel near Nantes, France was used to predict and gather data on plant-produced mix resistance to rutting and fatigue cracking. To cross-check, further analyze, and extrapolate the APT data, AASHTOWare® Pavement M-E Design software was used to predict critical pavement distress trends over a multitude of scenarios. From the analyses and predictive modeling completed as a part of this research, the following conclusions can be made:

- Computer software predictive modeling can be used to extrapolate APT carrousel rutting trends. However, these predictions are likely conservative as they do not account for aging phenomena and their impact on rutting resistance.
- APT facility data can be coupled with computer modeling data to generate models of pavement distress trends over time based on respective critical temperature ESALs. Models based on critical temperature ESALs can be used to predict pavement performance with respect to rutting and fatigue behavior in different climate zones.
- These novel mixes (BF, SY, and EMS) are most sensitive to field compaction air void contents. Lower air void contents drastically improve resistance to fatigue cracking (bottom-up and top-down) as well as rutting for BF and EMS while the SY mix has greater rutting resistance at higher air voids (7%).

In addition to the important conclusions offered, Table 4.14 shows a summary of each mix and its associated critical ESALs to failure for rutting, bottom-up fatigue cracking, and top-down fatigue cracking based on computer modeling outcomes for lab-produced mixes compacted to 4% air voids and traffic speeds of 89 km/h (55mph).

www.manaraa.com

Table 4.14: Mix Performance Summary

Mix I.D.	Rutting (AC Layer) 10-mm Max.		Bottom-Up Fatigue Cracking (25% Max.)		Top-Down Longitudinal Cracking (380-m/lane-km Max)	
	mm	Critical ESALs	Total ESALs	Critical ESALs	Total ESALs	Critical ESALs
EME	0.25	637,000	9,346,000	7,921,000	1,401,000	1,117,000
BF	2.29	637,000	7,331,000	6,164,000	1,075,000	879,000
SY	4.32	637,000	3,776,000	3,108,000	750,000	606,000
EMS	1.02	637,000	9,346,000	7,921,000	1,228,000	975,000

Because all computer-simulated pavements compacted to 4% air voids passed rutting criteria up to the maximum-tested 9.75 million total ESALs, the total rutting at the end of 20-year design life is shown for comparison. Even though the SY mix has a greater rutting resistance at higher air voids, it has greater cracking resistance at lower air voids. Table 4.14 shows that the top-down longitudinal fatigue cracking is the predicted critical failure distress for each pavement mix tested. Although plant-produced mixes had better cracking resistance that the lab-produced mixes, these results lead to the conclusion that top-down cracking governs the life expectancy of these mixes and should be carefully considered prior to implementation. Results also show that these novel mixes have high performances against bottom-up fatigue cracking and rutting. It is expected that cracking would increase over time as the pavements age and become more prone to brittle failure mechanisms which is not accounted for in the software analyses. With the exception of the SY mix, the BF and EMS mixes performed as well, or similarly, as the high-performance EME control with regards to all three distress criteria investigated.

References

1. FHWA, U.S. Department of Transportation Federal Highway Administration. “Reclaimed Asphalt Pavement in Asphalt Mixtures: State of the Practice.” *FHWA Publication No. FHWA-HRT-11-021*. April 2011.

www.manaraa.com

2. National Center for Asphalt Technology (NCAT): *Hot Mix Asphalt Materials, Mixture Design and Construction, 3rd ed.*, NCAT. 1991.

3. EAPA (European industry association), Asphalt in Figures, 2016. [www.eapa.org]

4. Ali, Hesham. "Long-Term Aging of Recycled Binders." Florida International University: Civil and Environmental Engineering Department; submitted to the Florida Department of Transportation. July 2015.

5. Haghshenas et al. "Research on High-RAP Asphalt Mixtures with Rejuvenators and WMA Additives." University of Nebraska-Lincoln: Nebraska Department of Roads Research Reports. September 2016.

6. Kowalski et al. "Thermal and Fatigue Evaluation of Asphalt Mixtures Containing RAP Treated with a Bio-Agent." *Applied Sciences, Vol. 7, Issue 3*. February 2017.

7. Mogawer, Walaa & Booshehrian, Abbas & Vahidi, Siavash & Austerman, Alexander. (2013). "Evaluating the effect of rejuvenators on the degree of blending and performance of high RAP, RAS, RAP/RAS mixtures." *Road Materials and Pavement Design*. 14. 10.1080/14680629.2013.812836.

8. Zaumanis et al. "Influence of Six Rejuvenators on the Performance Properties of Reclaimed Asphalt Pavement (RAP) Binder and 100% Recycled Asphalt Mixtures." *Construction and Building Materials.* November 2014.

9. Jiménez del Barco Carrión, A., Pérez-Martínez, M., Themeli, A., Lo Presti, D., Marsac, P., Pouget, S., Chailleux, E., Airey, G. D. (2017). Evaluation of bio-materials' rejuvenating effect on binders for high-reclaimed asphalt content mixtures. *Materiales de Construcción, 67*(327), 1–11.

10. Jiménez del Barco Carrión, A., Lo Presti, D., Pouget, S., Airey, G., & Chailleux, E. (2017). Linear viscoelastic properties of high reclaimed asphalt content mixes with biobinders. *Road Materials and Pavement Design*, 1–11.

11. Shirzad, Sharareh & Aguirre, Max & Bonilla, Luis & A Elseifi, Mostafa & Cooper, Samuel & Mohammad, Louay. (2018). Mechanistic-empirical pavement performance of asphalt mixtures with recycled asphalt shingles. Construction and Building Materials. 160. 687-697.

www.manaraa.com

12. Buss, A., & Williams, R. C. (2012). Warm Mix Asphalt Performance Modeling Using the Mechanistic-Empirical Pavement Design Guide. In A. Scarpas, N. Kringos, I. Al-Qadi & L. A (Eds.), *7th RILEM International Conference on Cracking in Pavements* (Vol. 4, pp. 1323-1332): Springer Netherlands.

13. Joseph H. Podolsky, Ashley Buss, R. Christopher Williams & Eric Cochran (2017). "Mechanistic empirical performance of warm-mix asphalt with select bio-derived additives in the Midwestern United States using AASHTOWare pavement ME design." *Road Materials and Pavement Design*, 18:4, 800-816, DOI: 10.1080/14680629.2016.1194880.

14. Biophalt patent US 8,652,246 B2

15. Pouget S. & Loup L. "Thermo-mechanical behaviour of mixtures containing bio-binders." *Road Materials and Pavement Design*, vol.14, Special Issue EATA, pp. 212-226, 2013.

16. Porot, L. and W. Grady. "Effectiveness of a bio-based additive to restore properties of aged asphalt binder". Proc., International Society for Asphalt Pavements (ISAP) Symposium. 2016.

17. Elkashef, Mohamed Elsayed, "Using soybean-derived materials to rejuvenate reclaimed asphalt pavement (RAP) binders and mixtures" (2017). Graduate Theses and Dissertations. 15514. https://lib.dr.iastate.edu/etd/15514

18. ASTM D2172. "Standard Test Methods for Quantitative Extraction of Asphalt Binder from Asphalt Mixes." Standard Specifications for Transportation Materials and Methods of Sampling and Testing, Washington D.C., 2007.

19. ASTM D7906. "Standard Practice for Recovery of Asphalt from Solution Using Toluene and the Rotary Evaporator." Standard Specifications for Transportation Materials and Methods of Sampling and Testing, Washington D.C., 2007.

20. Asphalt Institute. Asphalt Mix Design Methods, 7th Edition. MS-2. 2014.

21. AASHTO T 331-13. "Standard Method of Test for Bulk Specific Gravity (Gmb) and Density of Compacted Hot Mix Asphalt (HMA) Using Automatic Vacuum Sealing Method." Standard Specifications for Transportation Materials and Methods of Sampling and Testing, Washington D.C., 2015.

www.manaraa.com

22. AASHTO T 209. "Theoretical Maximum Specific Gravity and Density of Hot Mix Asphalt (HMA)." Standard Specifications for Transportation Materials and Methods of Sampling and Testing, Washington D.C., 2015.

23. AASHTO TP 79-13. "Determining the Dynamic Modulus and Flow Number for Asphalt Mixtures Using the Asphalt Mixture Performance Tester (AMPT)." Standard Specifications for Transportation Materials and Methods of Sampling and Testing, Washington D.C., 2013.

24. ASTM D2872. "Standard Test Method for Effect of Heat and Air on a Moving Film of Asphalt (Rolling Thin-Film Oven Test)." Standard Specifications for Transportation Materials and Methods of Sampling and Testing, Washington D.C., 2013.

25. ASTM D7175. "Standard Test Method for Determining the Rheological Properties of Asphalt Binding Using a Dynamic Shear Rheometer." Standard Specifications for Transportation Materials and Methods of Sampling and Testing, Washington D.C., 2008.

26. FHWA, U.S. Department of Transportation Federal Highway Administration. "Asphalt Material Characterization for AASHTOWare® Pavement ME Design Using an Asphalt Mixture Performance Tester (AMPT)." *FHWA Publication No. FHWA-HIF-13-060*. September 2013.

27. A Kamal, M & Arshid, Muhammad & I Sha, M & A Khan, E. (2018). "Relationship between Dynamic Deformation Modulus (Evd) and CBR for Common and Granular Materials." *Technical Journal, University of Engineering and Technology (UET)* Taxila, Pakistan Vol. 23 No. 1-2018. ISSN:1813-1786 (Print) 2313-7770 (Online).

28. Y.H. Huang. *Pavement Analysis and Design*. Second Edition, Prentice Hall, New Jersey, 2004.

29. Solaimanian, Mansour & Kennedy, Thomas W. (1993). "Predicting Maximum Pavement Surface Temperature Using Maximum Air Temperature and Hourly Solar Radiation." Transportation Research Board, Washington D.C., 1993. Issue No. 1417, ISSN: 0361-1981.

30. A. A. Shamsipour, Gh. Azizi, M. Karimi Ahmadabad, M. Moghbel. "Surface Temperature Pattern of Asphalt, Soil and Grass in Different Weather Condition." *Journal of Biodiversity and Environmental Sciences*, Vol. 3, No. 9, p. 42-50, 2013. ISSN: 2220-6663 (Print) 2222-3045 (Online).

www.manaraa.com

31. Pennsylvania Department of Transportation. “Truck Factors Table, Table 7.1”. http://www.dot.state.pa.us/public/Bureaus/BOMO/Marcellus/TruckFactorsTable.pdf.

32. Stempihar, Jeffrey John. (2004). “Quantifying the Lateral Displacement of Heavy Vehicles on Michigan’s Highways and its Incorporation into Flexible Pavement Design.” Thesis for the Degree of M.S., Michigan Technological University.

33. Md S. Rahman, Joseph H. Podolsky, R. Christopher Williams & Todd Scholz (2017). “A study of top-down cracking in the state of Oregon.” *Road Materials and Pavement Design*. DOI: 10.1080/14680629.2017.1345782.

www.manaraa.com

CHAPTER 5: GENERAL CONCLUSIONS

This chapter is a summation of all significant conclusions highlighted within the prior chapters. These conclusions are those that are deemed of most importance as a result of the totality of the analyses and data that make up this research.

5.1. Laboratory Performance of a Novel Bio-Binder

The first part of this research showed the viability of a novel bio-binder as a complete replacement to conventional bituminous neat binder in a mix with 50% RAP. At the laboratory-preparation scale, the binder derived from refined pine-chemistry was shown to significantly improve the resistance to thermal cracking of a mix with 50% RAP. While the beam fatigue test results showed a slightly greater rate of damage accumulation for the mix with the bio-binder, these results also show the increased viscous response of the restored RAP mix as compared to the control mix. Flow number testing showed that the mix stiffness at high temperatures was decreased by the bio-binder replacement, yet still retained enough stiffness to resist rutting at high temperatures. Comparisons with industry standards and Superpave recommendations showed that a mix with 50% RAP and non-bituminous binder can pass all performance criterion for a pavement with a 20-year design traffic loading of greater than 10 million but less than 30 million ESALs.

5.2. Bio-Additive Performance Sensitivity to Mix Scale

The second part of this research showed that the novel bio-binder has very little performance sensitivity to the change in mix scale and associated process control variations when going from a laboratory-produced mix to a large-scale continuous asphalt mix plant. The two rejuvenators had little sensitivity to mix scale and process control variations at low temperatures

www.manaraa.com

but did show increased stiffness at intermediate and high temperature performance. Although the rejuvenated mixes still passed performance criteria at both scales, the increased stiffness at intermediate and high temperatures indicates that rejuvenating effectiveness potentially decreases at the larger mix scale. A decrease in rejuvenator effectiveness is likely attributable to the increased mixing temperatures, variable application rates, and variable short-term aging conditions at the two scales. Such changes should be considered when assessing laboratory-based performance testing on rejuvenated high RAP content mixes and using results to predict in-situ field performance.

5.3. APT and Computer Predictions for Mix Performance

Accelerated pavement test result analysis showed that predicted asphalt layer rutting can be separated out from raw measurements by using incremental rutting trends. Rutting progression can further be evaluated based on critical high temperature ESALs. These models can be extrapolated using fitted mechanistic-empirical computer modeling to create rutting progression prediction models over a wide range of critical ESALs which can be used in different climate regions. Similarly, APT fatigue measurements and observations can be supplemented with computer modeling to analyze the critical types of cracking attributable to each mix tested. For this research, it was found that all three mixes with bio-additives perform exceptionally well against rutting on a large scale. Further, computer predictions and field performance measurements showed that the mixes with bio-additives perform as well or better than a high-performance control mix with 20% RAP against fatigue cracking. All four mixes were predicted to have critical distresses of top-down longitudinal cracking that limit the pavements' design lives. The bio-additives did show good performance against bottom-up fatigue cracking at air void contents of 4% with greater fatigue cracking at higher air void contents.

www.manaraa.com

5.4. Future Research

Future research should determine more accurate methods of analyzing and predicting fatigue performance of high RAP content mixes incorporating bio-additives with rejuvenating properties. Conventional methods of testing consider the viscous damping component added by the restorative rejuvenation as accelerated rates of damage accumulation. However, this may due to self-heating of the binder due the added "softness" and may not be necessarily a negative attribute considering fatigue performance as was seen in the APT testing of this research. Further research could also be conducted on rejuvenator sensitivities to process control variables associated with changing mix scales from the laboratory to an asphalt plant. Data collection on the plant process control variables and laboratory conditions could be used to assess relative degrees of volatilization, rejuvenator mass loss, or short-term aging conditions. Finally, APT testing could be conducted using an increased number of load cycles to further verify computer modeling extrapolations. Distress modeling using critical ESALs could be used and verified in other climate locations to develop universal prediction models for pavement mix performance. Demonstration pavement sections used on actual in-situ roadway paving projects could also be instrumented and used for data collection with time to calibrate both the APT test results as well as the computer software M-E predictions for these types of mix designs.

www.manaraa.com